40454

National Library of Canada | Bibliothèque nationale du Canada

CANADIAN THESES ON MICROFICHE | THÈSES CANADIENNES SUR MICROFICHE

NAME OF AUTHOR/*NOM DE L'AUTEUR* Laila Abdelaziz MAAROUF

TITLE OF THESIS/*TITRE DE LA THÈSE* An Analysis of Solar Radiation Measurements at Edmonton and Their Bearing on Atmospheric Transmission

UNIVERSITY/*UNIVERSITÉ* Alberta

DEGREE FOR WHICH THESIS WAS PRESENTED/*GRADE POUR LEQUEL CETTE THÈSE FUT PRÉSENTÉE* M. Sc.

YEAR THIS DEGREE CONFERRED/*ANNÉE D'OBTENTION DE CE GRADE* ~~Prof. G. W. Sadler~~ 1979

NAME OF SUPERVISOR/*NOM DU DIRECTEUR DE THÈSE* Prof. G. W. Sadler

Permission is hereby granted to the NATIONAL LIBRARY OF CANADA to microfilm this thesis and to lend or sell copies of the film.

The author reserves other publication rights, and neither the thesis nor extensive extracts from it may be printed or otherwise reproduced without the author's written permission.

L'autorisation est, par la présente, accordée à la BIBLIOTHÈQUE NATIONALE DU CANADA de microfilmer cette thèse et de prêter ou de vendre des exemplaires du film.

L'auteur se réserve les autres droits de publication; ni la thèse ni de longs extraits de celle-ci ne doivent être imprimés ou autrement reproduits sans l'autorisation écrite de l'auteur.

DATED/*DATÉ* 1 Dec, 1978 SIGNED/*SIGNÉ* Laila Maarouf

PERMANENT ADDRESS/*RÉSIDENCE FIXÉ* Box 3295, station D, Willowdale, Ontario M2R- 3G6

NL-91 (3-74)

National Library of Canada

Cataloguing Branch
Canadian Theses Division

Ottawa, Canada
K1A 0N4

Bibliothèque nationale du Canada

Direction du catalogage
Division des thèses canadiennes

NOTICE

The quality of this microfiche is heavily dependent upon the quality of the original thesis submitted for microfilming. Every effort has been made to ensure the highest quality of reproduction possible.

If pages are missing, contact the university which granted the degree.

Some pages may have indistinct print especially if the original pages were typed with a poor typewriter ribbon or if the university sent us a poor photocopy.

Previously copyrighted materials (journal articles, published tests, etc.) are not filmed.

Reproduction in full or in part of this film is governed by the Canadian Copyright Act, R.S.C. 1970, c. C-30. Please read the authorization forms which accompany this thesis.

THIS DISSERTATION
HAS BEEN MICROFILMED
EXACTLY AS RECEIVED

AVIS

La qualité de cette microfiche dépend grandement de la qualité de la thèse soumise au microfilmage. Nous avons tout fait pour assurer une qualité supérieure de reproduction.

S'il manque des pages, veuillez communiquer avec l'université qui a conféré le grade.

La qualité d'impression de certaines pages peut laisser à désirer, surtout si les pages originales ont été dactylographiées à l'aide d'un ruban usé ou si l'université nous a fait parvenir une photocopie de mauvaise qualité.

Les documents qui font déjà l'objet d'un droit d'auteur (articles de revue, examens publiés, etc.) ne sont pas microfilmés.

La reproduction, même partielle, de ce microfilm est soumise à la Loi canadienne sur le droit d'auteur, SRC 1970, c. C-30. Veuillez prendre connaissance des formules d'autorisation qui accompagnent cette thèse.

LA THÈSE A ÉTÉ
MICROFILMÉE TELLE QUE
NOUS L'AVONS REÇUE

THE UNIVERSITY OF ALBERTA

AN ANALYSIS OF SOLAR RADIATION MEASUREMENTS AT EDMONTON AND THEIR BEARING ON ATMOSPHERIC TRANSMISSION

by

© LAILA ABDELAZIZ MAAROUF

A THESIS

SUBMITTED TO THE FACULTY OF GRADUATE STUDIES AND RESEARCH

IN PARTIAL FULFILMENT OF THE REQUIREMENTS FOR THE DEGREE

OF MASTER OF SCIENCE

IN

MECHANICAL ENGINEERING

DEPARTMENT OF MECHANICAL ENGINEERING

EDMONTON, ALBERTA

SPRING, 1979

THE UNIVERSITY OF ALBERTA

FACULTY OF GRADUATE STUDIES AND RESEARCH

The undersigned certify that they have read, and recommend to the Faculty of Graduate Studies and Research, for acceptance, a thesis entitled "An Analysis of Solar Radiation Measurements at Edmonton and Their Bearing on Atmospheric Transmission", submitted by Laila Abdelaziz Maarouf in partial fulfilment of the requirements for the degree of Master of Science in Mechanical Engineering.

.....Gerald W. Sadler.....

Supervisor

.....Ron Tweed.....

.....Keith C. Hay.....

Date..28 November 1978...

ABSTRACT

An analysis of the integral wavelength direct normal incidence solar radiation and its spectral components passing through the RG2 and RG8 filters has been made for measurements taken at Edmonton, Alberta, Canada during the period May 1972 to September 1975 under clear sky conditions. The basic terms and equations useful in solar energy calculations are presented. The annual variations of the apparent solar constant and the apparent extinction coefficient have been examined. The diurnal and annual variations of the direct radiation and of its spectral components have been studied. The average spectral composition of the direct radiation is found to be 56% in the infrared region, 37.5% in the shortwave region and 6.5% in the red region for solar altitudes between 60 and 20 degrees. Expressing the infrared and shortwave fractions as functions of the optical air mass resulted in linear relationships. For the same altitude, the atmospheric transmission factors for the direct radiation and its spectral components are lower in summer than in winter. The average ratios of the extinction coefficients for the infrared and the shortwave regions to that for the integral wavelength are 0.79 and 1.15 during the summer, respectively. The corresponding values in the winter are 0.66 and 1.4. The atmospheric turbidity and the water vapor absorption have been determined and they show marked annual variations with maximum values during the summer.

ACKNOWLEDGEMENTS

The author takes the pleasure in expressing her sincere thanks and appreciation to Professor G.W. Sadler for his continuing encouragement and capable supervision.

I am also indebted to my sister, Alia, who volunteered to take full care of my children when I needed her assistance.

TABLE OF CONTENTS

	Page
ABSTRACT	iv
ACKNOWLEDGEMENTS	v
TABLE OF CONTENTS	vi
LIST OF TABLES	ix
LIST OF FIGURES	xi
NOMENCLATURE	xiv
CHAPTER	
1. PRINCIPLES OF SOLAR ENERGY CALCULATIONS	1
1.1 Introduction	2
1.2 The Sun and the Earth	3
1.3 Basic Earth-Sun Angles	5
1.4 Solar Time	14
1.5 The Solar Constant, The Solar Spectral Irradiance and the Air Mass	17
1.6 Data and Computations	19
2. CLEAR SKY DIRECT NORMAL INCIDENCE SOLAR RADIATION	22
2.1 Solar Extraterrestrial Radiation	23
2.2 Atmospheric Effects on Extraterrestrial Energy	23
2.3 Extinction of Solar Radiation and Atmospheric Transmission Factor	24

2.4 Apparent Solar Insolation at Air Mass Zero and Apparent Atmospheric Extinction Coefficient 28

2.5 Measurement of the Apparent Solar Constant and the Apparent Extinction Coefficient at Edmonton, Alberta 30

2.6 Annual Variation of the Direct Solar Radiation at Normal Incidence, IDN, at Various Hour Angles as Measured at Edmonton 35

3. DISTRIBUTION OF SOLAR ENERGY IN DIFFERENT WAVELENGTH REGIONS 47

3.1 The Solar Radiation at the Earth Surface 48

3.2 Characteristics of Cutoff Glass Filters Used in Solar Radiation Measurements 49

3.3 Application of the Filter Measurements 53

3.4 Filter Measurements at Edmonton 56

3.5 The Annual Variation of the Spectral Distribution of the Normal Incidence Insolation Measured at Edmonton at Different Hour Angles 58

3.6 Variation of the Normal Insolation with the Solar Altitude 75

3.7 Variation of the Infrared and Shortwave Fractions of the Normal Insolation with the Optical Air Mass 78

Page

3.8 Determination of Atmospheric Transmission Factors and Extinction Coefficients for Direct Radiation within the Whole Solar Spectrum and the Five Spectral Bands 86

4. TURBIDITY OF THE ATMOSPHERE AND ABSORPTION OF SOLAR RADIATION BY ATMOSPHERIC WATER VAPOR 92

4.1 Atmospheric Turbidity 93

4.2 Determination of Linke's Turbidity Factor for Edmonton 101

4.3 Determination of Ångström's Turbidity Coefficient for Edmonton 105

4.4 Absorption of Solar Radiation by Atmospheric Water Vapor 107

4.5 Determination of Water Vapor Absorption at Edmonton 109

5. DISCUSSION AND CONCLUSIONS 113

5.1 Apparent Solar Constant and Apparent Extinction Coefficient 114

5.2 Diurnal and Annual Variations of the Direct Radiation and Its Spectral Composition 115

5.3 Variation of the Infrared and Shortwave Fractions with Solar Altitude and Optical Air Mass 117

5.4 Atmospheric Transmission Factors and Extinction Coefficients 117

5.5 Atmospheric Scattering and Absorption 118

REFERENCES 120

LIST OF TABLES

Table		Page
1.1	Comparison of the terrestrial, the equatorial and the horizon systems	7
2.1	Comparison between Sadler's and present monthly average values for A and I* obtained at Edmonton	35
2.2	Monthly average direct normal incidence solar radiation (IDN) measured at Edmonton at different hour angles	46
3.1	Solar intensity above the longwave cutoff of the filters ΔIL as a function of atmospheric humidity $m_h \cdot w$	52
3.2	Spectral regions of the solar spectrum obtained by filter measurements	55
3.3	Monthly average percentage of the direct normal incidence solar radiation in the infrared spectrum band Iip and the shortwave spectrum band Ikp at Edmonton at different hour angles	67
3.4	Monthly average normal incidence solar radiation in the red and infrared band Ir and the shortwave band Ik measured at Edmonton at different hour angles	71
3.5	Monthly average normal incidence solar radiation in the infrared band Ii and the visible band Iv measured at Edmonton at different hour angles	72

Table

Page

3.6 Monthly average normal incidence solar radiation in the wavelength range of 626 to 690 millimicron measured at Edmonton at different hour angles 73

3.7 Equations representing the infrared fractions of the normal incidence solar radiation in terms of the optical air mass m and the solar altitude α .. 84

3.8 Equations representing the shortwave fraction of the normal incidence solar radiation in terms of the optical air mass m and the solar altitude α .. 85

3.9 Normal incidence solar radiation, IDN, at different solar altitudes and its distribution in different spectral bands throughout the year 87

3.10 Atmospheric transmission factors for the whole solar spectrum and the five bands calculated at different solar altitudes throughout the year 88

3.11 Extinction coefficients for the whole solar spectrum and the five bands calculated at different solar altitudes throughout the year 90

4.1 Polynomials for calculating the factor P(m) as a function of the air mass m 102

4.2 Mean monthly value of Linke's turbidity factor ... 103

4.3 Mean monthly value of Ångström's turbidity factor β_p for Edmonton 107

4.4 Mean monthly value of water vapor absorption at Edmonton 111

LIST OF FIGURES

Figure		Page
1.1	Equatorial astronomical coordinate system	8
1.2	Horizontal astronomical coordinate system	9
1.3	Illustration of the three basic earth-sun angles: Latitude L, Hour angle h and Declination δ	9
1.4	Illustration of derived solar angles	13
2.1	Annual variation of the apparent extinction coefficient, A, measured at Edmonton	32
2.2	Annual variation of the apparent solar insolation at air mass zero, I^*, measured at Edmonton	33
2.3	Annual variation of clear sky direct normal incidence solar radiation, IDN, measured at Edmonton at hour angle zero	37
2.4	As in figure 2.3 but for hour angle 1	38
2.5	As in figure 2.3 but for hour angle 2	39
2.6	As in figure 2.3 but for hour angle 3	40
2.7	As in figure 2.3 but for hour angle 4	41
2.8	As in figure 2.3 but for hour angle 5	42
2.9	As in figure 2.3 but for hour angle 6	43
2.10	As in figure 2.3 but for hour angles zero to six	44
3.1	Annual variation of the fractions of the clear sky direct normal incidence solar radiation within different spectral bands measured at Edmonton at hour angle zero	60

Figure		Page
3.2	As in figure 3.1 but for hour angle 1	61
3.3	As in figure 3.1 but for hour angle 2	62
3.4	As in figure 3.1 but for hour angle 3	63
3.5	As in figure 3.1 but for hour angle 4	64
3.6	As in figure 3.1 but for hour angle 5	65
3.7	As in figure 3.1 but for hour angle 6	66
3.8	Annual variation of the infrared, Iip, shortwave, Ikp, and red, Iep, fractions of the direct normal incidence solar radiation measured at Edmonton at hour angles zero to six	69
3.9	Variation of the infrared fraction, Iip, of the direct normal incidence solar radiation with the solar altitude α	76
3.10	Variation of the shortwave fraction, Ikp, of the direct normal incidence solar radiation with the solar altitude α	77
3.11	Variation of the infrared fraction, Iip, of the direct normal incidence solar radiation with the optical air mass for the solar altitude interval 20 to 60 degrees throughout the year ..	80
3.12	As in figure 3.11 but for the solar altitude interval 5 to 20 degrees	81
3.13	Variation of the shortwave fraction, Ikp, of the direct normal incidence solar radiation with the optical air mass for the solar altitude interval 20 to 60 degrees throughout the year	82

Figure Page

3.14 As in figure 3.13 but for the solar altitude interval 5 to 20 degrees 83

4.1 Annual variation of Linke's turbidity factor, T_n, for Edmonton 104

4.2 Annual variation of Ångström's turbidity coefficient, β_p, for Edmonton 106

4.3 Annual variation of water vapor absorption, WA, at Edmonton 112

NOMENCLATURE

A	Apparent atmospheric extinction coefficient
ADN	Atmospheric extinction coefficient for the whole solar spectrum
Ae	Atmospheric extinction coefficient for red radiation
Ai	Atmospheric extinction coefficient for infrared radiation
Ak	Atmospheric extinction coefficient for shortwave radiation
Ar	Atmospheric extinction coefficient for red and infrared radiation
Av	Atmospheric extinction coefficient for visible radiation
$A(\lambda)$	Atmospheric extinction coefficient as a function of the wavelength λ
$a_D(\lambda)$	Extinction coefficient of atmospheric dust as function of λ
$a_o(\lambda)$	Extinction coefficient of ozone as function of λ
$a_R(\lambda)$	Extinction coefficient of clean dry, Rayleigh, atmosphere as function of λ
$\bar{a}_R(m)$	Mean value over all wavelengths of the extinction coefficient of clean dry atmosphere as function of the air mass m
$a_w(\lambda)$	Absorption coefficient of water vapor in the atmosphere as function of λ
B	Schüepp's turbidity coefficient
ET	Equation of time (minutes)
F1	Filter factor for the filter OG1
F2	Filter factor for the filter RG2
F8	Filter factor for the filter RG8
G	Longitude (degrees)
Gs	Longitude of a standard meridian (degrees)

h	Hour angle of the sun (degrees)
I	Intensity of direct radiation at normal incidence at the earth's surface ($Btu.ft^{-2}.hr^{-1}$.)
Ib	Intensity of direct blue and violet radiation at normal incidence ($Btu.ft^{-2}.hr^{-1}$.)
ID	Intensity of direct yellow and red radiation at normal incidence ($Btu.ft^{-2}.hr^{-1}$.)
IDN	Intensity of clear sky direct normal incidence solar radiation measured at Edmonton ($Btu.ft^{-2}.hr^{-1}$.)
Ie	Intensity of direct red radiation at normal incidence ($Btu.ft^{-2}.hr^{-1}$.)
Iep	Fraction of IDN within the red radiation
Ii	Intensity of direct infrared radiation at normal incidence ($Btu.ft^{-2}.hr^{-1}$.)
Iip	Fraction of IDN within the infrared radiation
Ik	Intensity of direct shortwave radiation at normal incidence ($Btu.ft^{-2}.hr^{-1}$.)
Ikp	Fraction of IDN within the shortwave radiation
Ir	Intensity of direct red and infrared radiation at normal incidence ($Btu.ft^{-2}.hr^{-1}$.)
Irp	Fraction of IDN within the red and infrared radiation
Iv	Intensity of direct visible radiation at normal incidence ($Btu.ft^{-2}.hr^{-1}$.)
Ivp	Fraction of IDN within the visible radiation
I1	Intensity of radiation measured by OG1 filter ($Btu.ft^{-2}.hr^{-1}$.)
I2	Intensity of radiation measured by RG2 filter ($Btu.ft^{-2}.hr^{-1}$.)
I8	Intensity of radiation measured by RG8 filter ($Btu.ft^{-2}.hr^{-1}$.)
I_o	Solar constant ($Btu.ft^{-2}.hr^{-1}$.)
$I_{o\lambda}$	Intensity of parallel monochromatic beam of wavelength λ outside the earth's atmosphere ($Btu.ft^{-2}.hr^{-1}$.)

$I_0(\lambda)$	Solar constant as a function of wavelength λ ($Btu.ft^{-2}.hr^{-1}$.)
I_λ	Intensity of parallel monochromatic solar beam of wavelength λ at the earth's surface ($Btu.ft^{-2}.hr^{-1}$.)
I^*	Apparent solar constant ($Btu.ft^{-2}.hr^{-1}$.)
i	Inclination angle of a surface (degrees)
L	Latitude (degrees)
m	Absolute optical air mass
m_h	Relative optical air mass
n	Day of year measured from January one
P	Pressure of the earth's surface at mean sea level (millibars)
P_o	Pressure of the earth's surface at time and place of observation (millibars)
R	Reduction factor to mean earth-sun distance
R_i	Earth-sun distance at time of observation (miles)
R_o	Mean earth-sun distance (miles)
S	Azimuth of inclined surface (degrees)
T	Linke's turbidity factor
TDN	Atmospheric transmission factor for clear sky direct normal incidence solar radiation
Te	Atmospheric transmission factor for direct normal red radiation
Ti	Atmospheric transmission factor for direct normal infrared radiation
Tk	Atmospheric transmission factor for direct normal shortwave radiation
Tr	Atmospheric transmission factor for direct normal red and infrared radiation
Tv	Atmospheric transmission factor for direct normal visible radiation
T_p	Linke's turbidity factor extrapolated to mean sea level

T_λ	Atmospheric transmission of parallel monochromatic solar beam of wavelength λ
w	Precipitable water content of the vertical column of the atmosphere (cm)
WA	Solar energy absorbed by water vapor in the atmosphere ($Btu.ft^{-2}.hr^{-1}$.)
z	Zenith angle of the sun (degrees)
α	Altitude angle of the sun (degrees)
β	Ångstrom's turbidity coefficient
β_p	Ångstrom's turbidity coefficient extrapolated to mean sea level
γ	A wavelength exponent
δ	Declination of the sun (degrees)
ΔIL	Intensity of solar radiation above the longwave cutoff of the filters ($Btu.ft^{-2}hr^{-1}$)
θ	Incidence angle of sun's rays on inclined surface (degrees)
λ	Wavelength (microns)
τ_λ	Monochromatic transmission of the atmosphere in a unit air mass
$\tau_{CO_2}(\lambda)$	Transmission due to carbon dioxide in a unit air mass
$\tau_D(\lambda)$	Transmission due to dust in a unit air mass
$\tau_o(\lambda)$	Transmission due to ozone in a unit air mass
$\tau_R(\tau)$	Transmission due to Rayleigh atmosphere of unit air mass
$\tau_w(\lambda)$	Transmission due to water vapor in a unit air mass
ϕ	Zenith angle of the sun (degrees)

T_λ Atmospheric transmission of parallel monochromatic solar beam of wavelength λ

w Precipitable water content of the vertical column of the atmosphere (cm)

WA Solar energy absorbed by water vapor in the atmosphere ($Btu.ft^{-2}.hr^{-1}$.)

z Zenith angle of the sun (degrees)

α Altitude angle of the sun (degrees)

β Ångstrom's turbidity coefficient

β_p Ångstrom's turbidity coefficient extrapolated to mean sea level

γ A wavelength exponent

δ Declination of the sun (degrees)

ΔIL Intensity of solar radiation above the longwave cutoff of the filters ($Btu.ft^{-2}hr^{-1}$)

θ Incidence angle of sun's rays on inclined surface (degrees)

λ Wavelength (microns)

τ_λ Monochromatic transmission of the atmosphere in a unit air mass

$\tau_{CO_2}(\lambda)$ Transmission due to carbon dioxide in a unit air mass

$\tau_D(\lambda)$ Transmission due to dust in a unit air mass

$\tau_o(\lambda)$ Transmission due to ozone in a unit air mass

$\tau_R(\tau)$ Transmission due to Rayleigh atmosphere of unit air mass

$\tau_w(\lambda)$ Transmission due to water vapor in a unit air mass

ϕ Zenith angle of the sun (degrees)

CHAPTER 1

PRINCIPLES OF SOLAR ENERGY CALCULATIONS

1.1 INTRODUCTION

The sun is one of the main sources of natural energy, and since this energy source is undepleted while most of the other sources of energy are depleting, the utilization of solar energy in as many everyday living applications as possible is desirable. Engineering and scientific problems involved with utilizing solar energy on the earth must be studied, and in many countries research on fundamental and applied topics on harnessing of solar energy in thermal, electrical and chemical processes is expanding.

In solar radiation problems a quantitive knowledge of incident solar energy is needed for all types of solar weather including clear, partly cloudy, and cloudy days. One of the prime requirements is the prediction of the annual variation of solar energy on an oriented surface at any location on the earth's surface. A surface receives the maximum solar energy under clear sky conditions. Thus, an investigation was undertaken to measure and correlate the annual variation in the direct beam solar energy under clear sky conditions that will be received on a surface oriented perpendicular to the sun's rays at Edmonton, Alberta. In addition the distribution of energy within specific wavelength bands of the solar spectrum was also studied.

In sections 1.2 to 1.5 of this chapter, a brief review is given about the nature of the sun (the energy source) and

the earth (the receiver). Also the basic relationships and essential terms required in the calculations are defined. In section 1.6 of this chapter the procedure for collecting data, the basic calculations and specific information about the selected location are presented. In chapter 2 the transmission of the direct solar beam through the earth's atmosphere and the energy carried within the whole spectrum will be studied. Chapter 3 will deal with the filter measurements of solar radiation and the energy distribution in specific wavelength regions reaching the ground. Finally, in chapter 4 the turbidity of the atmosphere and the energy absorbed by the atmospheric water vapor will be determined from the solar radiation measurements. Conclusions are summarized in chapter 5.

1.2 THE SUN AND THE EARTH

1.2.1 THE SUN: One of the stars of the universe. The diameter of the sharp circular boundary of the sun is about 865,400 miles, and its mass is about 332,000 times that of the earth. It is entirely gaseous. Astrophysicists generally divide the structure of the sun into three regions:
i) the interior which is the main mass of the sun is believed to have a central temperature of many millions of degrees and a central gas pressure of perhaps a billion atmospheres. It is here that the sun's energy output is generated. Astrophysicists have established that the sun's main constituent

is hydrogen and it is believed that the sun's energy output occurs from conversion of hydrogen into helium in the presence of carbon and nitrogen.

ii) The photosphere is a thin layer of gas which forms the bright boundary of the sun. Both pressure and density are very low in this layer and the temperature is about 10,000°F. The greatest part of the sun's thermal radiation is emitted from the photosphere.

iii) The solar atmosphere is composed of the chromosphere and corona. Both regions of the solar atmosphere offer little resistance to the sun's radiation output. The chromosphere is a relatively thin layer of gas at extremely low temperature and low density. The corona which is the extremity of the sun, consists of rarified gases which extend beyond the chromosphere for a million miles or more.

1.2.2 THE EARTH: The planet earth is nearly spherical with a diameter of about 7,900 miles. It makes one rotation about its axis every 24 hours and completes an orbit about the sun in a period of 365.25 days approximately. The earth's orbit about the sun is approximately circular, with the sun located slightly off the center of the circle. The earth's mean distance from the sun is about 92,900,000 miles and about January 1, the earth is closest to the sun while about July 1, it is most remote, the variation being 3.3 percent. The earth's axis of rotation is tilted 23.5 degrees with

respect to its orbit plane and is of profound significance, for together with the earth's daily rotation and yearly revolution it accounts for the distribution of solar radiation over the earth's surface, the changing length of hours of daylight and darkness, and the changing of the seasons.

1.3 BASIC EARTH-SUN ANGLES

The zenith angle, altitude angle, azimuth angle and incidence angle are earth-sun angles used in solar calculations. They may be calculated for any location P on the earth's surface if the latitude L and hour angle h for that location, and the sun's declination δ are known. It is convenient to illustrate these angles using the astronomical coordinate systems [27].

The systems of astronomical spherical coordinates are all analogous to the system of latitudes and longitudes on the earth. The most important difference being that the earth is viewed from the outside and the celestial sphere which is a fictitous sphere of indeterminate radius, with its center at the observer, and the sun is imagined to be projected on the inside surface of it is viewed from the inside. Every such system contains two diametrically opposite poles, a north pole and a south pole, the north pole being the one that is visible from the north pole of the earth. There is a primary circle, which is a great circle of the sphere, so

placed that each pole is 90 degrees from it. The latitudinal coordinate of an object is its angular distance measured northward or southward from the primary circle. The longitudinal coordinate of an object is the angular distance measured along the primary circle from a specified origin to the point of intersection with a great circle passing through the object and the two poles. Three basic systems, the terrestrial system, and the two astronomical systems most used for locating the sun (the equatorial system and the horizon system), are compared in table 1.1. The equatorial system, Fig. 1.1, is the geometrical extension of the terrestrial system. The horizon system shown in Fig. 1.2 is fixed relative to the observer.

Now it is easy to define the three basic angles, the latitude L, the local hour angle h, and the sun's declination δ. Figure 1.3 illustrates these angles.

1.3.1 LATITUDE,L: The angular distance of the point P north or south of the earth's equator.

1.3.2 HOUR ANGLE, h: The angle through which the earth must turn to bring the meridian of P directly in line with the sun's rays. At solar noon the hour angle is zero. The hour angle is measured on either side of solar noon and one hour of time equals 360/24 or 15 degrees of earth's rotation.

TABLE 1.1 Comparison of the terrestrial, the equatorial, and the horizon systems.

The name of the system	The Poles of the system	The primary circle	The latitudinal coordinate	The longitudinal coordinate	The origin of the longit. coordinate
Terrestrial	The poles of the rotation of the earth	The equator	latitude	longitude	The meridian[1] of Greenwich.
Equatorial	The intersections of the earth's axis of rotation with the celestial sphere	The celestial equator	declination	hour angle	The intersection of the celestial equator with the observer's celectial meridian[2].
Horizon	zenith[3] and the nadir	The horizon	altitude or zenith[4]	azimuth	The north point of the horizon.

(1) The terrestrial meridian is that half of a great circle on earth that passes through points having the same longitude and terminates at the north and south poles.

TABLE 1.1
(continued)

(2) The celestial meridian is a great circle on the celestial sphere passing through the two celestial poles and the observer's zenith.

(3) The zenith is the point directly overhead.

(4) The altitudinal coordinate is latitude if it is measured from the horizon or zenith if it is measured downward from the zenith.

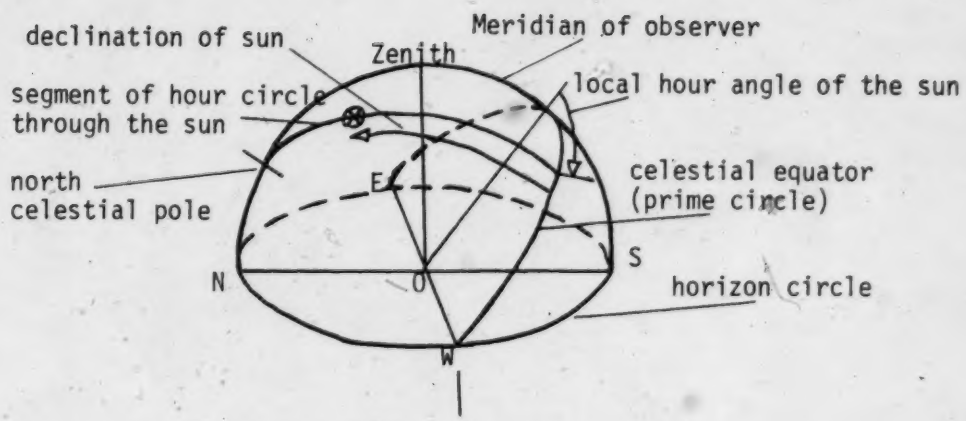

Figure 1.1 Equatorial astronomical coordinate system.

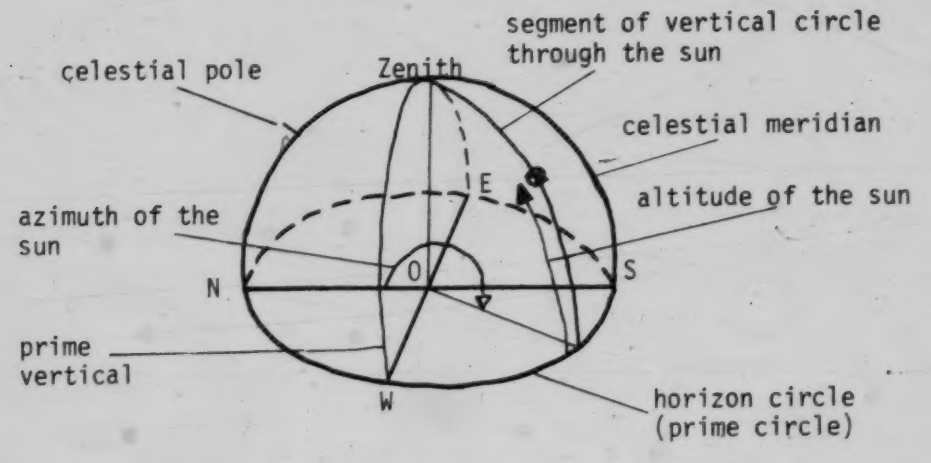

Figure 1.2 Horizon system of astronomical coordinates.

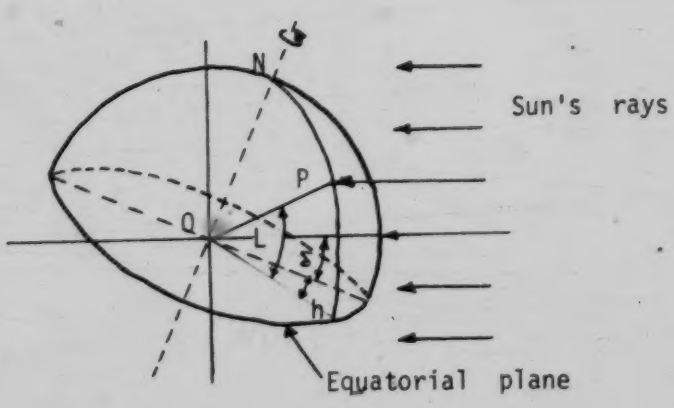

Figure 1.3 Illustration of the three basic earth-sun angles; Latitude L, Hour angle h and Declination δ.

1.3.3 DECLINATION, δ: The sun's declination is the angular distance of the sun north or south of the celestial equator. The tilt of the earth's axis is the direct cause of the sun declination. The sun's declination would be 23.5 degrees south of the equator at the winter solstice, 23.5 degrees north of the equator at the summer solstice, and at the equinoxes, the declination is zero. Because the period of the earth's complete revolution about the sun does not coincide exactly with a calendar year, the declination varies slightly for the same day from year to year. A declination formula is given by [14]:

$$\delta = 23.45 \sin[(360/365)(284 + n)]$$

where n is the day of the year measured from January 1. The sun's declination may be obtained from Solar Ephemeris Publications [22].

1.3.4 DERIVED SOLAR ANGLES: With the sun's declination δ, the hour angle h, and the latitude L for a specific locality known, the sun's zenith z, altitude α, azimth angle ϕ and incidence angle θ can be calculated using the following equations:

$$\cos z = \cos L \cdot \cos h \cdot \cos \delta + \sin L \cdot \sin \delta \quad (1.1)$$

Since the altitude angle $\alpha = (\pi/2)$ - the zenith angle z

therefore, $\sin \alpha = \cos L \cdot \cos h \cdot \cos \delta + \sin L \cdot \sin \delta \quad (1.2)$

and the azimuth angle ϕ, measured from south is given by

$$\cos \phi = \sec \alpha \ (\cos L \cdot \sin \delta - \cos \delta \cdot \sin L \cdot \cos h) \qquad (1.3)$$

In applying equations 1.1 to 1.3 north latitudes are considered positive and south latitudes negative. The declination will be positive for the summer period between the vernal equinox and autumnal equinox (March 22 to September 22 approximately) and negative at other times. The hour angle in degrees is measured on either side of solar noon. Thus h is limited to values between zero and π. If $h < \pi/2$, cos h is positive and if $h > \pi/2$, cos h is negative.

For a particular surface orientation the sun's incidence angle θ is given by:

$$\cos \theta = \cos i \cdot \sin \alpha + \sin i \cdot \cos \alpha \cdot \cos(\phi - s)$$

where: i is the inclination angle of the surface under consideration, and is expressed in degrees from the horizontal, and

s is the aspect of the surface, and is expressed in degrees from the south with a westerly component being positive.

For example a vertical east facing surface would have an inclination angle of 90 degrees and an aspect of -90 degrees.

The solar angles z, α, ϕ, the incidence angle θ and the surface angles i and s can be defined through the geometrical relationships between the sun and the horizontal plane and the inclined surface at the point of observation on the ground. Figure 1.4 illustrates these angles. The three reference axes are Z(vertical), W(west) and S(south) and P is the point of observation, then by definition

Line AP is the sun's ray

Line BP is the projection of the sun's ray on the horizontal plane

Line CP is the normal to the inclined surface

Line DP is the projection of the normal to the inclined surface on the horizontal plane.

Sun altitude angle, α: the angle in the vertical plane between the sun's ray and the projection of the sun's ray on the horizontal plane (angle APB),

Sun zenith angle z: the angle between the sun's rays and a line perpendicular to the horizontal plane (angle APZ),

Sun azimuth angle, ϕ: the angle in the horizontal plane measured from south to the horizontal projection of the sun's rays, in the northern hemisphere, (angle BPS),

Incident angle, θ: the angle between the sun's rays and the normal to the surface (angle APC),

Surface inclination angle, i, is measured from the horizontal plane.

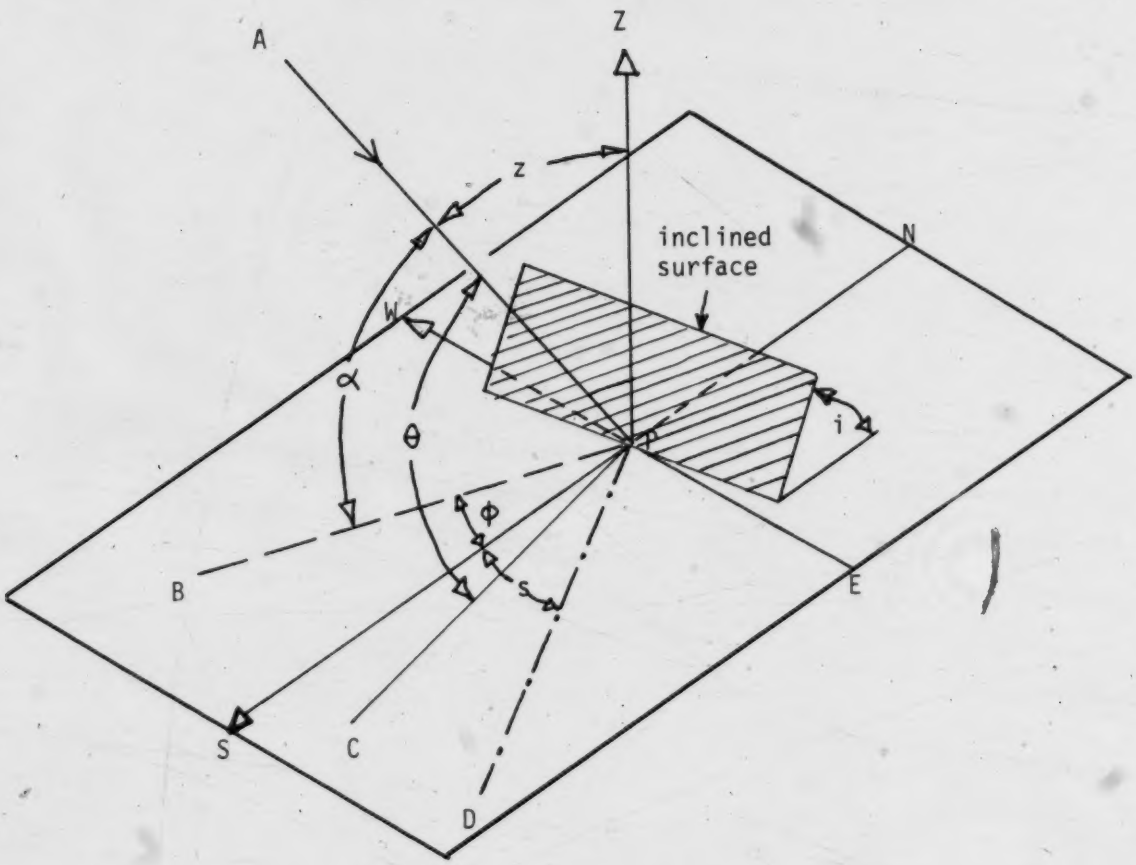

Figure 1.4 Illustration of solar angles.

Surface azimuth angle, s (also known as the aspect of the surface): It is the angle in the horizontal plane measured from south to the horizontal projection of the normal line to the surface (angle DPS).

1.4 SOLAR TIME

Solar radiation calculations must be made in terms of solar time, usually with respect to solar noon which occurs with the sun at the zenith for the station meridian. In order to calculate mean solar noon from true solar noon some terms should be clearly defined.

1.4.1 TRUE SOLAR TIME, TST: The time that would be shown by a sun dial, or it is the hour angle of the sun and it is measured by the diurnal motion of the sun. An apparent solar day at any place is the interval of time between two successive transits of the sun over the meridian of that place, with the transit from midnight to midnight as being more adaptable to the civil day. True solar time is the known angle of the sun plus 12 hours. Whereas a civil day is precisely 24 hours, a true solar day is slightly different due to irregularities of the earth's rotation, obliquity of the earth's orbit and other factors.

1.4.2 MEAN SOLAR TIME, MST: It is measured by the diurnal motion of a fictitious body called the mean sun, which

is supposed to move uniformly in the celestial equator, completing the circuit in one tropical year. A mean solar day at any place is the interval of time between two successive transits of the mean sun over the meridian of that place. Since mean solar time is uniform and regular in its passage, clocks and watches are regulated to it. Mean solar time is called civil time.

1.4.3 THE EQUATION OF TIME, ET: The equation of time is the difference in hour angle between true sun and mean sun, or it is the quantity added to mean solar time to obtain true solar time. The true sun is sometimes ahead and sometimes behind the mean sun by an amount which varies from zero to about 16 minutes.

$$TST = MST + ET \tag{1.4}$$

1.4.4 GREENWICH CIVIL TIME, GCT: Time reckoned from midnight at the greenwich meridian (zero longitude) is known as Greenwich civil time or universal time. Such time is expressed on an hour scale from zero to 24. Thus, midnight is 0 and noon is 12.

1.4.5 LOCAL CIVIL TIME, LCT: The mean solar time reckoned from the precise longitude of the observer. At the same instant, LCT is more advanced by four minutes for each degree difference in longitude east of Greenwich meridian and

is less advanced by four minutes for each degree difference in longitude west of Greenwich.

1.4.6 ZONE AND STANDARD TIMES, ZST: To avoid the inconvenience of the continuous change of mean solar time with longitude, zone time or civil time is used. The earth is divided into 24 zones each approximately 15 degrees wide, and centered on standard longitudes 0, 15, 30 and so on until 180 degrees east and west of Greenwich. Within each of these zones the clock time is the same for all locations of the zone and is kept at the mean solar time of the standard meridian.

Now the true solar time TST at any instant at any location on the earth's surface of longitude G can be computed from equation 1.4, substituting for MST as follows:

$$\begin{aligned} TST &= MST + ET \\ &= LCT + ET \\ &= ZST + (GS - G) * 4 + ET \end{aligned} \qquad (1.5)$$

where GS is the longitude of the standard meridian of the zone including that location. The values of ET can be obtained from Nautical Almanac or Solar Ephemeris publications.

1.5 THE SOLAR CONSTANT, THE SOLAR SPECTRAL IRRADIANCE AND THE AIR MASS:

1.5.1 THE SOLAR CONSTANT, I_o: The total solar energy received per unit time per unit area exposed normally to the sun's rays at the mean sun-earth distance in the absence of the terrestrial atmosphere.

The value of the solar constant which had been proposed by F.S. Johnson in 1954 [21] is 442 Btu $ft^{-2}hr^{-1}$ (2 cal $cm^{-2}min^{-1}$). Recently a new value of 429 Btu ft^{-2} hr^{-1} (1.94 cal cm^{-2} hr^{-1}) has been proposed for the solar constant [33]. This is 3% lower than the Johnson value.

1.5.2 SOLAR SPECTRAL IRRADIANCE: The distribution of the solar constant as a function of wavelength. The spectrum of the sun extends from x-rays of wavelength 1 Angström or less to radio emission of wavelength 100 meters and more. However, the wavelength range 0.275 to 4.95μm contains 99% of the energy and 99.9% is within the range 0.220 to 11.8μm. The proposed standard for zero air mass solar spectral irradiance which is presented in reference [33] was used in this research.

1.5.3 THE AIR MASS, m: The air mass is the ratio of the length of the path of the sun's rays through the atmosphere to the length of the path when the sun is at the zenith. In solar radiation calculations, unit depth of the atmosphere is

taken as the depth when the sun is at the zenith for sea level.

For solar altitude angles greater than or equal to 20 degrees, the air mass is equal to the cosecant of the altitude angle α:

$$\text{Air mass} = 1/\sin\alpha, \qquad \alpha \geq 20 \text{ degrees} \tag{1.6}$$

Below 20 degrees a more accurate method should be used and the formula proposed by Robinson for calculating the air mass of a homogeneous spherical atmosphere is often used [27]. It is given by:

$$\text{Air mass} = [(r/H \cdot \sin\alpha)^2 + 2(r/H) + 1]^{\frac{1}{2}} - r/H \cdot \sin\alpha \tag{1.7}$$

Where r is the radius of the earth, $H = P_o/\rho_o g$

Where P_o is the pressure of the earth's surface (sea level), and ρ_o is the density at the earth's surface. On substituting P_o = 760 mm Hg and ρ_o corresponding to the temperature of 273°K, it is found that H = 7.991 km.

The air mass calculated from equation 1.6 or 1.7 is the relative optical air mass m_h. The absolute optical air mass m can then be computed using the relation:

$$m = m_h \cdot P/p_o \tag{1.8}$$

where p is the surface pressure at the place and time of observation.

1.6 DATA AND COMPUTATIONS

The data in this study are the values of the normal incidence insolation and the insolation passing the RG2 and RG8 filters measured by Eppley normal incidence pyrheliometers under clear sky conditions. The Pyrheliometers are mounted on the roof of the Mechanical Engineering building of the University of Alberta campus at Edmonton, Alberta and the output is recorded by a strip chart recorder. A continuous record is available during the months of April to September, but only a partial record is available during the months of October to March. Clear sky conditions during both forenoon and afternoon are difficult to obtain in the region as there is a tendency for a clear sky during the forenoon, but light fluffy clouds often appear just before solar noon and these may remain for the rest of the day [28]. About 200 days were chosen from a 4-year period, (1972 to 1975), with about 70% of them during the months of May to September. The days selected showed a high value of normal incident insolation at midday, and a symmetrical shape for forenoon and afternoon. Whenever possible, full day data was used in the analysis but, due to infrequency of occurrence, these days were supplemented by half-day data, and part-day data that were deemed to be clear sky conditions.

The sun crosses the local meridian at local apparent noon each day, i.e. the local hour angle is zero and the true solar time is 12. Edmonton (113° 31'W and 53° 34'N) is

included in the zone with a standard meridian of 105°W and the local standard time, LST, corresponding to the true Solar noon on any given day was computed from equation 1.8 as follows:

$$12 = LST + [4\cdot(105° - 113° 31') + ET]/60$$

$$LST = 12 + (34.08 - ET)/60 \qquad (1.9)$$

This means that on any given day when the sun crosses the local meridian at Edmonton, the local clock indicates 12 hour and 34.08 - ET minutes. In other words, the true solar time lags the local standard time by 34.08 - ET minutes. The values of the equation of time ET substituted in equation 1.9 were obtained from Solar Ephemeris [22] and the chart records were adjusted to true solar time. The readings were taken from the charts every 15 minutes whenever it was possible, starting from solar noon as hour angle zero till hour angle 6 for both forenoon and afternoon periods during the months of April to September and to hour angle 4 during the rest of the year. These values were entered on computer cards and the quantities of the solar energy were computed for normal incidence insolation and insolation passing the RG2 and RG8 filters. It was found that the data showed only a small change during any 15-minute interval, so, only the values at the exact hour angle from 0 to 6 were used in most of the analysis. The remaining data was utilized to augment the material for certain calculations especially when the best

fit was obtained by the computer.

For each day the altitude of the sun was calculated every 15 minutes from equation 1.2 using the declination values published in Solar Ephemeris [22]. The corresponding relative optical air mass (termed hereinafter as relative air mass) was calculated using equations 1.6 and 1.7, then corrected to absolute optical air mass (termed hereinafter as optical air mass) according to equation 1.8. For this correction the average daily pressure values for forenoon and afternoon were obtained from Upper Air Bulletins [11]. In these Bulletins pressure values are published for Stony Plain, Alberta (776 meters above mean sea level) and a correction for elevation level was applied to get the pressure at Edmonton (668 meters above mean sea level).

For some calculations, it was necessary to reduce the measured values of the solar insolation to the mean distance R_o between the sun and the earth by multiplication by the factor $(R_i/R_o)^2$, obtained from the tables published in Nautical Almanac [25], where R_i is the earth-sun distance at time of observation.

CHAPTER 2

CLEAR SKY DIRECT NORMAL INCIDENCE SOLAR RADIATION

2.1 SOLAR EXTRATERRESTRIAL RADIATION

The extraterrestrial solar radiation at normal incidence at any instant, I_{0i}, will differ from the solar constant, I_0, because of the variation in the earth-to-sun distance throughout the year. This results in a maximum variation of irradiation of ±3.5 percent. To obtain I_{0i} the solar constant should be multiplied by the factor $(R_0/R_i)^2$. On January 1 the value of I_{0i} is 7 percent higher than on July 1.

The solar radiation is depleted as it penetrates the earth's atmosphere. The intensity of the direct beam received at the earth's surface depends upon the path length traversed by the sun rays. The length of the path through the atmosphere depends on the solar declination, the time of the day, and the location on the earth's surface. The extent to which any particular air mass depletes the sun rays depends on the components of the earth's atmosphere.

2.2 ATMOSPHERIC EFFECTS ON EXTRATERRESTRIAL ENERGY

Scientific studies of the effects of the earth's atmosphere upon solar radiation has shown that, in general, the atmospheric elements absorb and scatter part of the incident solar energy. Scattering may be accomplished by dry gas molecules (nitrogen, oxygen, and other molecular components of the atmosphere), by dust, aerosols and water droplets. Small amounts of many substances absorb solar energy, but the

principal absorbing mediums are ozone, water vapor, carbon dioxide, and cloud particles.

The remaining portion of the original direct radiation may reach the earth's surface unchanged in wavelength and is known as the direct solar radiation or normal incidence insolation. A portion of the scattered energy will return to space, but some of it also reaches the earth's surface as diffused radiation. It comes from the entire sky vault and therefore is usually termed diffuse sky radiation. On clear days (cloudless sky), diffuse sky radiation is small compared to direct solar radiation but during extremely cloudy days, only diffuse radiation may reach the ground. In general a surface on the earth receives solar energy associated with radiation of two forms; direct radiation and diffuse radiation. This research is concerned with the incidence of direct solar radiation on clear days (cloudless sky).

2.3 EXTINCTION OF SOLAR RADIATION AND ATMOSPHERIC TRANSMISSION FACTOR

The intensity I_λ of parallel monochromatic energy transmitted through the earth's cloudless atmosphere is given by [27]

$$I_\lambda = I_{0\lambda}\, e^{-A_\lambda \cdot m} \tag{2.1}$$

where A_λ is the monochromatic extinction coefficient,

m is the optical air mass,

$I_{0\lambda}$ is the intensity of parallel monochromatic beam of wavelength λ outside the atmosphere, air mass zero,

I_{λ} is the intensity of the parallel beam at the ground.

The atmospheric transmission T_{λ} of a parallel monochromatic beam of wavelength λ through the atmosphere gives the fraction of energy incident outside the earth's atmosphere (air mass zero) which penetrates the atmosphere to the earth's surface along optical air mass m. From equation 2.1 it is given by:

$$T_{\lambda} = \frac{I_{\lambda}}{I_{0\lambda}} = e^{-A_{\lambda} \cdot m} \tag{2.2}$$

$$= \tau_{\lambda}^{m} \tag{2.3}$$

where τ_{λ} is the monochromatic transmittance with the sun in the zenith i-e for unit air mass.

Several investigators have treated the monochromatic extinction coefficient A_{λ} in different ways, but as a compromise, it includes the effect of both scattering and absorption. They all have considered scattering due to main scattering agents in the atmosphere, dry gas molecules, dust and water vapor. Also they agreed that absorption is mainly by ozone, and water vapor in absence of clouds. On these bases the extinction coefficient A_{λ} can be written to

represent the sum of four parameters as follows:

$$A_\lambda = a_R(\lambda) + a_D(\lambda) + a_W(\lambda) + a_0(\lambda) \qquad (2.4)$$

where $a_R(\lambda)$ is the extinction coefficient for clean dry air and it accounts for scattering by air molecules according to Rayleigh's theory,

$a_D(\lambda)$ is the extinction coefficient of the atmospheric dust. It represents extinction due to turbidity of the atmosphere, taking into account scattering and absorption due to dust as well as scattering by water vapor in the atmosphere,

$a_W(\lambda)$ is the coefficient of absorption by the water vapor contained in the atmosphere, and

$a_0(\lambda)$ is the extinction coefficient due to ozone.

There is rarely more than 0.4 centimeters of ozone in the vertical column of the atmosphere and it is concentrated mainly at elevations between 15 and 35 kilometers above the ground. Yet the absorption coefficient of ozone is so large that the spectrum of solar energy at the ground is cut off below 0.29 micron. Therefore, from the view point of utilization of solar energy near the ground our attention is found on wavelengths longer than 0.29 micron. Then equation 2.4 can be written as:

$$A_\lambda = a_R(\lambda) + a_D(\lambda) + a_W(\lambda) \qquad (2.5)$$

The calculation of the extinction coefficients in equation 2.4 is illustrated in reference [12]. The extinction due to atmospheric turbidity, dust, and absorption by water vapor in the atmosphere will be discussed in chapter 4.

If equation 2.1 is integrated over all the solar spectrum and the factor $(R_0/R_i)^2$ is used, the basic relation for the extinction of solar radiation through the earth's atmosphere may be written as:

$$I = (R_0/R_i)^2 \int_0^\infty I_0(\lambda)\, e^{-A(\lambda)\cdot m}\, d\lambda \qquad (2.6)$$

where R_0 is the mean earth-sun distance,

R_i is the earth-sun distance at time of observation,

$I_0(\lambda)$ is the solar constant as a function of the wavelength λ,

I is the intensity of the direct solar radiation at the earth's surface,

m is the optical air mass, and

$A(\lambda)$ is the extinction coefficient and it is composed of four components depending on the wavelength λ as it is given in equation 2.4.

2.3.1 TRANSMISSION COEFFICIENT OR ATMOSPHERIC TRANSMISSION FACTOR FOR DIRECT SOLAR RADIATION:

This is defined as the fraction of the energy outside the

earth's atmosphere that is received at the earth's surface as normal incidence radiation. Therefore it is the result of the integration of equation 2.6 at certain air mass divided by the extraterrestrial radiation at air mass zero.

2.4 APPARENT SOLAR INSOLATION AT AIR MASS ZERO AND APPARENT ATMOSPHERIC EXTINCTION COEFFICIENT

Although equation 2.1 is theoretically applicable only for monochromatic radiation, it is suggested to be applicable for the total direct solar radiation in the method proposed by the American Society of Heating, Refrigerating, and Air Conditioning Engineers [1] of expressing solar energy quantities. This method represents the solar insolation at the earth's surface, under clear sky conditions, as a function of the apparent solar insolation at air mass zero, I^*, and the atmospheric extinction coefficient, A. The normal direct incidence insolation is represented by the equation:

$$I = I^* e^{-A \cdot m} \tag{2.7}$$

where I is irradiation on a plane normal to the solar beam at the ground,

I^* is the apparent solar irradiation at air mass zero, or the apparent solar constant,

A is the apparent extinction coefficient, and

m is the optical air mass.

The logarithm of equation 2.7 yields a straight line relationship between I and m and when plotted on semi logarithmic paper, has an intercept equal to I^* and the slope equal to A.

This method implies that the atmospheric extinction coefficient does not vary over the wavelength and also is constant during the period of measurements. To the extent that this is not practically true, equation 2.1 when applied to experimental data of the total direct solar spectrum, results in an ordinate I^* which is less than the solar constant I_0. The error introduced by applying this method is difficult to estimate. However, if the extinction coefficient does not have a large variation over the wavelength regions that contain the major portion of the solar energy, equation 2.7 will give results that can be used with sufficient accuracy for most design situations [28]. The values of I^* and A in equation 2.7 vary during the year because of seasonal changes in the dust and water vapor content of the atmosphere, and also because of the changing earth-sun distance.

The high altitude solar irradiance measurement from an air craft [32] indicate that the plot of the logarithm of normal incidence versus air mass produces a curve which is concaved up rather than a straight line. Measurements at ground level tend to support this curvature. Although the

curvature is small, representing the curve by a best fit straight line over a certain air mass range will give a different value of I^* and A than if the fit is taken over a different air mass range. Thus in using the straight line extrapolation to zero air mass method the value of I^* and A is influenced by the air mass range used in the computation and the local atmospheric conditions. Consideration should be given to the air mass range used in the calculation when comparing different stations' results or even different results at the same station.

2.5 MEASUREMENT OF THE APPARENT SOLAR CONSTANT AND THE APPARENT EXTINCTION COEFFICIENT AT EDMONTON, ALBERTA, CANADA

Taking the natural logarithm of equation 2.7 results in the straight line relationship

$$\ln (I) = -A \cdot m + \ln(I^*) \qquad (2.8)$$

which has a negative slope of magnitude A, and an ordinate value of $\ln(I^*)$ at air mass zero.

The annual variation at Edmonton, of apparent solar insolation at air mass zero, I^*, and the apparent extinction coefficient, A, were calculated using equation 2.8. About 80 of the clearest days in the period between May 1972 and September 1975 were selected for analysis. The criteria for

selection were: (1) high I value at solar noon, (2) close symmetrical shape for morning and afternoon and (3) full day data supplemented by half day data. The days that were selected represent all seasons, but there were more days in the months May to September than the remaining months. This may be a result of the short-term record or it may indicate that the frequency of clear sky is higher in the period May to September. For each selected day the measured values of the normal incidence insolation, IDN, were prepared at hour-angle 0, 1 and at successive 15-minute intervals thereafter till hour-angle 6 for the months of April to September and to hour-angle 4 for the months of October to March. The corresponding values of the optical air mass were computed as described in section 1.6. About 16 to 22 data points were available for each day (for each forenoon and afternoon) during the months of April to September, but only 8 to 16 data points for each day during the other months. The air mass and insolation values were entered on cards and the best straight line for equation 2.8 was fitted by computer, using a least squares technique. A separate line was calculated for each forenoon and afternoon and the calculations were cut off at air mass 8.

The resulting values for the apparent extinction coefficient A, and the apparent solar insolation at air mass zero I^* are presented in figures 2.1 and 2.2 respectively. The solid curves were fitted by eye through the data points to

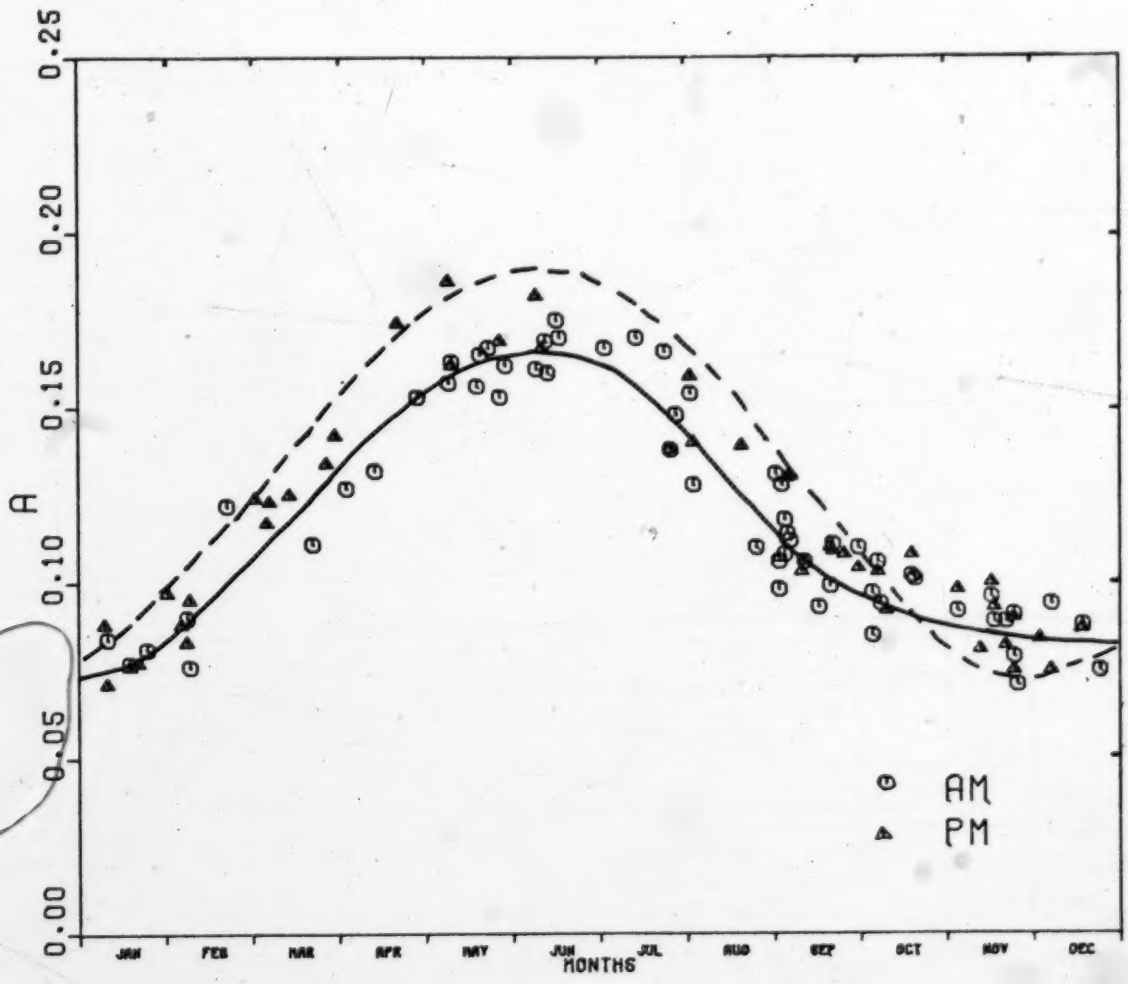

FIGURE 2.1 ANNUAL VARIATION OF THE APPARENT EXTINCTION COEFFICIENT ,A, MEASURED AT EDMONTON.

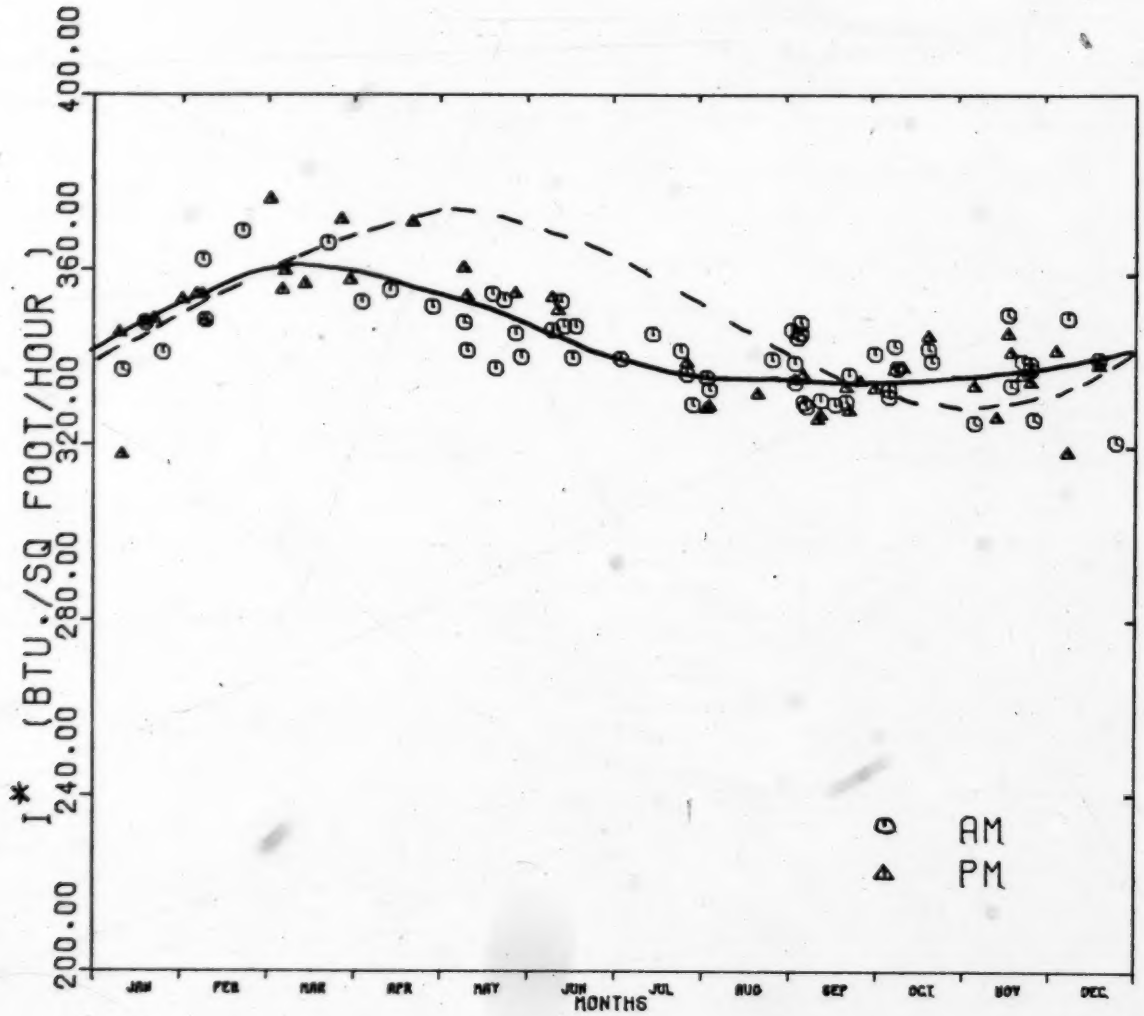

FIGURE 2.2 ANNUAL VARIATION OF THE APPARENT SOLAR INSOLATION AT AIR MASS ZERO ,I^*, MEASURED AT EDMONTON.

show the annual variation of both A and I^*.

A similar study was done by Sadler [28] at the same location using data for the period 1965-1968. He represented the annual variation of the apparent extinction coefficient, A, and the apparent solar insolation at air mass zero, I^*, by the following two periodic curves, respectively:

$$A = 0.134 + 0.056 \cos[360(n - 155)/365] \quad (2.9)$$

$$I^* = 351.4 + 21.0 \cos[360(n - 130)/365] \quad (2.10)$$

where n = day of year measured from 1 January. These periodic curves are shown as broken lines on figures 2.1 and 2.2

Table 2.1 lists the average values for A and I^* obtained from the periodic curves and from the present study for each month of the year. In general, a good agreement seems to exist between the two studies. However, the present results show about 5% lower values for I^* for the months April to August inclusive. A better agreement appears for the rest of the year. Comparing values for A, the present study shows slightly lower values for January through September and slightly higher values for October through December.

TABLE 2.1 Comparison between Sadler's and present monthly average values for A and I^* obtained at Edmonton.

Month	A		I^*, Btu.ft^{-2}.hr^{-1}.	
	Sadler	Present	Sadler	Present
January	0.096	0.085	345	342
February	0.123	0.103	356	356
March	0.149	0.125	365	363
April	0.174	0.152	371	353
May	0.188	0.164	372	350
June	0.188	0.171	367	347
July	0.172	0.152	358	340
August	0.146	0.141	347	330
September	0.117	0.110	337	335
October	0.092	0.100	331	334
November	0.079	0.087	331	334
December	0.080	0.083	335	336

2.6 ANNUAL VARIATION OF THE DIRECT SOLAR RADIATION AT NORMAL INCIDENCE, IDN, AT VARIOUS HOUR ANGLES AS MEASURED AT EDMONTON

The serial hourly values of the clear sky direct normal

incidence, IDN, solar radiation measured at Edmonton were made available in computer form as described in section 1.6. Figures 2.3 to 2.9 show these values in $Btu \cdot ft^{-2} \cdot hr^{-1}$ for hour angles zero to six throughout the year. The curves in these figures were best fitted by eye to show the approximate annual variation of IDN. Figure 2.10 depicts all seven curves on one graph for visual comparison. The annual variation at all hour angles shown is partly because of the variation of the earth-sun distance throughout the year, and because of seasonal change in the dust and water vapor content of the atmosphere. Dust and water vapor are the major factors attenuating solar radiation on its path through the atmosphere.

In Figure 2.10, at hour angle zero (solar noon) the intensity of the direct normal incidence radiation shows a slight variation from March through September. The maximum occurs in March and April. The lower values of IDN from October to February are primarily due to the longer path through the atmosphere. The curves at hour angles one and two are similar and close to the solar noon curve because of the small change in the path lengths for hour angles zero, one and two. At hour angles 3, 4, 5 and 6 the maximum energy is available during May to August. The available energy decreases rapidly in the other months due to rapid increases in the path length of the direct radiation through the atmosphere. The difference between the energy measured at two consecutive hours increases after hour angle two for any

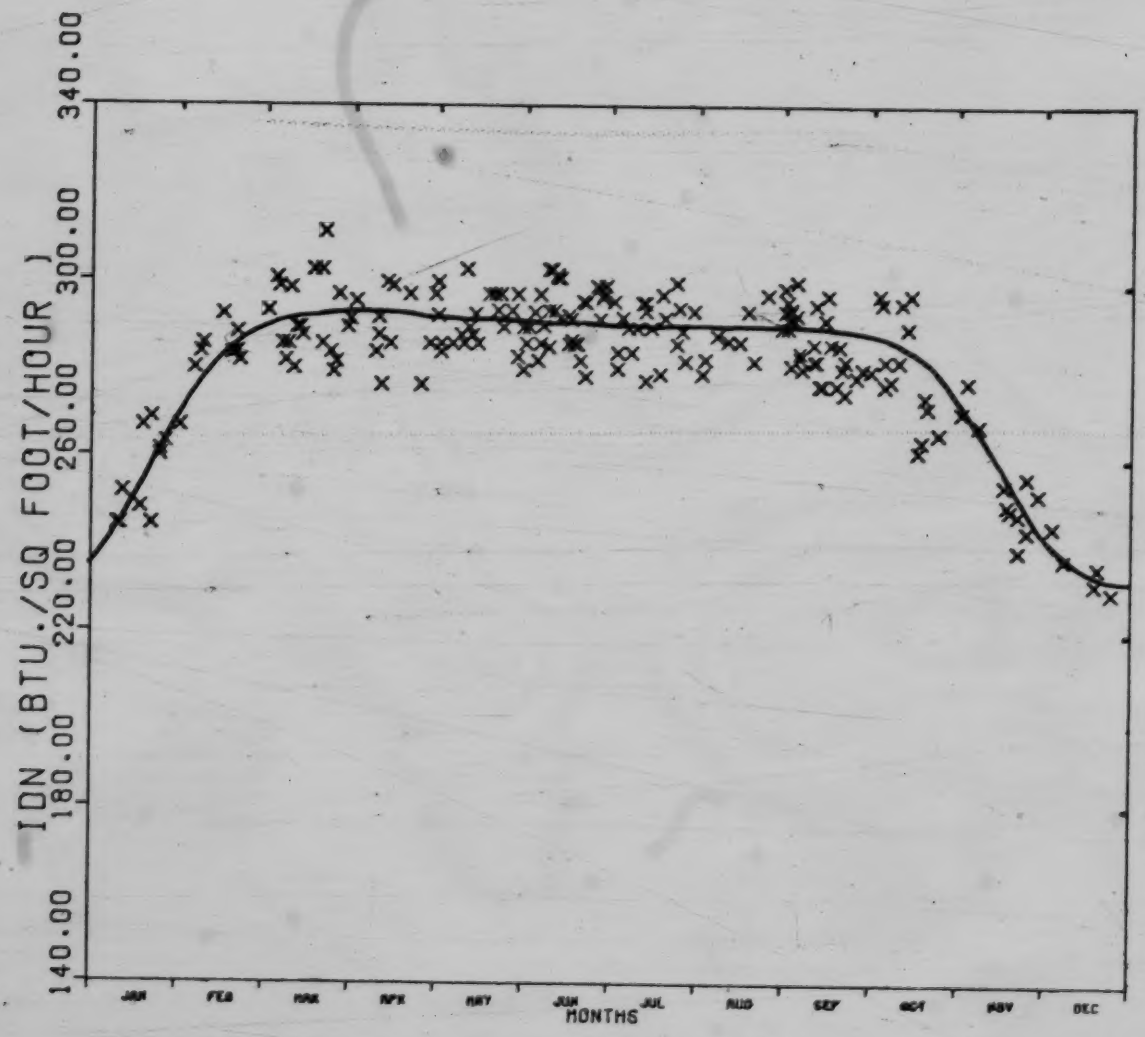

FIGURE 2.3 ANNUAL VARIATION OF THE CLEAR SKY DIRECT NORMAL INCIDENCE SOLAR RADIATION ,IDN, MEASURED AT EDMONTON AT HOUR ANGLE ZERO .

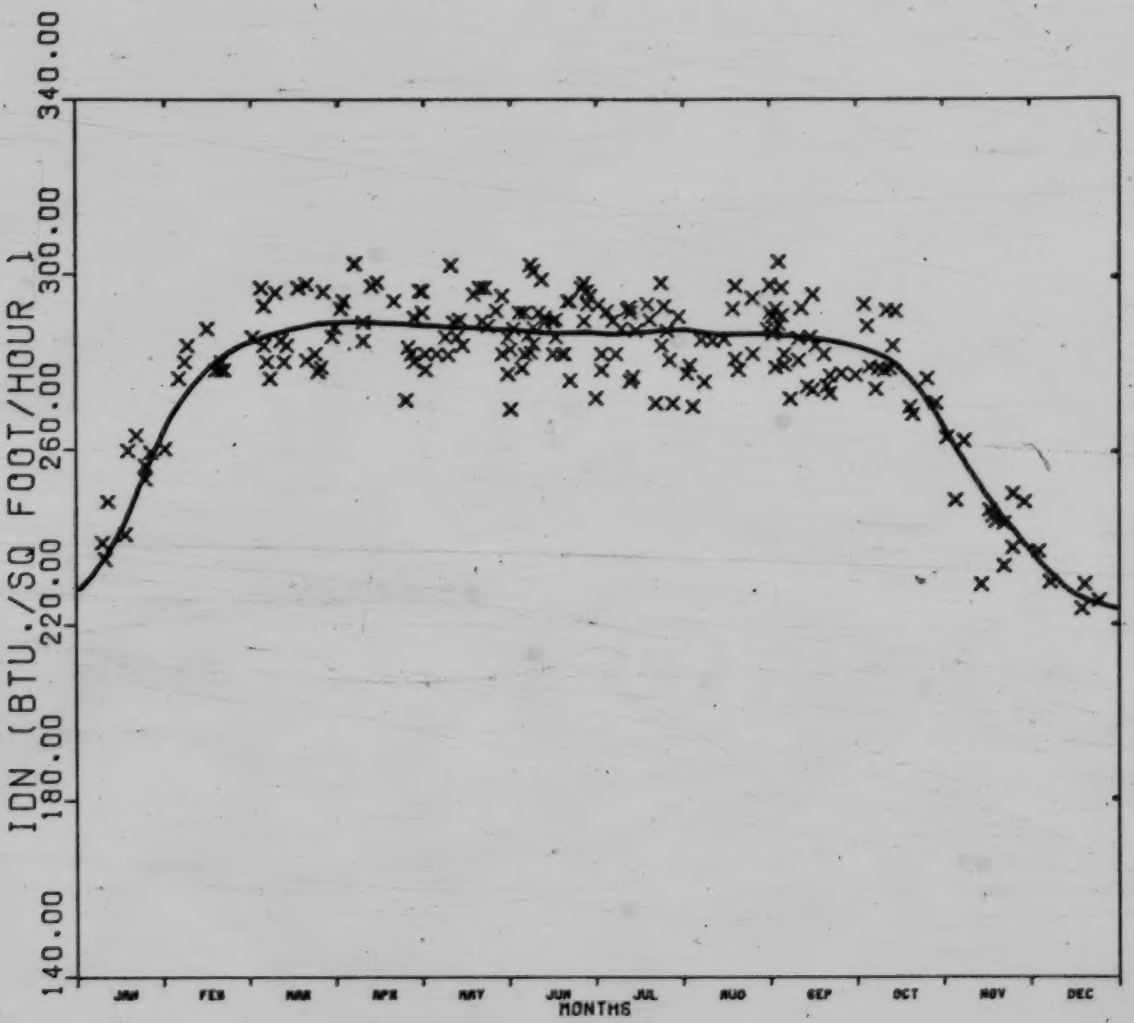

FIGURE 2.4 ANNUAL VARIATION OF THE CLEAR SKY DIRECT NORMAL INCIDENCE SOLAR RADIATION ,IDN, MEASURED AT EDMONTON AT HOUR ANGLE 1 .

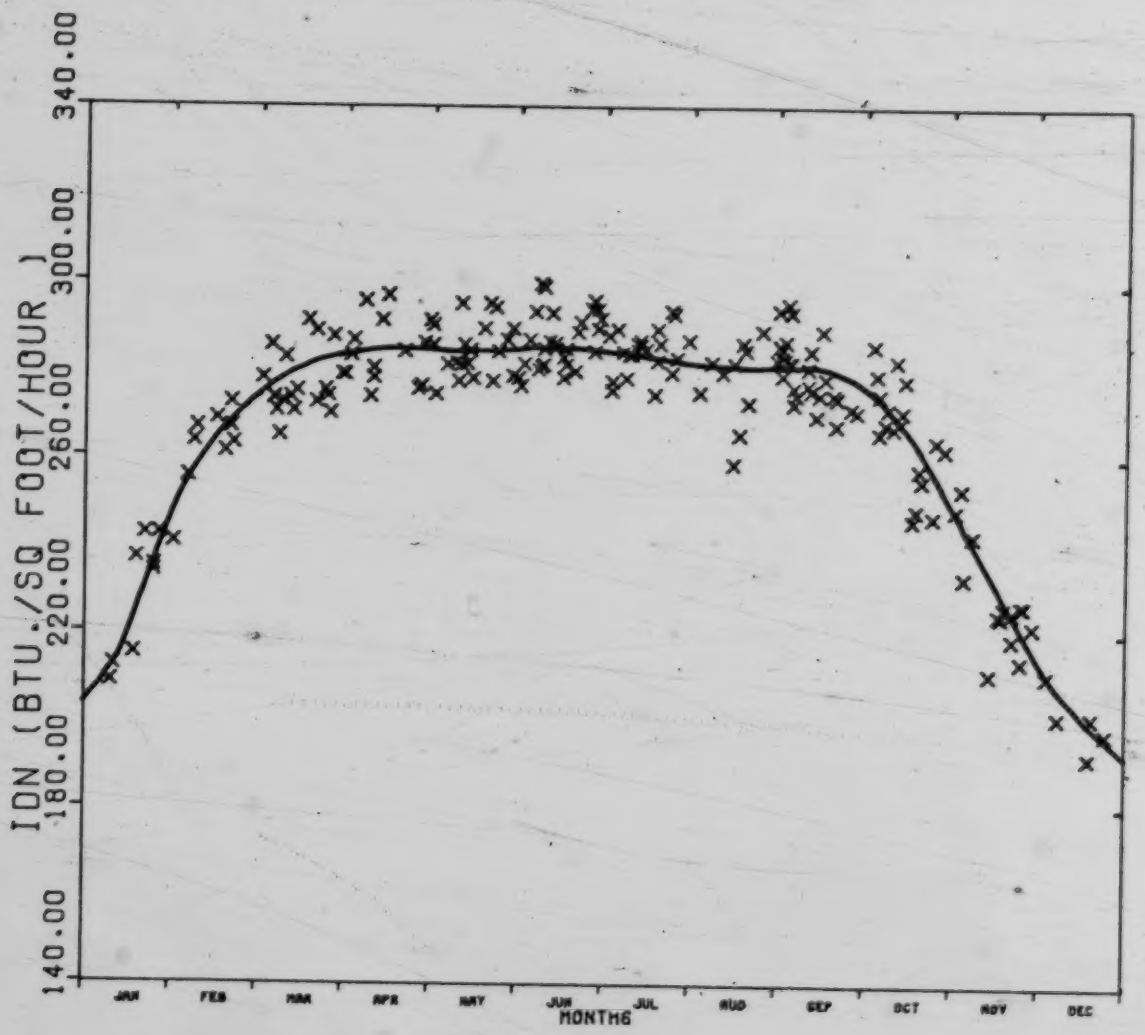

FIGURE 2.5 ANNUAL VARIATION OF THE CLEAR SKY DIRECT NORMAL INCIDENCE SOLAR RADIATION ,IDN, MEASURED AT EDMONTON AT HOUR ANGLE 2.

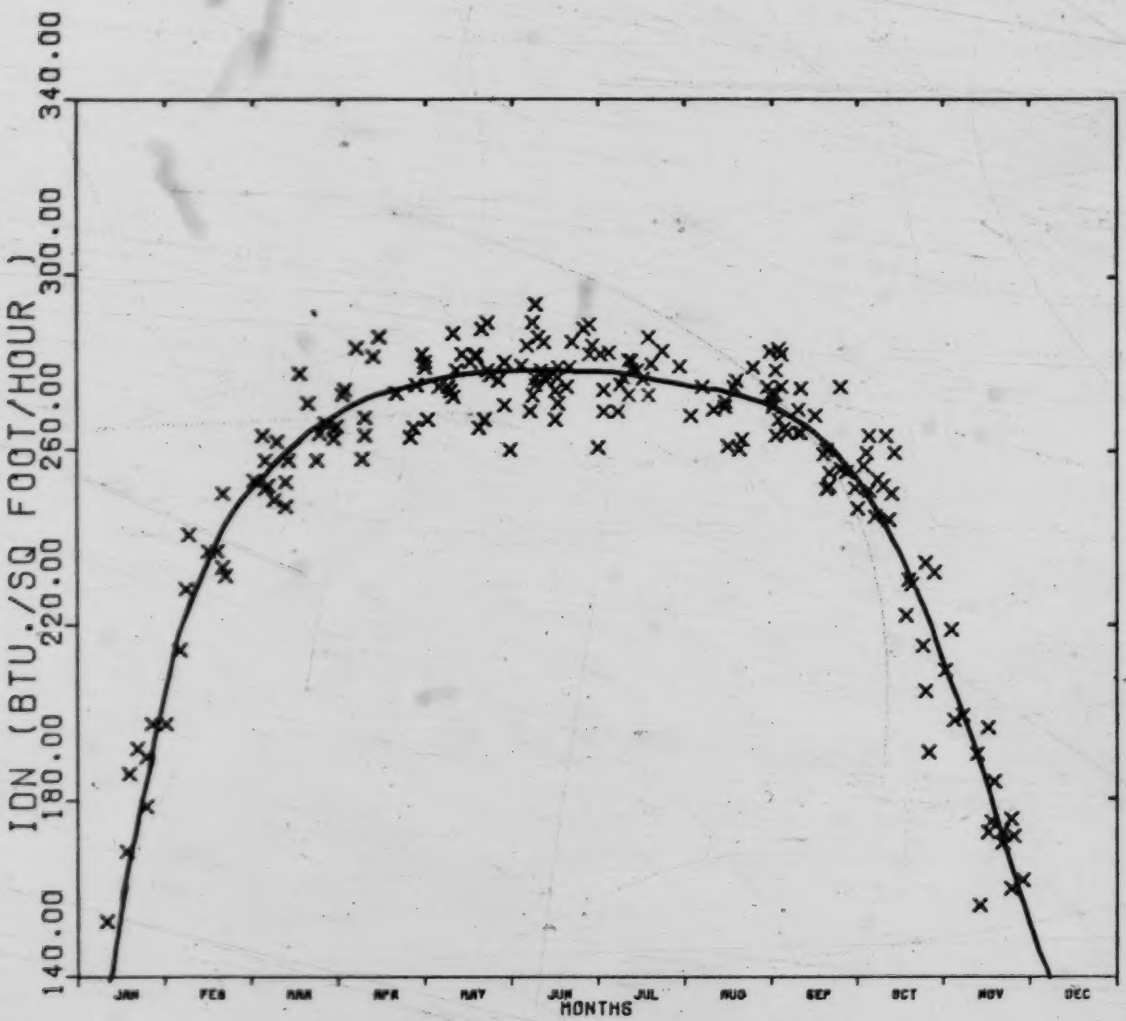

FIGURE 2.6 ANNUAL VARIATION OF THE CLEAR SKY DIRECT NORMAL INCIDENCE SOLAR RADIATION ,IDN. MEASURED AT EDMONTON AT HOUR ANGLE 3.

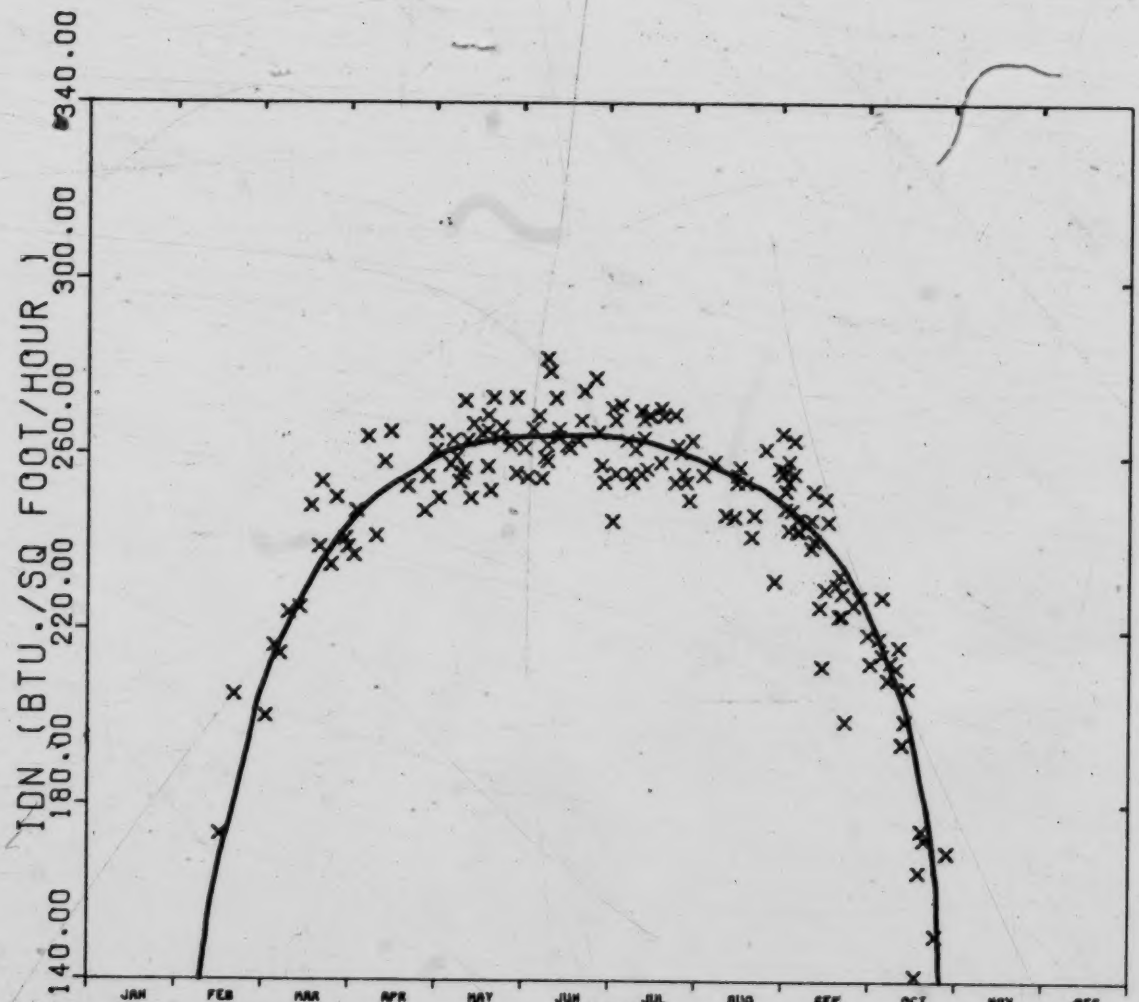

FIGURE 2.7 ANNUAL VARIATION OF THE CLEAR SKY DIRECT NORMAL INCIDENCE SOLAR RADIATION ,IDN, MEASURED AT EDMONTON AT HOUR ANGLE 4.

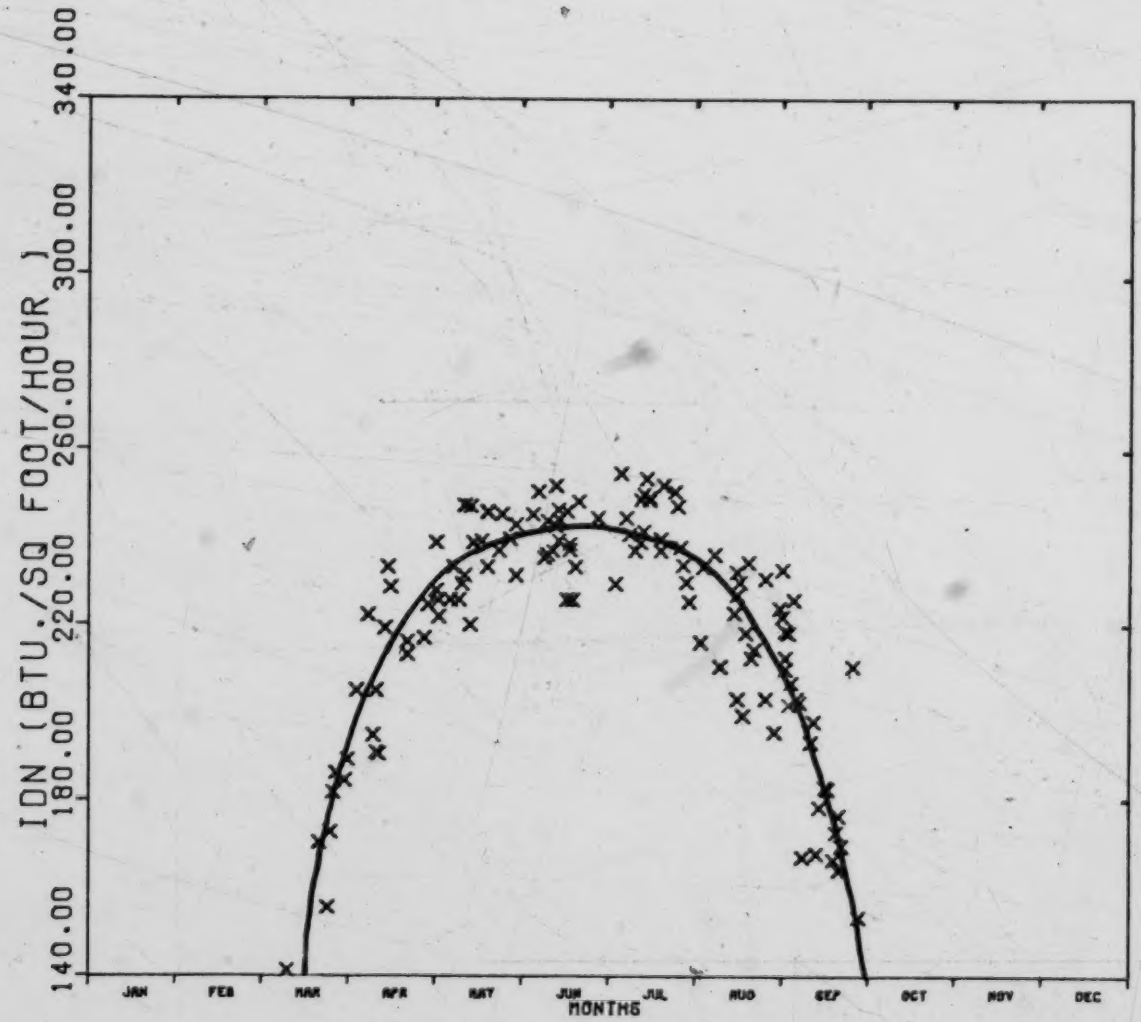

FIGURE 2.8 ANNUAL VARIATION OF THE CLEAR SKY DIRECT NORMAL INCIDENCE SOLAR RADIATION ,IDN, MEASURED AT EDMONTON AT HOUR ANGLE 5.

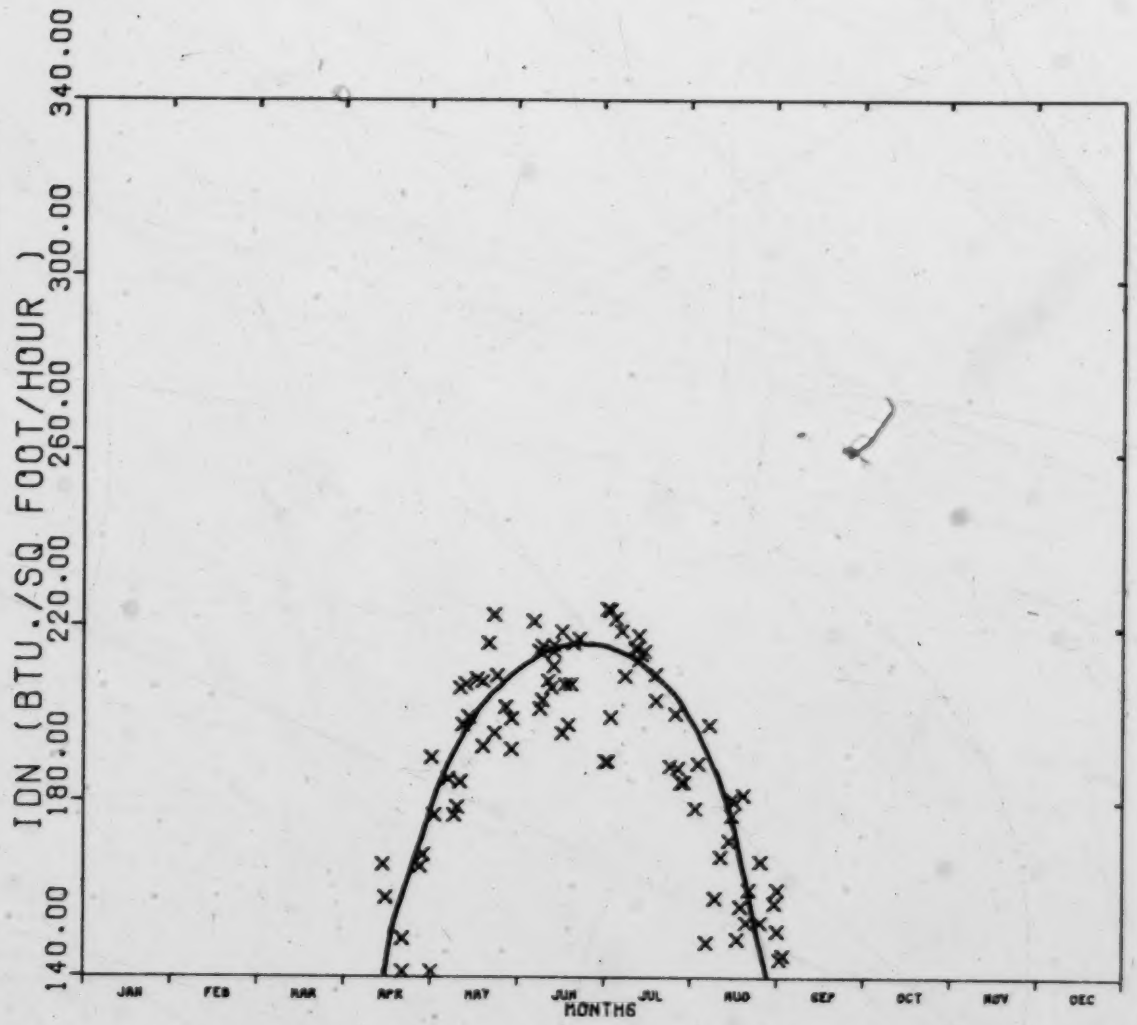

FIGURE 2.9 ANNUAL VARIATION OF THE CLEAR SKY DIRECT NORMAL INCIDENCE SOLAR RADIATION ,IDN, MEASURED AT EDMONTON AT HOUR ANGLE 6.

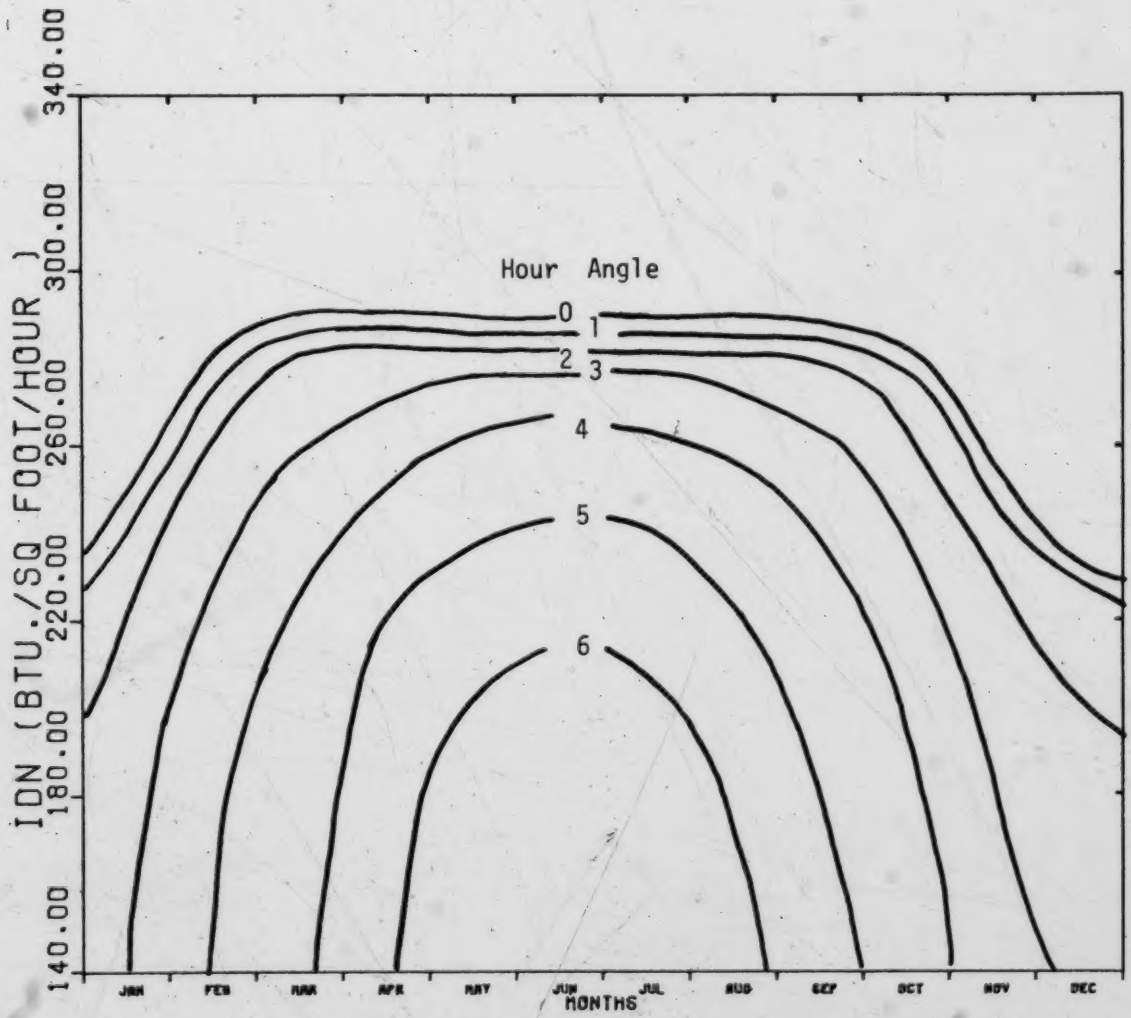

FIGURE 2.10 ANNUAL VARIATION OF THE CLEAR SKY DIRECT NORMAL INCIDENCE SOLAR RADIATION ,ION, MEASURED AT EDMONTON AT HOUR ANGLES 0 to 6.

particular day. This is mainly due to the rapid change of the sun's altitude which results in a large change of the air mass (path length through the atmosphere) in a short period of time.

Table 2.2 lists the monthly average of direct normal incidence, IDN, radiation measured at Edmonton at various hour angles. These values occur at about the third week of the month. Individual days may differ by $\pm$ 15 Btu$\cdot$ft$^{-2}\cdot$hr^{-1}.

TABLE 2.2 Monthly average normal incidence solar radiation (IDN) measured at Edmonton at different hour angles. Unit: Btu.ft.$^{-2}$hr.$^{-1}$

Month	Hour Angle From Solar Noon						
	0	1	2	3	4	5	6
January	255	250	227	180			
February	284	279	264	233	189		
March	291	286	275	262	232	178	
April	294	291	284	272	250	216	152
May	291	286	285	278	262	236	194
June	290	286	285	277	265	241	210
July	288	284	282	274	258	238	204
August	286	284	279	270	250	222	168
September	286	285	280	269	243	200	153
October	281	272	262	243	201	154	
November	252	251	235	193	170		
December	234	228	198	156			

CHAPTER 3

DISTRIBUTION OF SOLAR ENERGY IN DIFFERENT WAVELENGTH REGIONS

3.1 THE SOLAR RADIATION AT THE EARTH'S SURFACE

Although the spectrum emitted by the sun extends from x-rays of wavelength of a fraction of an Ångström ($1\text{Å} = 10^{-10}$ meter) to radio emission of hundreds of meters wavelength, only the spectral region from 0.3 micron to 3.0 microns ($1\mu = 10^{-6}$ meter) reaches the earth's surface as direct solar radiation. Almost all the energy associated with radiation of wavelength less than 0.24μ is absorbed by oxygen in the upper atmosphere and this leads to the formation of ozone. At about 60 kilometers above the ground the atmosphere becomes so rich in ozone that all the energy in the wavelengths shorter than 0.3μ is absorbed and ground measurements are not possible. The emitted solar energy at wavelengths less than 0.3μ is 0.485 percent. At wavelengths longer than 3.0μ in the infrared range, which accounts for 2.17 percent of the emitted solar energy, most of the energy is absorbed by atmospheric water vapor and carbon dioxide.

As mentioned in chapter two the intensity of the direct normal solar radiation incident on a given surface on the earth depends on the sun's elevation and shows a diurnal and annual variation. It also depends on its attenuation along its path through the earth's atmosphere. The attenuation of the solar beam by the atmosphere is not uniform over the solar spectrum. The influences which cause diminution in the incident energy passing through the atmosphere may be divided into two major effects:

(i) An effect which is generally ascribed to the scattering and general absorption in the atmosphere. It affects all wavelengths, and in fact the shortwaves more than the long ones. It is due to two factors. One is the scattering by air molecules (Rayleigh scattering). The other factor is that part of the incident energy scattered and absorbed by the dust in the atmosphere.

(ii) The second effect is limited to certain wavelengths of the spectrum and is called the selective absorption by the gases of the atmosphere. This absorption is practically negligible for the wavelength range 0.3 to 0.6 μ and the largest absorption occurs in the infrared region ($\lambda > 0.63\mu$) of the solar spectrum and it is mainly due to water vapor.

Between 0.3 and 3.0 microns, considerable variation in attenuation of the solar beam occurs for the different wavelengths. Therefore, it is desirable to divide the solar spectrum into several wavelength regions and study the distribution of energy in each region in addition to the total energy that reaches the ground.

3.2 CHARACTERISTICS OF CUTOFF GLASS FILTERS USED IN SOLAR RADIATION MEASUREMENTS

For the separation of the solar spectrum into reasonably well defined bands, filters are more practical and easier to handle than a spectrophotometer [9]. Absorbing glass filters

can be readily employed with normal incidence pyrheliometers by simple positioning of the filter in front of the detector, and the transmitted radiation can be expressed directly in absolute units. The filters recommended for use by the International Radiation Commission are the three Schott glass filters OG1, RG2 and RG8.

Each of the Schott glass filters OG1, RG2 and RG8 has a main transmission band in which an ideal filter shows almost uniform transparency and shows no transmission outside this region. Practically, each filter has a sharp lower cutoff separating the wavelengths almost totally transmitted from those totaly absorbed. The transmission change occurs over a 20 to 50 mμ range and the center of the lower cutoff is defined by the wavelength λ_m at which the transmission of the filter is 50 percent. The center of cutoff for filters with the same main transmission characteristics but made of different melts may differ in the position. Also it is slightly temperature dependent.

The transmission characteristics of each filter may be expressed as a filter factor and, by multiplying the measured radiation behind the filter by this factor, the solar radiation in front of the filter is obtained. If the filter is used with a pyrheliometer having a weather protective window in front of the receiver, the filter factor has to be reduced by one percent to compensate for the effect of the multiple reflections between the filter and the window.

To compare measurements taken at different locations or taken by filters made of different melts, a correction may be made to account for the shift in the positions of the center of the lower cutoff for the filter from the cutoff position of a standard filter. This correction is made to reduce the measurement to that which would be obtained by the standard filter. One method of applying this correction is to test the filter in use by a national standarizing laboratory to obtain a correction to the filter factor. This method is applicable for shifts of less than 10 mμ in the position of the lower cutoff, and may usually be applied to filters of the same type but from different melts [10]. Another method, which calculates the correction as a function of the shift in the center of cutoff, the air mass, and the turbidity coefficient of the atmosphere, has been introduced by Ångström and Drummond [9]. They suggested that if the shift is more than 10 mμ, the correction is evidently so large that it ought to be taken into account in all instances; also for accurate measurements and for truly comparable values, the correction should be applied whenever the shift exceeds ±5 mμ. However, to produce a shift in the cutoff position in excess of 5 mμ, a temperature difference of 30 to 40 degrees Celsius is necessary, which implies that, in general, a correction need not be applied for daily variations in temperature, and only in rare cases that corrections for seasonal temperature variations are necessary.

The solar energy above the upper cutoff wavelength for the filters (which is at about 2800 mμ for the three filters OG1, RG2 and RG8) reaching the earth's surface is small and is a function of the precipitable water vapor in the atmosphere. But in order to obtain more accurate results for the energy distribution of the solar radiation reaching the earth's surface within different spectral bands, a small correction ΔIL should be added to the filtered radiation being reduced to the standard conditions. This correction is small and difficult to calculate, so it is often omitted. However, the correction ΔIL has been calculated as a function of the product of air mass and precipitable water. Table 3.1, which is a reproduction of table 1, Page 399, Reference [10], lists this correction.

TABLE 3.1 Solar intensity above the longwave cutoff of the filters ΔIL (in mcal . cm^{-2} . min^{-1}) as a function of atmospheric humidity m_h.w (in cm).

$m_h \cdot w$	ΔIL	$m_h \cdot w$	ΔIL	$m_h \cdot w$	ΔIL
0.10	34	0.60	20	4.30	8
0.13	32	0.80	18	6.30	6
0.16	30	1.00	16	11.00	4
0.21	28	1.10	16	22.00	2
0.26	26	1.50	14	44.0	0
0.34	24	2.10	12		
0.45	22	3.00	10		

3.3 APPLICATION OF THE FILTER MEASUREMENTS

The method of dividing the solar spectrum into two regions by means of each filter is illustrated by considering the red filter RG2. Its wavelength range is from 630 to 2800 mμ, and F2 is the filter factor. If the intensity of the total direct solar radiation I and also, practically simultaneously, the intensity of the radiation behind the filter I2 are measured, then by multiplying I2 by the filter factor F2 and adding ΔIL, the following two radiation integrals can be calculated

$$\int_{630}^{\infty} I(\lambda)d\lambda = F2.I2 + \Delta IL = Ir \qquad (3.1)$$

$$\int_{0}^{630} I(\lambda)d\lambda = I - Ir = Ik \qquad (3.2)$$

where $I(\lambda)$ represents the energy distribution within the solar spectrum,

Ir represents the red and infrared radiation,

Ik represents the ultraviolet and visible radiation.

The first integral (3.1) covers the red and infrared spectrum where all the strong absorption bands of water vapor and carbon dioxide occur. The second integral (3.2) covers the short wave radiation, where there is almost no selective absorption apart from the ozone absorption in high layers of the atmosphere, and attenuation of the radiation in this region is

mainly due to scattering by dry gas, dust and other aerosols.

If I1 and I8 are the intensities measured with the filters OG1 and RG8, F1 and F8 are the respective filter factors and the transmission region is from 530 to 2800 mμ for OG1 and from 710 to 2800 mμ for RG8, then the intensity of the solar radiation covered by the following integrals can be determined

$$\int_{530}^{\infty} I(\lambda)d\lambda = F1 \cdot I1 + \Delta IL = Id \qquad (3.3)$$

$$\int_{0}^{530} I(\lambda)d\lambda = I - Id = Ib \qquad (3.4)$$

and

$$\int_{710}^{\infty} I(\lambda)d\lambda = F8 \cdot I8 + \Delta IL = Ii \qquad (3.5)$$

$$\int_{0}^{710} I(\lambda)d\lambda = I - Ii = Iv \qquad (3.6)$$

where Id represents the yellow and green radiation,
Ib represents the blue and violet radiation,
Ii represents the infrared radiation and
Iv represents the visible radiation.

In general, a filter is used to separate the spectrum of solar radiation into two well defined regions. The intensity of the radiation below the short-wave cutoff of the filter is

mainly dependent on the atmospheric scattering and the intensity of the radiation above the short-wave cutoff is mainly dependent on the selective absorption of the atmosphere. Data concerning the variation of the two integrals of any of the three filters with location and time of the day and of the year is of value not only for studying the energy distribution in specific wavelength ranges but also for studying the constitution of the atmosphere with regards to turbidity and water vapor content. The latter will be discussed in chapter four. The use of the three filters OG1, RG2 and RG8 allows the energy distribution to be calculated for seven designated solar spectrum bands as shown in table 3.2.

TABLE 3.2 Spectral regions of the solar spectrum obtained by filter measurements

Denomenation	Abbreviation	Wavelength range (millimicrons)	Calculation
Blue and violet	Ib	$\lambda \leq 525$	I-F1.I1
Yellow and green	Id	$525 < \lambda < 630$	F1.I1-F2.I2
Short-wave (ultraviolet and visible)	Ik	$\lambda \leq 630$	I-F2.I2
Yellow and red	ID	$525 < \lambda < 710$	F1.I1-F8.I8
Visible	Iv	$\lambda < 710$	I-F8.I8
Red and infrared	Ir	$\lambda > 630$	F2.I2
Infrared	Ii	$\lambda > 710$	F8.I8

3.4 FILTER MEASUREMENTS AT EDMONTON

The output of the three normal incidence pyrheliometers mounted on a tracking unit monitored the normal incidence insolation over the observable spectral region (i.e. approximately 0.3 to 3 microns) and the insolation passing the RG2 and RG8 filters under clear sky conditions at Edmonton. This allowed the study for the solar energy distribution in five spectral bands. The procedures of preparing the hourly records of the solar energy carried within the total normal incidence radiation and the radiation passing RG2 and RG8 filters were described in section six of chapter one.

The filters used in this study were supplied by The Eppley Laboratory. They were 2 millimeters thick and, at 20 degrees Celsius, had a center of lower cutoff at 628 mμ for RG2 filter and 692 mμ for RG8 filter and upper cutoff at 2800 mμ. For calculations, it was assumed that the lower center of cutoff was at 626 mμ for RG2 filter and 690 mμ for RG8 filter which were about the values expected at the average yearly outdoor temperature. No correction was applied for the shift in center of cutoff. The filter factors were 1.10 for RG2 filter and 1.12 for RG8 filter and, since the Eppley normal incidence pyrheliometers have a quartz window between the radiation receiver and the filter, each filter factor was reduced by one percent to correct for multiple reflection between the window and the filter.

The correction ΔIL for the energy above 2800 mμ not

measured by the filters was calculated using table 3.1. This table was divided into two intervals, one covering the range of atmospheric humidity (precipitable water w along the path of the sun's rays) for which $m_h \cdot w \leq 2$ and the other covering the range of $m_h \cdot w > 2$. Using a least squares technique a polynomial was fitted for each interval. The correction for the solar intensity above the longwave cutoff of the filters ΔIL was calculated using the polynomials:

$$\Delta IL = 33.61 - 33.25(m_h \cdot w) + 19.76(m_h \cdot w)^2 - 0.22(m_h \cdot w)^3, \quad m_h w \leq 2 \qquad (3.7)$$

$$\Delta IL = 17.35 - 2.74(m_h \cdot w) + 0.14(m_h \cdot w)^2, \quad m_h w > 2 \qquad (3.8)$$

where ΔIL is in $mcal.cm^{-2}.min^{-1}$,

($1\ cal\ cm^{-2}\ min^{-1} = 221.2\ Btu\ ft^{-2}hr^{-1}$)

w is the precipitable water, and

m_h is the relative air mass.

The appropriate relative air mass values were calculated and the average daily precipitable water vapor for forenoon and afternoon were calculated using the published values in reference [11].

The use of the two filters RG2 and RG8 allowed the energy distribution to be calculated for the five solar spectral bands: $\lambda \leq 626$, $\lambda > 626$, $\lambda \leq 690$, $\lambda > 690$ and $626 < \lambda \leq 690$ millimicrons. Let IDN, I2 and I8 be the measured intensities

of the total direct normal solar radiation, the radiation passing the RG2 filter and the radiation passing the RG8 filter respectively and let ΔIL be the intensity of the radiation above the long wave cutoff of the filters. The intensities of the radiation within the five spectral bands were calculated at Edmonton as follows:

$$Ir = (1.10 \cdot I2) + \Delta IL, \qquad \lambda > 626m\mu$$

$$Ik = IDN - Ir, \qquad \lambda \leq 626m\mu$$

$$Ii = (1.11 \cdot I8) + \Delta IL, \qquad \lambda > 690m\mu$$

$$Iv = IDN - Ii, \qquad \lambda < 690m\mu$$

$$Ie = Ir - Ii, \qquad 626 < \lambda \leq 690m\mu$$

where Ir, Ik, Ii and Iv are as defined previously and Ie represents the red band radiation.

3.5 THE ANNUAL VARIATION OF THE SPECTRAL DISTRIBUTION OF THE NORMAL INCIDENCE INSOLATION MEASURED AT EDMONTON AT DIFFERENT HOUR ANGLES

Full day, half day and part day data were used in the analysis. For each forenoon and afternoon, the energy within each band was calculated at hour angles zero to six when it was possible. As discussed in chapter two, the normal incidence insolation was also calculated and then the percentage of the normal incidence insolation carried by the radiation

within each band was determined. Figures 3.1 to 3.7 show the latter quantity for hour angles zero to six throughout the year. The curves in these figures were best fitted by eye to show the approximate annual variation of the fraction of the normal insolation with the five spectral bands. The fraction of the normal insolation for the three bands $\lambda < 626m\mu$ (short-wave fraction), $\lambda > 690m\mu$ (infrared fraction) and $626 < \lambda < 690m\mu$ (red fraction) should be read on the left hand axis from the curves named Ikp, Iip and Iep respectively, and the fractions for the two bands $\lambda > 626m\mu$ and $\lambda < 690m\mu$ should be read on the right-hand axis from the curves Ikp and Iip, respectively.

The curves in figures 3.1 to 3.7 show that the fraction Iip has a similar annual trend at different hour angles. The same type of results are also found for the fraction Ikp. The infrared fractions Iip have flat minima during the summer months June, July and August and increase gradually during the rest of the year. The curves representing the short wave fractions Ikp have flat maxima during the summer months and decrease gradually during the rest of the year. The curves representing the red fractions Iep show slight annual variation at all hour angles. Table 3.3 lists the monthly average of the infrared fractions and the shortwave fractions of the normal insolation. The fractions of the normal insolation within the two bands $\lambda < 690m\mu$ (Ivp) and $\lambda > 630m\mu$ (Irp) can be easily determined as follows:

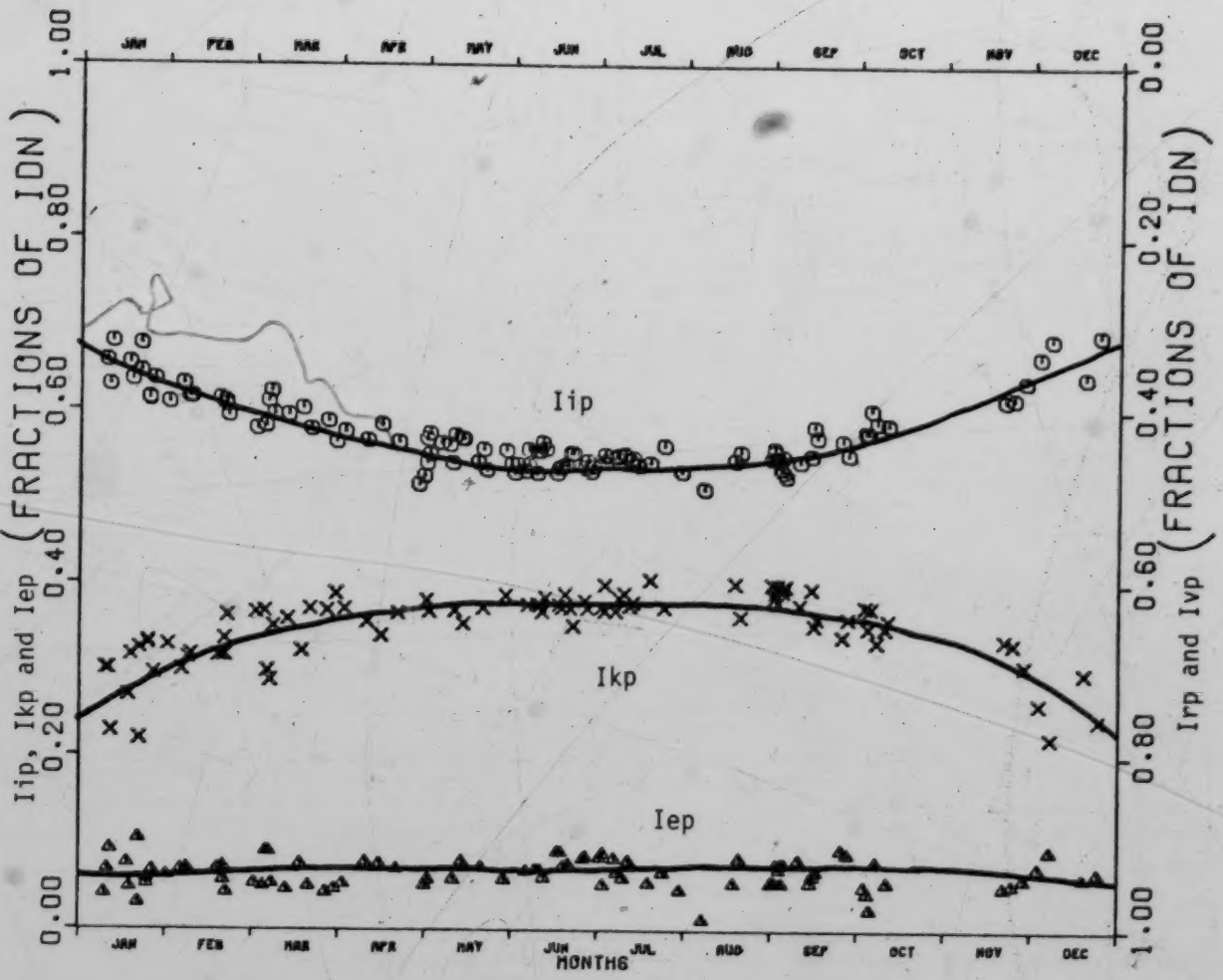

FIGURE 3.1 ANNUAL VARIATION OF THE FRACTIONS OF ION WITHIN DIFFERENT WAVELENGTH REGIONS COMPUTED AT EDMONTON AT HOUR ANGLE ZERO.

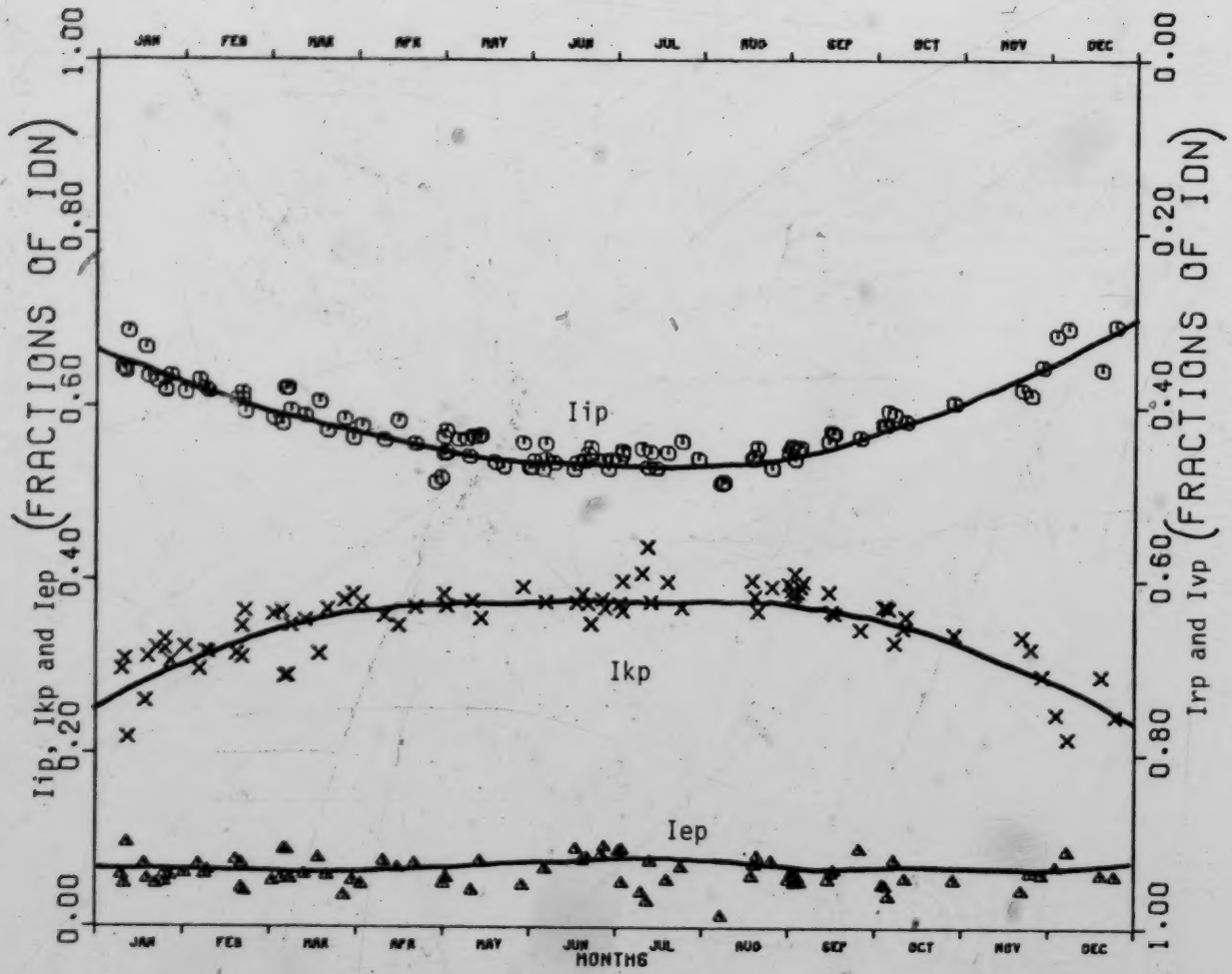

FIGURE 3.2 ANNUAL VARIATION OF THE FRACTIONS OF IDN WITHIN DIFFERENT WAVELENGTH REGIONS COMPUTED AT EDMONTON AT HOUR ANGLE 1.

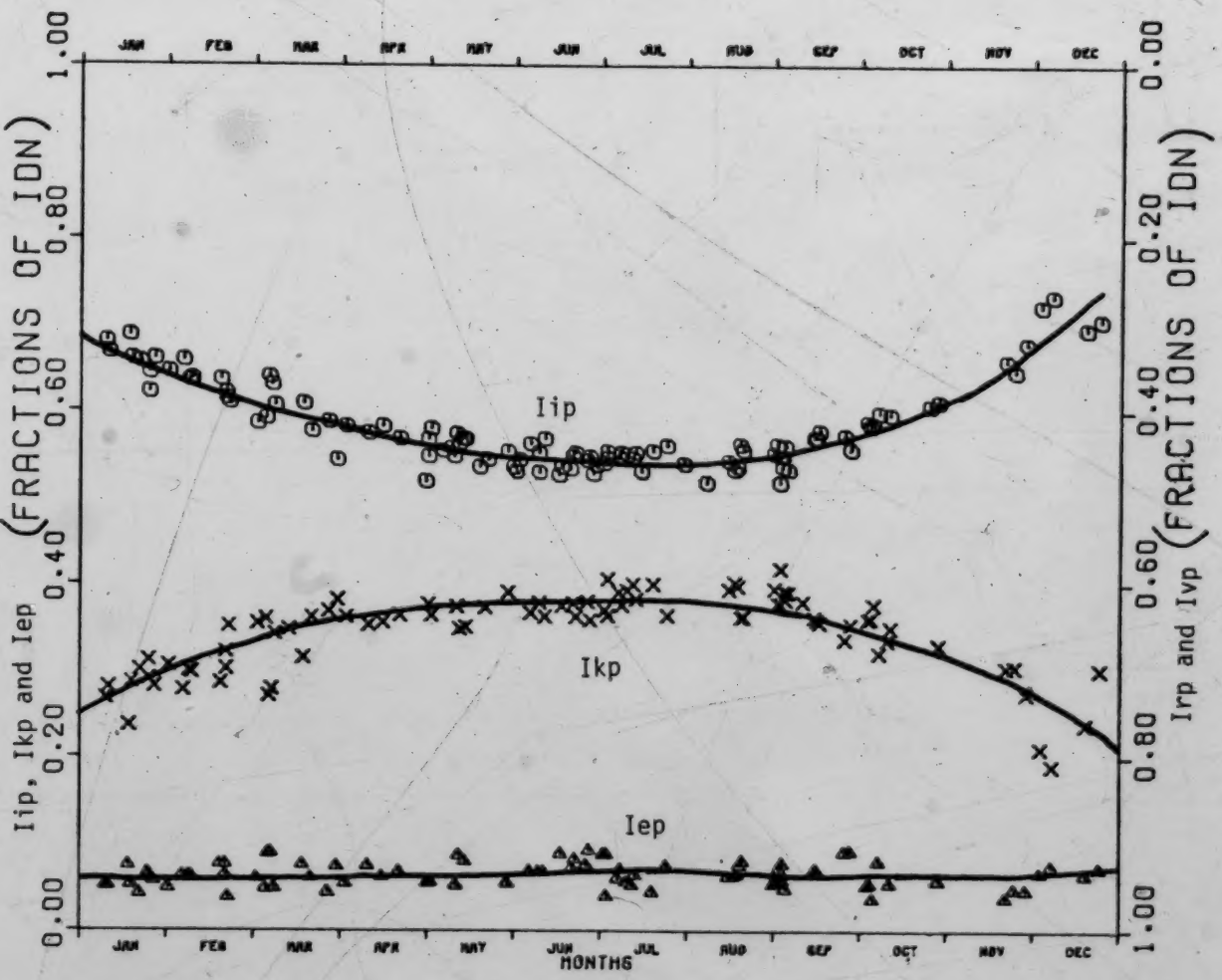

FIGURE 3.3 ANNUAL VARIATION OF THE FRACTIONS OF IDN WITHIN DIFFERENT WAVELENGTH REGIONS COMPUTED AT EDMONTON AT HOUR ANGLE 2.

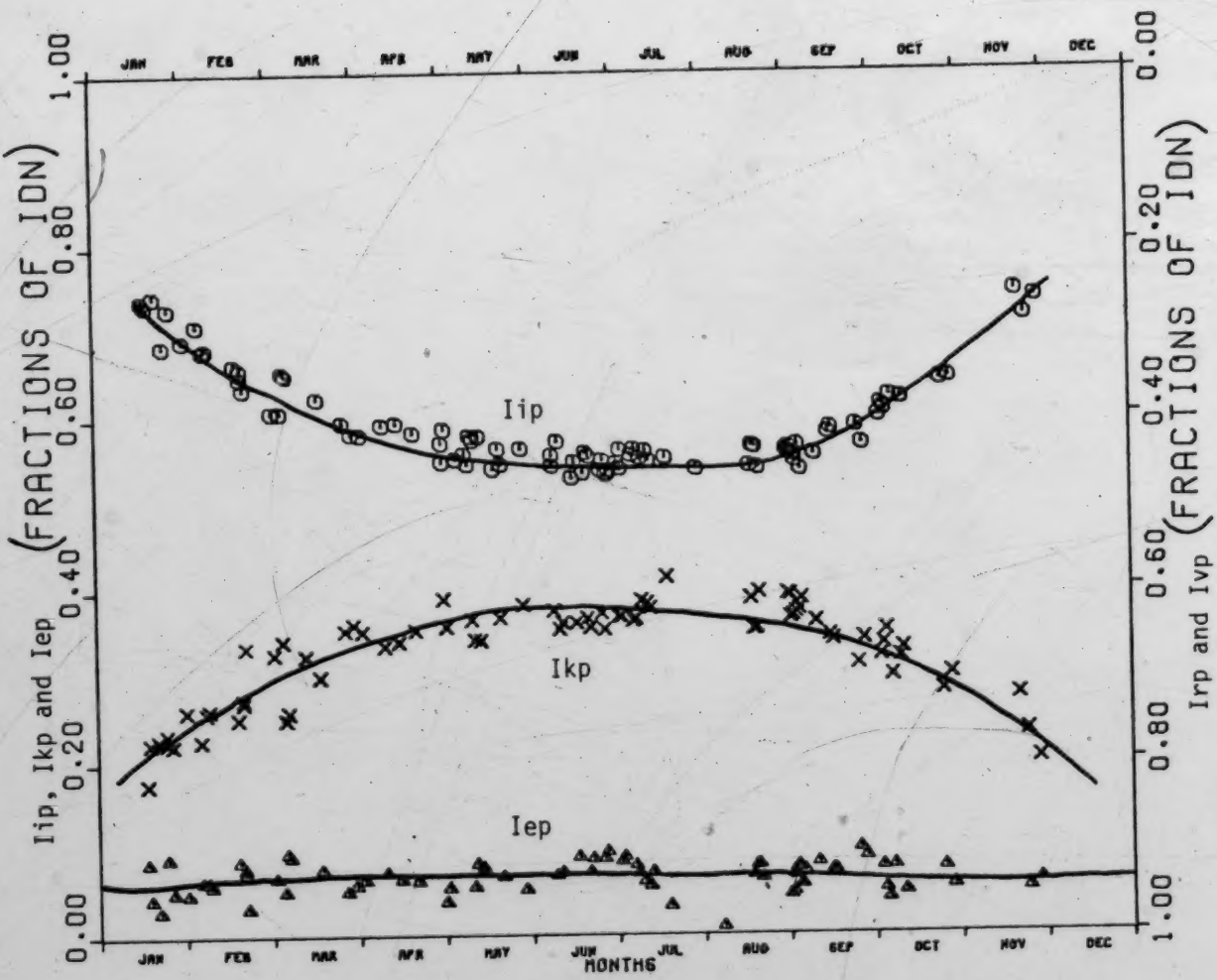

FIGURE 3.4 ANNUAL VARIATION OF THE FRACTIONS OF ION WITHIN DIFFERENT WAVELENGTH REGIONS COMPUTED AT EDMONTON AT HOUR ANGLE 3.

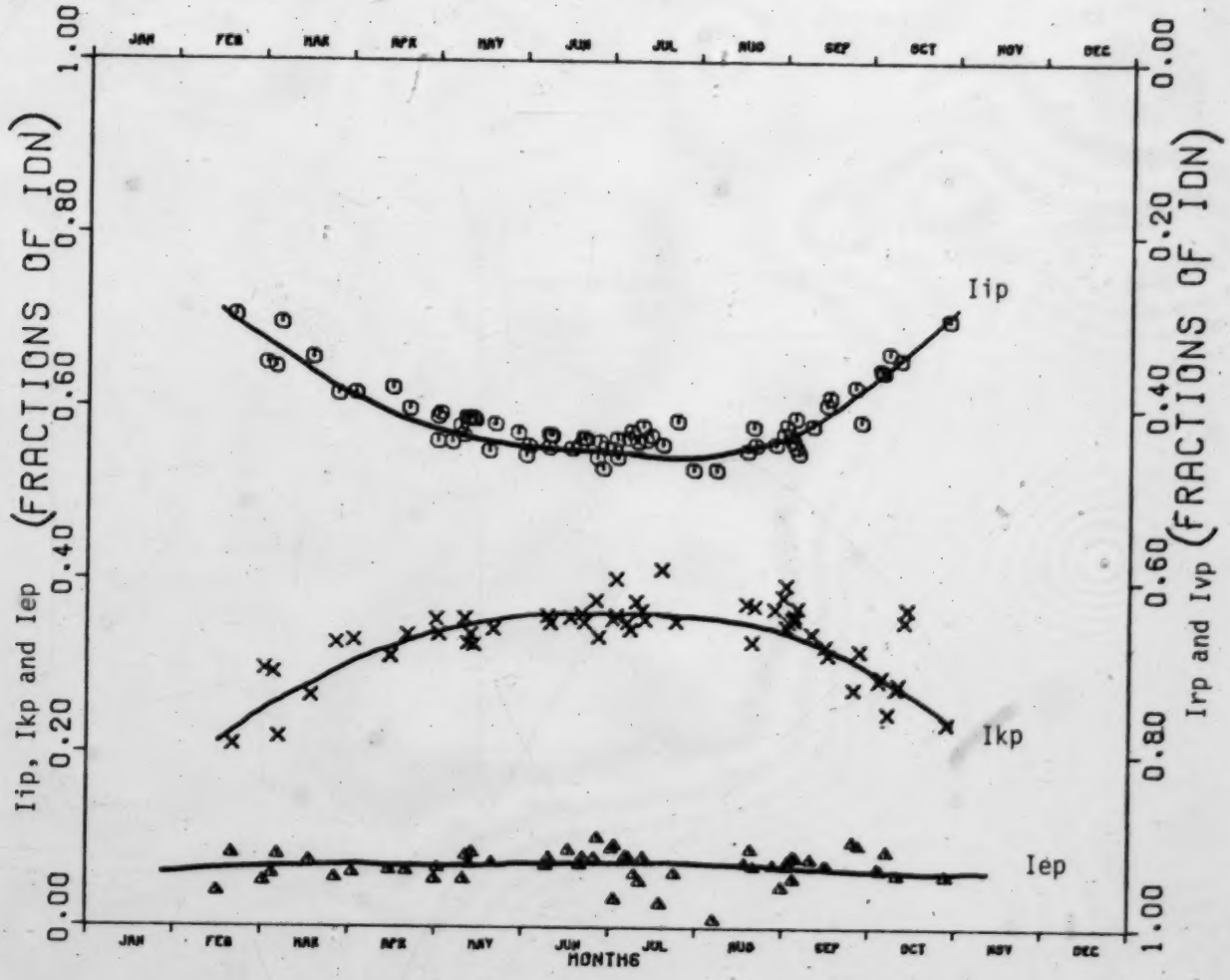

FIGURE 3.5 ANNUAL VARIATION OF THE FRACTIONS OF IDN WITHIN DIFFERENT WAVELENGTH REGIONS COMPUTED AT EDMONTON AT HOUR ANGLE 4.

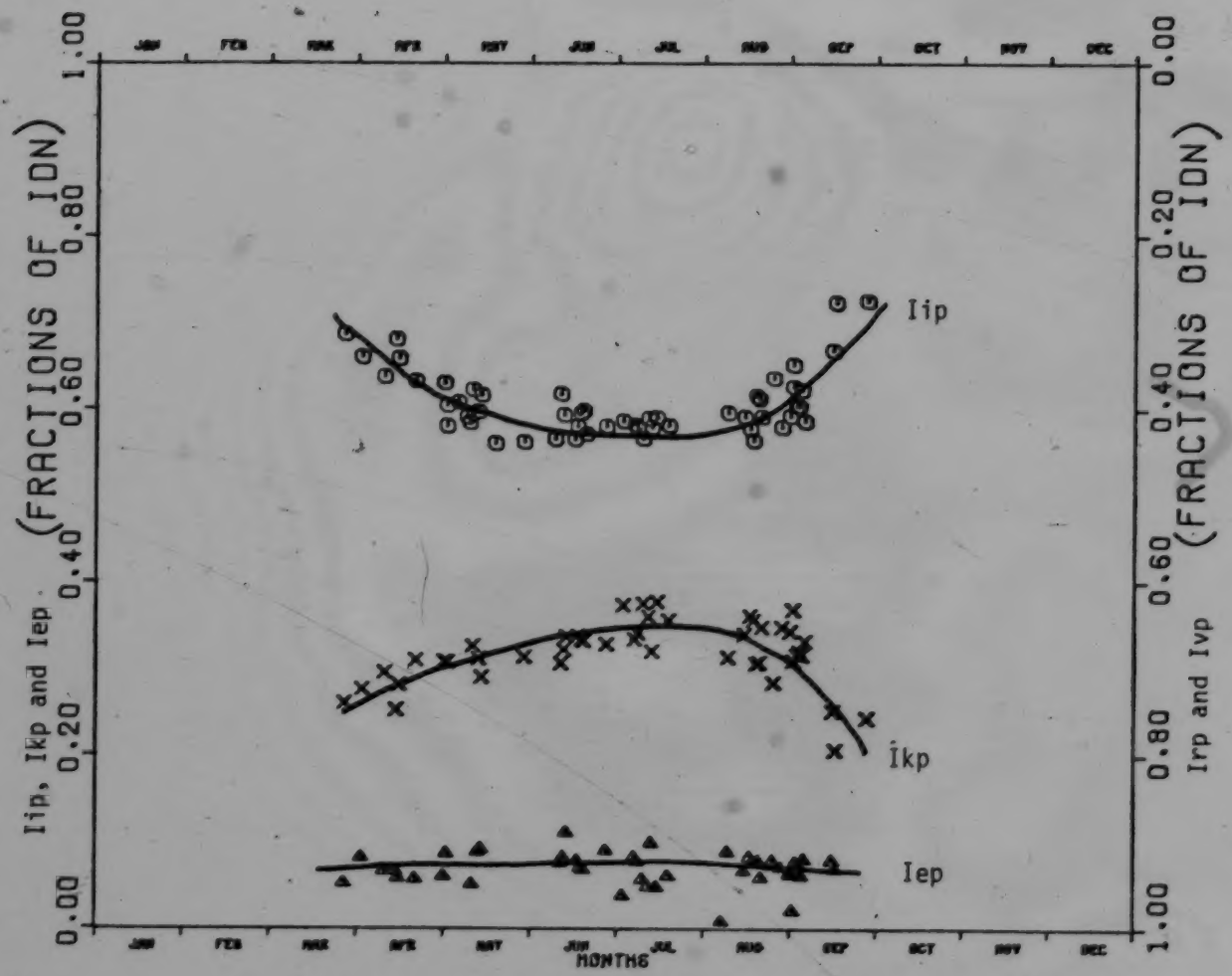

FIGURE 3.6 ANNUAL VARIATION OF THE FRACTIONS OF IDN WITHIN DIFFERENT WAVELENGTH REGIONS COMPUTED AT EDMONTON AT HOUR ANGLE 5.

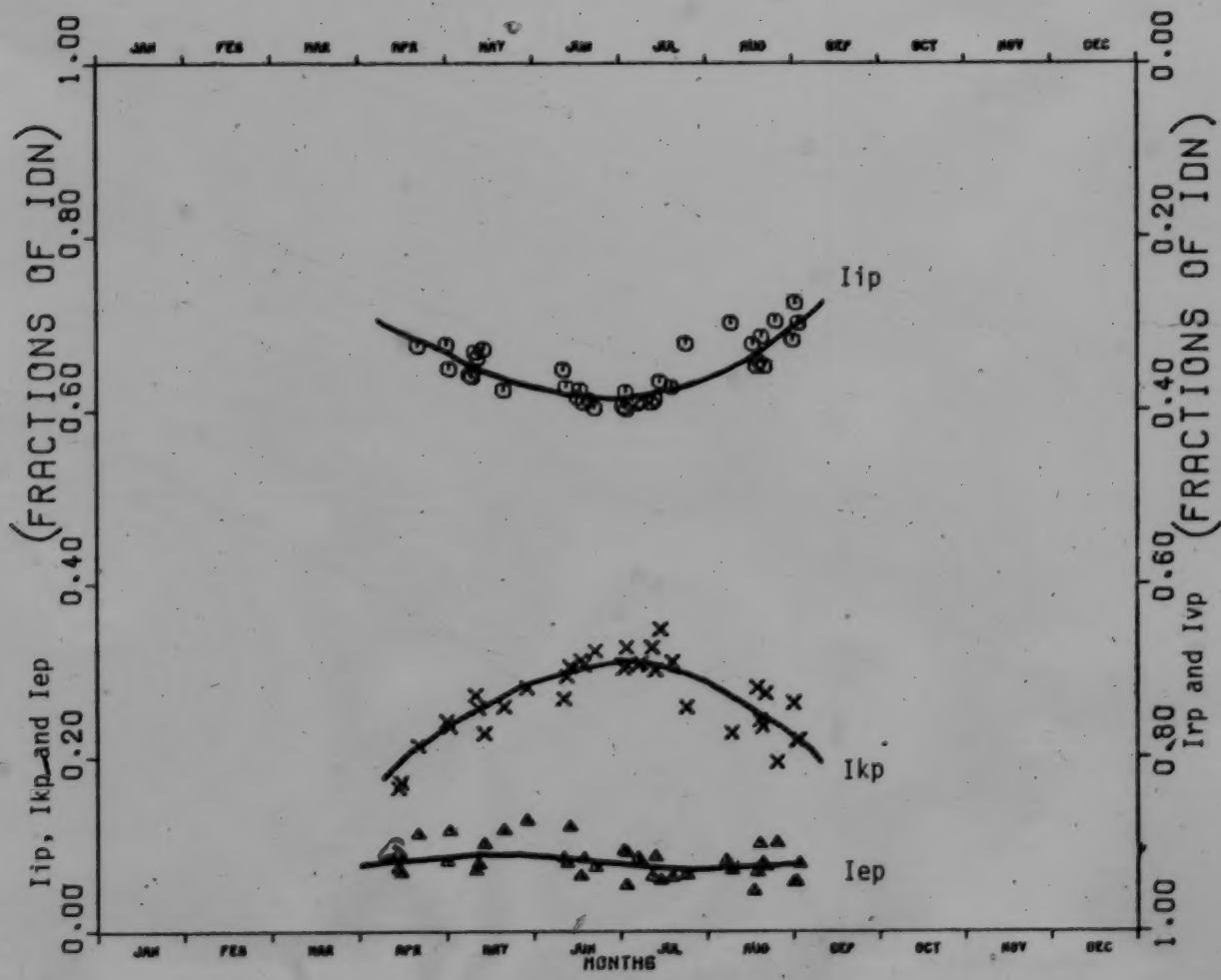

FIGURE 3.7 ANNUAL VARIATION OF THE FRACTIONS OF ION WITHIN DIFFERENT WAVELENGTH REGIONS COMPUTED AT EDMONTON AT HOUR ANGLE 6.

TABLE 3.3 Monthly average percentage of the normal incidence radiation in the infrared spectrum band Iip(λ>690mμ) and the shortwave spectrum band Ikp(λ<626mμ) at Edmonton at different hour angles.

Month		Hour Angle From Solar Noon						
		0	1	2	3	4	5	6
January	Iip	64.6	64.6	66.2	73.0			
	Ikp	28.7	28.9	27.6	21.5			
February	Iip	61.2	61.3	63.0	66.3	70.6		
	Ikp	32.2	32.1	30.2	26.7	21.0		
March	Iip	59.2	59.3	59.7	61.7	65.3	68.7	
	Ikp	34.8	34.5	33.8	31.5	28.1	26.1	
April	Iip	56.4	56.6	57.8	58.8	61.2	65.4	67.4
	Ikp	36.0	35.9	35.2	34.6	32.8	28.4	24.6
May	Iip	55.6	55.7	55.8	56.1	57.4	59.6	65.6
	Ikp	37.6	37.2	36.8	36.4	34.2	31.0	26.4
June	Iip	54.1	54.3	54.5	55.2	55.9	58.1	62.8
	Ikp	37.5	37.2	37.1	36.3	35.7	32.9	30.2
July	Iip	54.1	54.5	54.6	55.5	56.4	58.3	62.2
	Ikp	39.9	39.9	39.7	39.4	38.4	35.8	31.5
August	Iip	54.1	54.5	54.9	55.3	56.0	59.9	67.2
	Ikp	39.0	38.2	38.0	37.4	35.2	32.8	25.2
September	Iip	55.0	55.2	55.4	56.3	58.1	62.9	69.7
	Ikp	38.6	38.4	38.2	38.2	35.9	31.8	24.2
October	Iip	58.7	58.9	59.6	62.1	64.6		
	Ikp	35.3	35.2	34.5	31.8	29.0		
November	Iip	61.5	61.6	63.2	65.7	70.3		
	Ikp	33.4	32.9	31.7	27.8	23.7		
December	Iip	65.5	66.2	70.3	73.7			
	Ikp	28.8	27.1	24.2	20.2			

$$Ivp = 100 - Iip$$

and $$Irp = 100 - Ikp$$

Figure 3.8 depicts all the curves in figures 3.1 to 3.7 on one graph for visual comparison at different hour angles. The infrared fraction curves have close agreement at hour angles 0, 1 and 2 with an average value of 54 percent in May, June, July and August with a variation of ±1 percent about the average. This average increases to about 62 percent for the rest of the year with a variation of ±6 percent about the average. As the hour angle exceeds 2 the infrared fractions increase, a characteristic which occurs for all days throughout the year. Close agreement between the curves up to hour angle 4 is noticed during the summer months, an average value of about 55 percent can be assumed for May to August at hour angles 0 to 4. At hour angle 5 and 6 the solar energy is available for a short period of the year, approximately from April to September, and the infrared fractions have an average value of about 66 percent.

The shortwave fraction curves show that the maximum fraction of about 38 percent occurs in the summer at hour angles 0, 1 and 2 then the fractions decrease on both sides of the curve to about 31±6 percent for the rest of the year. As the hour angle exceeds 2 the shortwave fractions decrease, a characteristic which occurs for all days throughout the year. At hour angle six the shortwave fractions reach a value

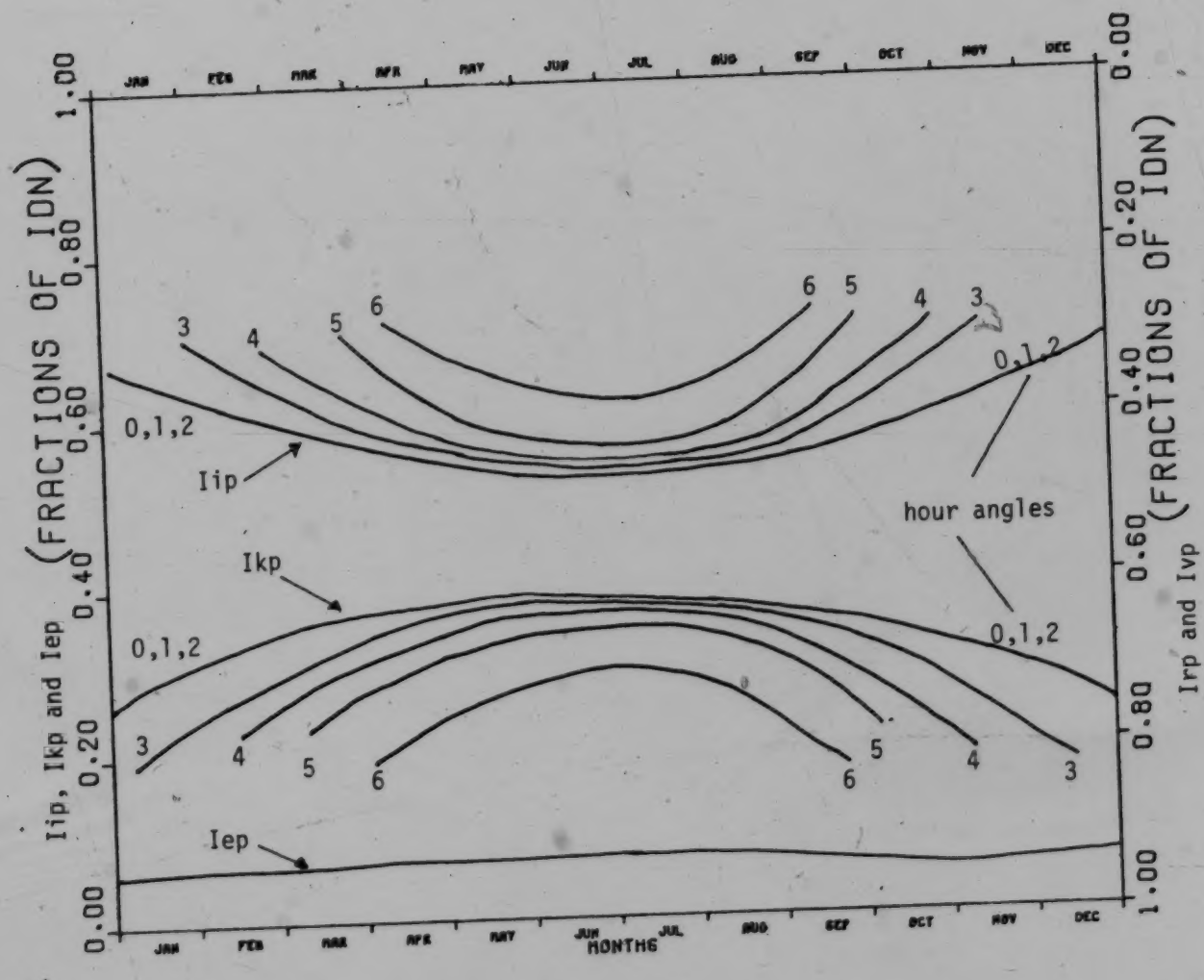

FIGURE 3.8 ANNUAL VARIATION OF THE FRACTIONS OF ION WITHIN DIFFERENT WAVELENGTH REGIONS COMPUTED AT EDMONTON AT HOUR ANGLES 0 to 6.

of 25±5 percent.

The fractions within the red band have slight variation at different hour angles for all days throughout the year and the average value is about 6.5 percent.

The variation of the fractions of the normal insolation in different bands with time of the day and the year shows an agreement with the fact that the attenuation of the solar beam due to dry air molecules, water vapor, dust and other aerosols in the atmosphere is not uniform over the solar spectrum.

The closer agreement between the infrared fraction curves at different hour angles till hour angle 4 during the summer months is due to relatively small change in the path length of the radiation through the atmosphere while the precipitable water, which is the major attenuating factor of the infrared radiation, is at about the same level during the summer.

The decrease of the shortwave fractions as the hour angle increases and also in the winter months is due to the longer path through the atmosphere where more attenuation is caused by scattering by dust and other aerosols, which are the major attenuating factors of the shortwave radiation, as well as scattering by air molecules which attenuate the shortwave radiation more than the infrared radiation.

The monthly averages at different hour angles of the magnitude of the energy within each of the five spectral bands calculated at Edmonton are listed in tables 3.4 to 3.6.

TABLE 3.4 Monthly average normal incidence solar radiation in the red and infrared band Ir (λ>626mμ) and the shortwave band Ik (λ<626mμ) measured at Edmonton at different hour angles. Unit: Btu.ft^{-2}.hr^{-1}.

Month		Hour Angle From Solar Noon						
		0	1	2	3	4	5	6
January	Ir	181	178	164	139			
	Ik	73	72	63	40			
February	Ir	192	188	183	170	149		
	Ik	91	89	79	62	41		
March	Ir	190	189	181	178	158	138	
	Ik	101	99	94	82	64	45	
April	Ir	189	186	183	179	171	150	127
	Ik	106	105	102	94	83	60	29
May	Ir	185	182	181	176	175	159	133
	Ik	104	110	105	102	90	75	48
June	Ir	184	182	182	178	175	159	145
	Ik	110	108	107	102	97	79	62
July	Ir	177	174	172	170	162	153	143
	Ik	113	112	110	100	94	86	66
August	Ir	174	172	170	164	155	141	115
	Ik	120	118	104	105	92	73	48
September	Ir	178	178	171	168	155	132	111
	Ik	112	111	103	106	95	65	35
October	Ir	179	178	174	165	151	126	
	Ik	106	104	99	84	64	42	
November	Ir	174	171	163	146	129		
	Ik	89	85	76	57	40		
December	Ir	171	168	153	129			
	Ik	66	62	48	32			

TABLE 3.5 Monthly average normal incidence solar radiation in the infrared band Ii (λ>690mμ) and the visible band Iv (λ<690mμ) measured at Edmonton at different hour angles. Unit: Btu.ft^{-2}.hr^{-1}

Month		Hour Angle From Solar Noon						
		0	1	2	3	4	5	6
January	Ii	164	161	150	121			
	Iv	90	89	77	63			
February	Ii	168	166	162	153	135		
	Iv	109	107	97	79	55		
March	Ii	173	169	163	161	143	128	
	Iv	119	116	112	100	77	58	
April	Ii	165	167	165	160	154	138	114
	Iv	131	130	121	113	98	73	43
May	Ii	162	160	158	154	148	136	111
	Iv	130	129	126	122	111	94	67
June	Ii	158	155	154	152	147	137	126
	Iv	137	133	130	126	118	100	81
July	Ii	158	156	153	152	147	132	130
	Iv	132	131	129	126	115	99	79
August	Ii	155	153	151	149	139	128	107
	Iv	132	131	126	122	109	89	54
September	Ii	161	160	159	155	137	122	101
	Iv	130	127	121	116	105	78	44
October	Ii	165	164	160	153	130	110	
	Iv	121	115	112	98	80	43	
November	Ii	157	155	151	135	119		
	Iv	99	95	89	64	50		
December	Ii	154	152	142	120			
	Iv	82	78	59	42			

TABLE 3.6 MOnthly average normal incidence solar radiation in the wavelength range of 626 to 690 millimicrons (red band Ie) measured at Edmonton at different hour angles. Unit: $Btu \cdot ft^{-2} \cdot hr^{-1}$.

Month	Hour Angle From Solar Noon						
	0	1	2	3	4	5	6
January	17	16	14	12			
February	19	19	18	14	11		
March	19	19	18	14	12	7	
April	18	16	15	12	11	9	8
May	16	14	14	13	12	11	10
June	16	15	15	14	12	11	10
July	18	17	16	15	14	13	12
August	17	17	16	16	15	14	12
September	18	18	18	17	15	12	9
October	18	17	17	16	15	13	
November	16	14	12	10	8		
December	14	14	12	9			

The maximum energy within the red and infrared band Ir and the infrared band Ii occurs in March and April when the precipitable water vapor in the atmosphere is low. Lower energy is available in July and August when the atmosphere has a high precipitable water level. The least energy occurs during the winter months at large hour angles (when the solar altitude is less than 20 degrees).

For the shortwave band Ik and the visible band Iv the maximum energy occurs in the summer months May to August at hour angles 0 to 3 when the path length of the radiation through the atmosphere is relatively short. However, the magnitude of the energy is slightly larger than the values measured during April and September when the path length through the atmosphere is relatively longer. This is probably due to an increase of the dust particles in the atmosphere during May to August. The least energy is measured during the winter months at large hour angles. The magnitude of the energy within the red band Ie has a similar trend.

3.6 VARIATION OF THE INFRARED AND SHORTWAVE FRACTIONS OF THE NORMAL INSOLATION WITH THE SOLAR ALTITUDE

The variation of the infrared fraction and the shortwave fraction of the direct normal incidence solar radiation (normal insolation) was studied. The average fraction of the energy within each of the infrared band and the shortwave band was calculated for each one degree interval of change in solar altitude from 5 to 60 degrees. Figures 3.9 and 3.10 show the plot of these values. It seems that the infrared fraction increases somewhat uniformly from about 54 percent at 60 degrees to about 62 percent at 20 degrees and then increases rapidly to about 74 percent at 5 degrees solar altitude.

Also, it appears that the shortwave fraction decreases somewhat uniformly from about 40 percent at 60 degrees to about 35 percent at 20 degrees and then decreases to about 20 percent at 5 degrees solar altitude.

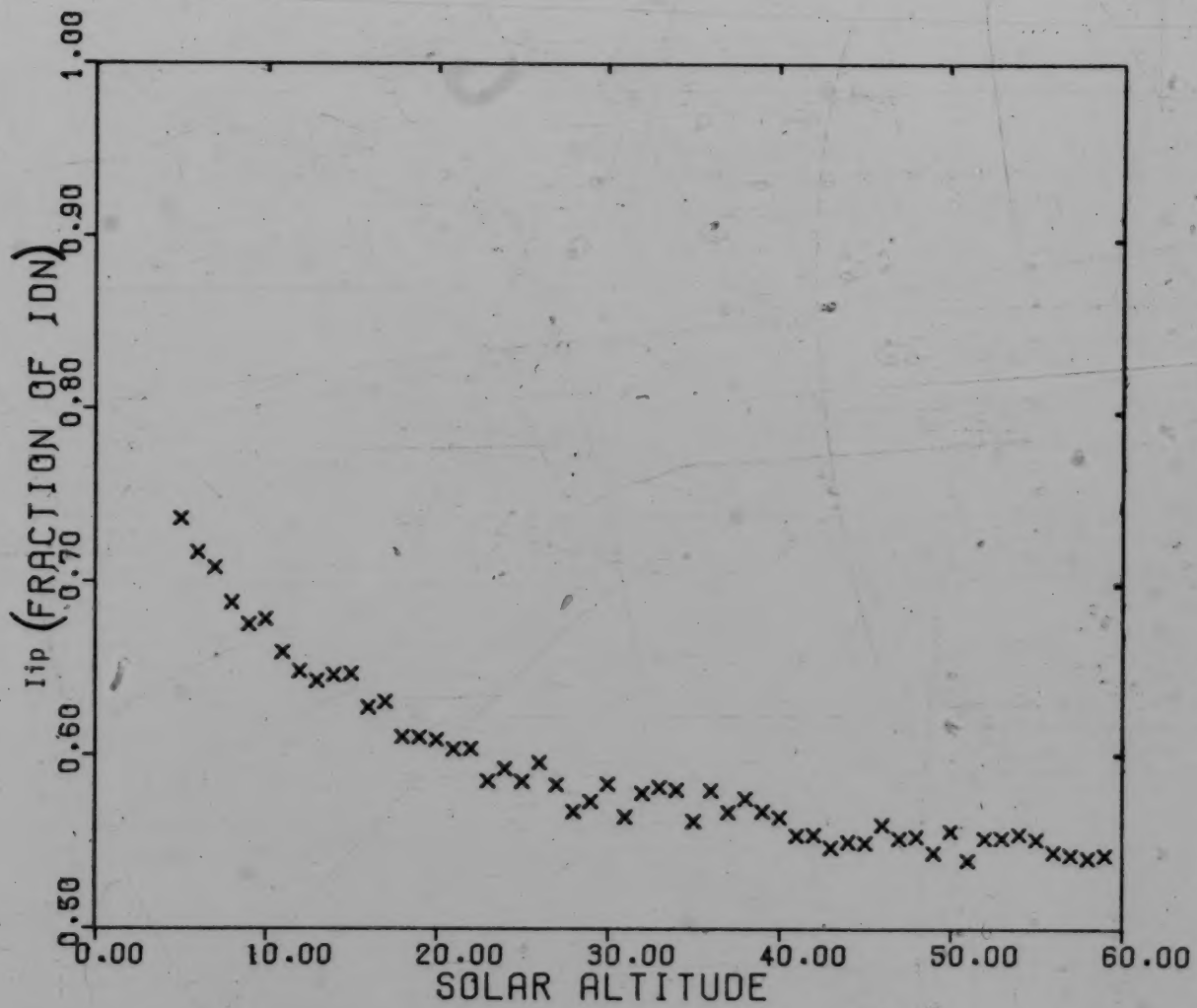

Figure 3.9 Variation of the infrared fraction, Iip, of the direct normal incidence solar radiation, IDN, with the solar altitude (degrees).

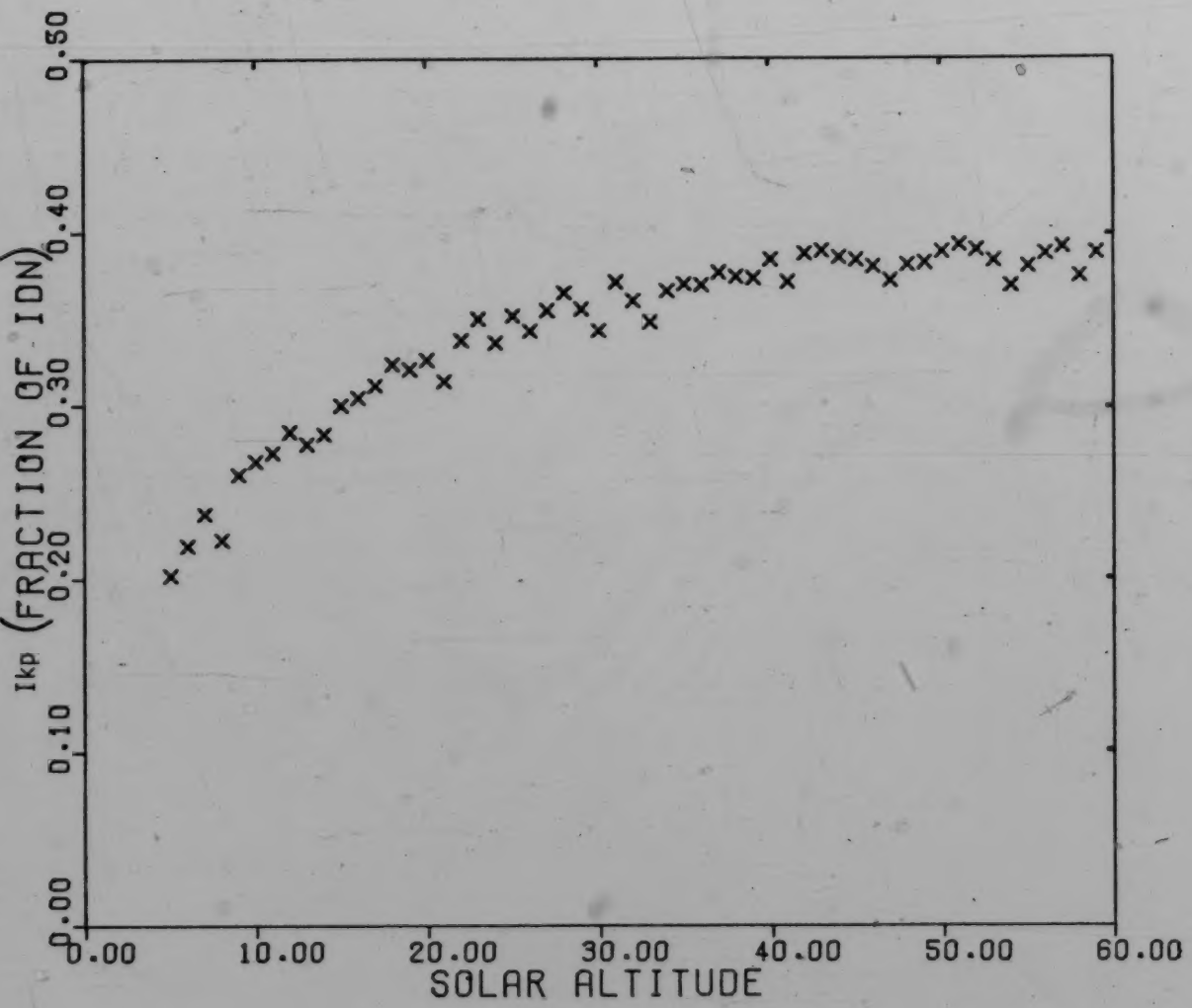

Figure 3.10 Variation of the shortwave fraction, Ikp, of the direct normal incidence solar radiation, IDN, with the solar altitude (degrees).

3.7 VARIATION OF THE INFRARED AND SHORTWAVE FRACTIONS OF THE NORMAL INSOLATION WITH THE OPTICAL AIR MASS

The attenuation of solar radiation is a function of the path length through the atmosphere and each station, due to elevation, has a different path length. To compensate for the effect of elevation, calculations are performed using the optical air mass. The optical air mass is obtained by multiplying the relative air mass (which is approximately equal to 1/sin (altitude)) by the ratio of the station pressure to standard atmospheric pressure. Representation of the fractions of the normal insolation as functions of optical air mass seems preferable.

From the results of the annual variation of the infrared and shortwave fractions and their variation with solar altitude, it was decided to represent the fractions as functions of the optical air mass at Edmonton for two periods of the year and two intervals of solar altitude. The first period includes April to September and the second period includes October to March. The solar altitude intervals are from 5 to 20 degrees and from 20 to 60 degrees. A study of the variation of the solar altitude with time of the day and time of the year at Edmonton showed that for the first period, the solar altitude is greater than 20 degrees on all days till hour angle 5 except in April, the second half of August and September where it is valid only till hour angle 4. The solar altitude is less than 20 degrees after hour angle 5

through out the first period. For the second period, the solar altitude is less than 20 degrees except in March from hour angle zero to three and in February and October till hour angle 2.

In Figures 3.11 to 3.14 the shortwave and the infrared fractions are represented as functions of the optical air mass for the two solar altitude intervals 5 to 20 degrees and 20 to 60 degrees for both periods April to September and October to March. The average optical air mass was calculated for each one degree interval of solar altitude. It appeared that the fractions could be represented by linear relationships and the best fit line was calculated for each set of data. The resulting equations representing the infrared fractions as functions of the optical air mass m are listed in table 3.7 for the two intervals of solar altitude and the two periods of the year. For solar altitude angles $\alpha > 20^\circ$ the relative air mass is given by $1/(\sin \alpha)$ and assuming that the optical air mass is calculated using mean annual station pressure (933 millibars), approximate equations can be written in terms of the solar altitude α for $\alpha > 20°$. These equations are also listed in table 3.7. Similar linear relationships for the shortwave fractions are given in table 3.8.

For the same optical air mass, the infrared fraction is less in the summer than in the winter by about 2.5 percent. On the other hand, the shortwave fraction is about 1.5 percent higher in the summer.

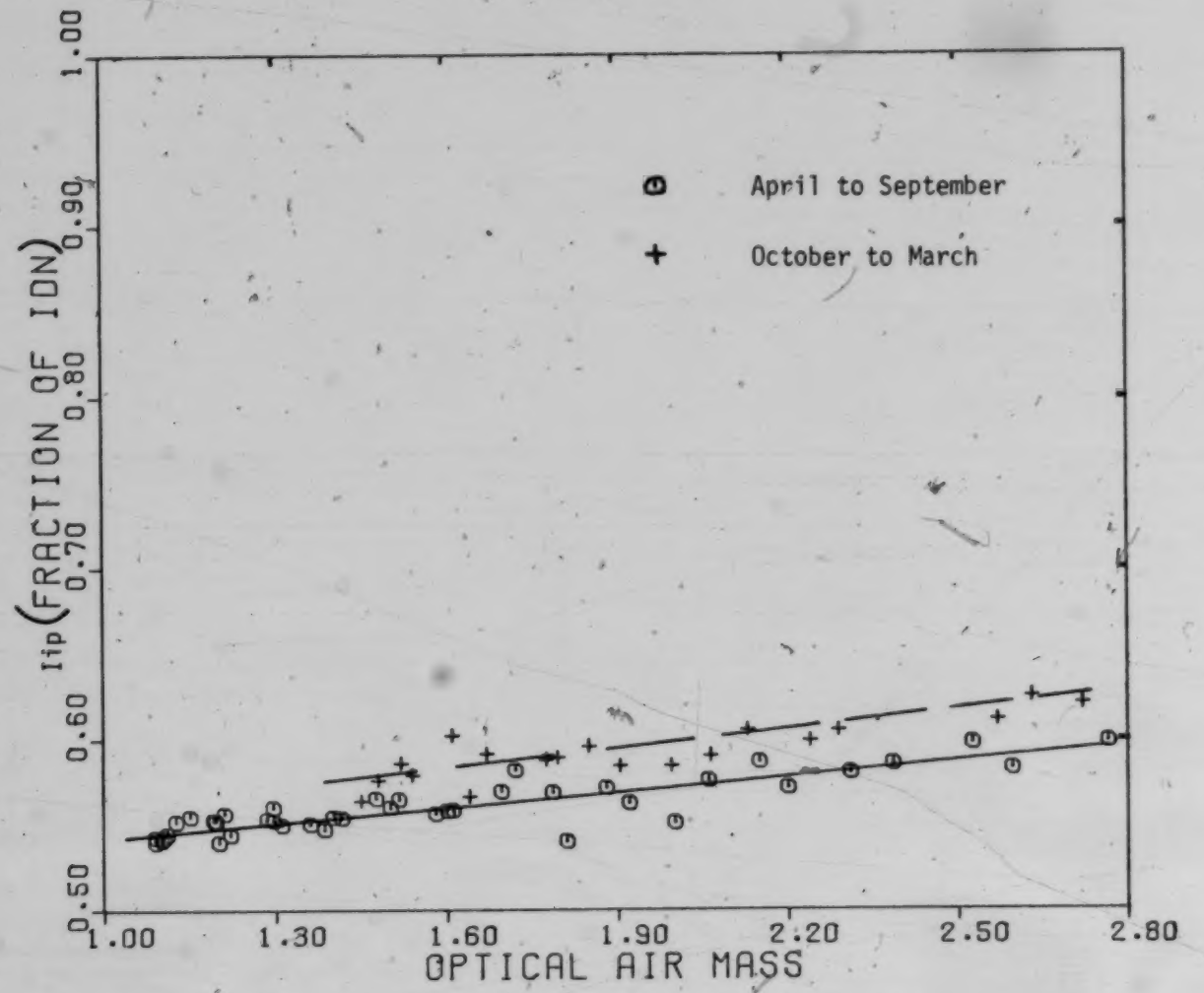

Figure 3.11 Variation of the infrared fraction, Iip, of the direct normal incidence solar radiation, IDN, with the optical air mass for the solar altitude interval 20 to 60 degrees throughout the year.

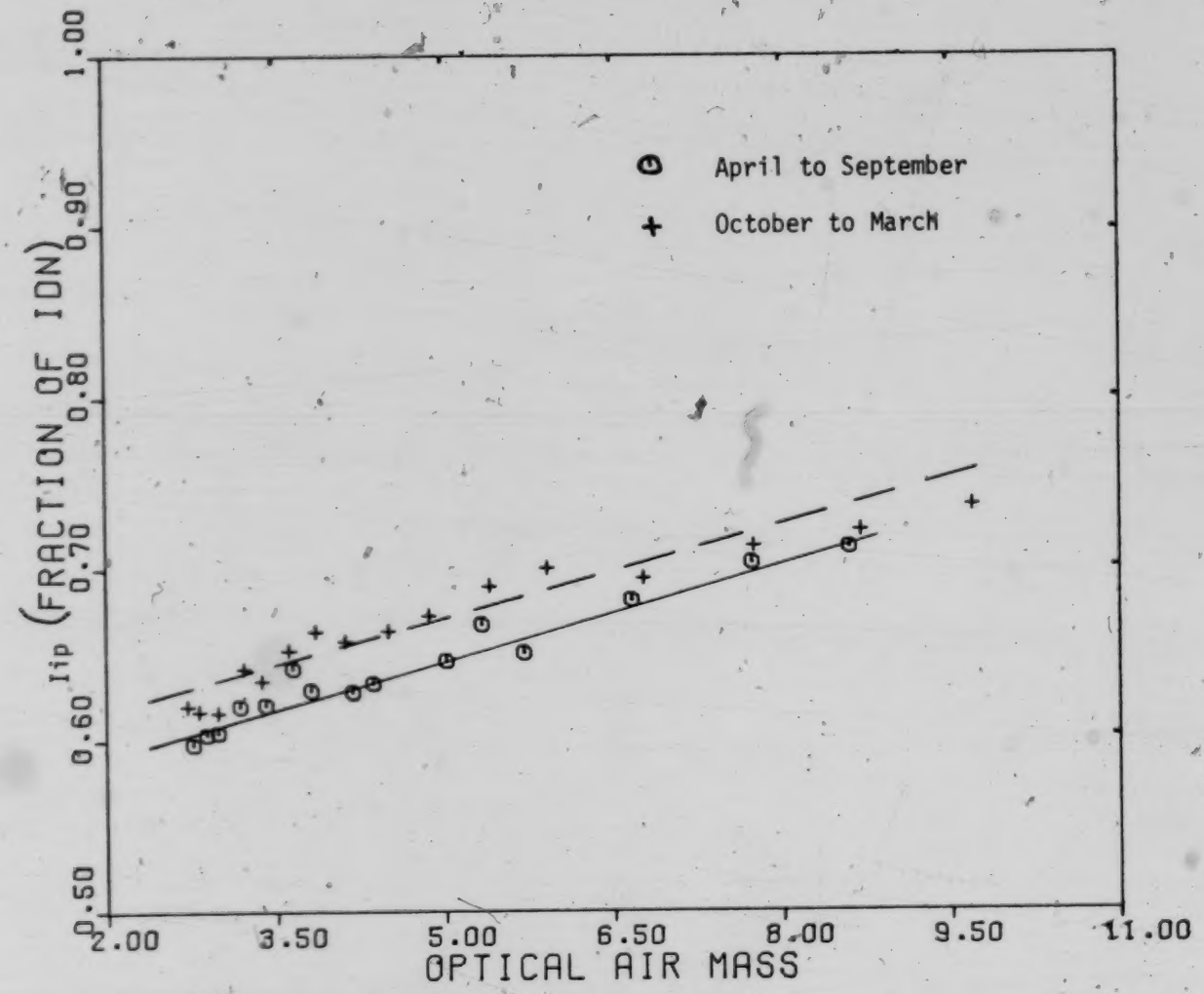

Figure 3.12 Variation of the infrared fraction, Iip, of the direct normal incidence solar radiation, IDN, with the optical air mass for the solar altitude interval 5 to 20 degrees throughout the year.

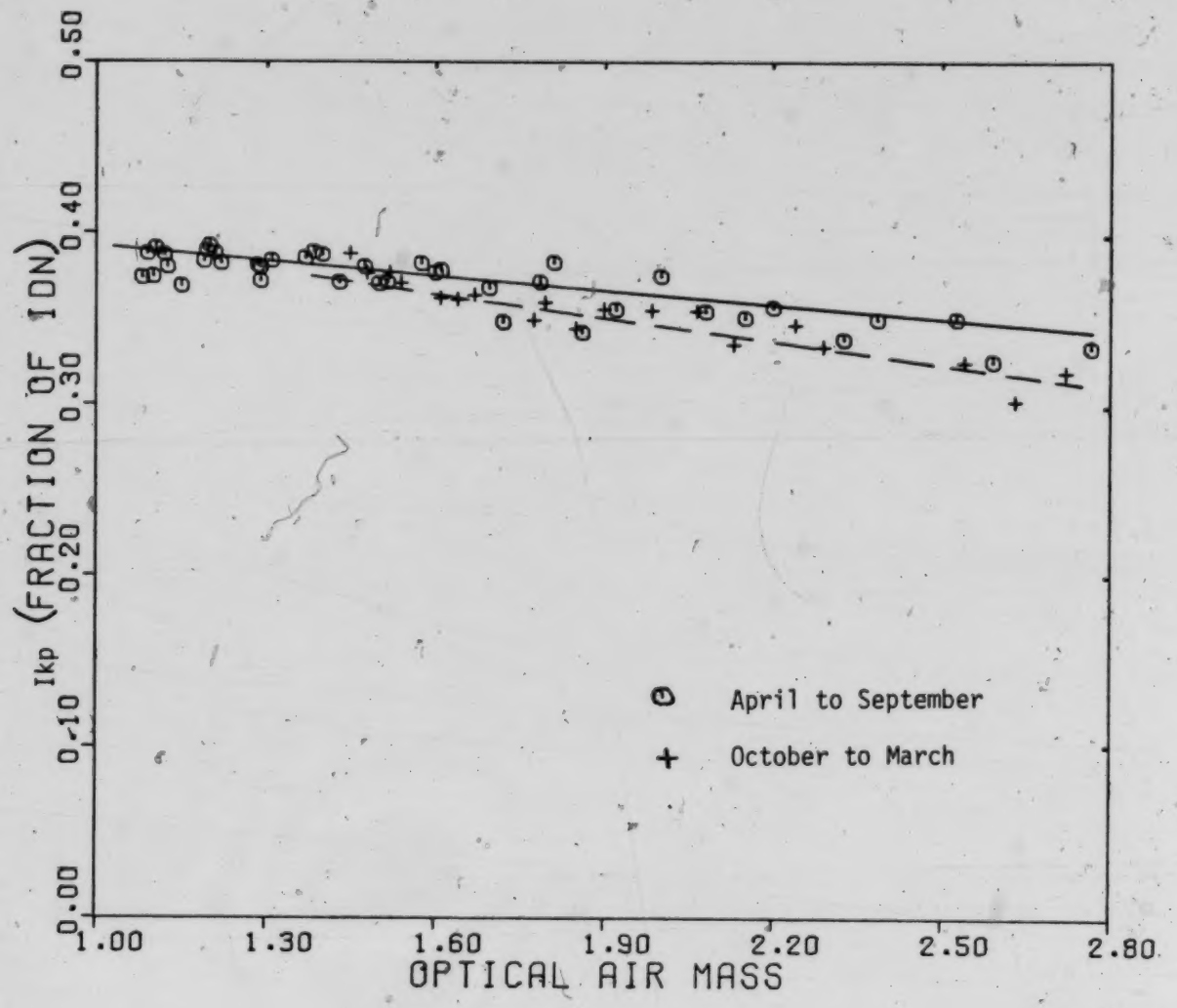

Figure 3.13 Variation of the shortwave fraction, Ikp, of the direct normal incidence solar radiation, IDN, with the optical air mass for the solar altitude interval 20 to 60 degrees throughout the year.

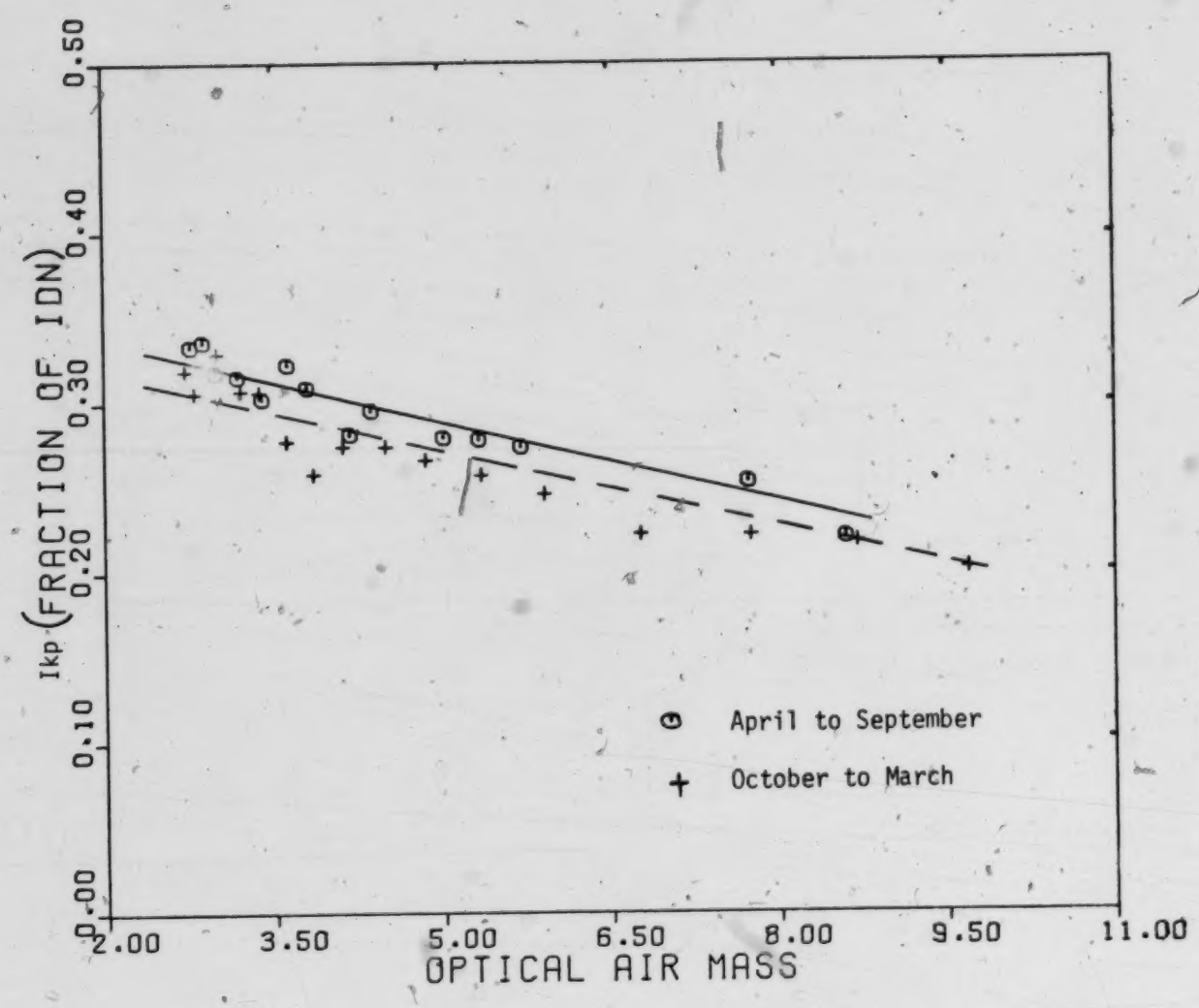

Figure 3.14 Variation of the shortwave fraction, Ikp, of the normal incidence solar radiation, IDN, with the optical air mass for the solar altitude interval 5 to 20 degrees throughout the year.

TABLE 3.7 Equations representing the infrared fraction ($\lambda > 690m\mu$) of the normal incidence solar radiation in terms of the optical air mass m and the solar altitude α.

Equation(*)	Altitude Interval	Time of the Year
Fraction = $0.513 + 0.030 \cdot m$	$20 \leq \alpha \leq 60$	April to September
$= 0.513 + 0.028 \cdot (1/\sin\alpha)$	"	"
Fraction = $0.528 + 0.033 \cdot m$	"	October to March
$= 0.528 + 0.031 \cdot (1/\sin\alpha)$	"	"
Fraction = $0.555 + 0.019 \cdot m$	$5 < \alpha < 20$	April to September
Fraction = $0.585 + 0.017 \cdot m$	"	October to March

(*) The straight lines are shown in figures 3.11 and 3.12.

TABLE 3.8 Equations representing the shortwave fraction ($\lambda < 626m\mu$) of the normal incidence solar radiation in terms of the optical air mass m and the solar altitude α.

Equation (*)	Altitude Interval	Time of the Year
Fraction = $0.420 - 0.031 \cdot m$	$20 \leq \alpha \leq 60$	April to September
$= 0.420 - 0.029 \cdot (1/\sin\alpha)$	"	"
Fraction = $0.451 - 0.051 \cdot m$	"	October to March
$= 0.451 - 0.048 \cdot (1/\sin\alpha)$	"	"
Fraction = $0.373 - 0.017 \cdot m$	$5 < \alpha < 20$	April to September
Fraction = $0.352 - 0.017 \cdot m$	"	October to March

(*) The straight lines are shown in figures 3.13 and 3.14.

3.8 DETERMINATION OF ATMOSPHERIC TRANSMISSION FACTORS AND EXTINCTION COEFFICIENTS FOR DIRECT RADIATION WITHIN THE WHOLE SOLAR SPECTRUM AND THE FIVE SPECTRAL BANDS

3.8.1 THE ATMOSPHERIC TRANSMISSION FACTORS: As mentioned in section 2.3 the atmospheric transmission factor for the integral wavelength direct normal incidence radiation can be calculated, using a simplified formula of equation 2.6, by dividing the measured radiation at the earth's surface reduced to mean earth - sun distance by the solar constant. The atmospheric transmission factors for a given band of the spectrum can be calculated by dividing the measured radiation within this band reduced to mean earth-sun distance by the portion of the solar constant within the same band.

The portion of the solar constant within each of the five spectral bands under investigation in this study was calculated from table 1 in reference [33]. The intensities of the direct radiation within the whole spectrum (IDN), infrared (Ii), visible (Iv), red and infrared (Ir), shortwave (Ik) and red (Ie) bands were reduced to mean earth-sun distance. The atmospheric transmission factors TDN, Ti, Tv, Tr, Tk and Te for the whole spectrum and the five bands were then calculated.

Tables 3.9 and 3.10 list the average values for the energy quantities IDN, Ii, Iv, Ir, Ik and Ie reduced to mean earth-sun distance, the average optical air mass m and the average values for the transmission factors TDN, Ti, Tv, Tr,

TABLE 3.9 Normal incidence solar radiation, IDN, at different solar altitudes α (degrees) and its distribution in different spectral bands throughout the year.
Unit: $Btu.ft^{-2}.hr^{-1}$.

α	Period(*)	m	Normal incidence radiation ($Btu.ft^{-2}.hr^{-1}$)					
			IDN	Ii	Iv	Ir	Ik	Ie
60	1	1.09	296	160	136	174	118	18
50	1	1.21	290	159	131	177	113	17
40	1	1.48	289	162	127	179	109	17
	2	1.45	289	163	126	181	108	17
30	1	1.88	264	150	113	168	96	17
	2	1.85	283	169	114	181	101	12
20	1	2.77	229	137	91	153	76	15
	2	2.72	262	162	99	178	83	15
15	1	3.63	210	132	77	146	63	14
	2	3.62	243	158	84	171	73	12
10	1	5.32	157	105	52	117	39	12
	2	5.70	203	140	62	152	51	8

(*) Period 1 includes the months April to September.
Period 2 includes the months October to March.

TABLE 3.10 Atmospheric transmission factors for the whole solar spectrum and the five bands calculated at different solar altitudes α (degrees) throughout the year.

α	Period (*)	m	Atmospheric transmission factors					
			TDN	Ti	Tv	Tr	Tk	Te
60	1	1.09	0.690	0.717	0.691	0.702	0.711	0.591
50	1	1.21	0.676	0.715	0.663	0.699	0.679	0.579
40	1	1.48	0.674	0.725	0.646	0.708	0.660	0.577
	2	1.45	0.674	0.731	0.640	0.714	0.651	0.577
30	1	1.88	0.615	0.675	0.577	0.663	0.577	0.580
	2	1.85	0.660	0.756	0.581	0.716	0.612	0.415
20	1	2.77	0.534	0.616	0.565	0.603	0.458	0.511
	2	2.72	0.611	0.729	0.504	0.704	0.504	0.515
15	1	3.63	0.489	0.593	0.395	0.578	0.382	0.469
	2	3.62	0.566	0.711	0.428	0.675	0.434	0.405
10	1	5.32	0.366	0.470	0.265	0.463	0.239	0.413
	2	5.70	0.473	0.631	0.316	0.602	0.305	0.291

(*) Period 1 includes the months April to September.
Period 2 includes the months October to March.

Tk and Te for the two periods of the year, April to September and October to March, at solar altitudes 60, 50, 40, 30, 20, 15 and 10 degrees. In general, for the same solar altitude, the atmospheric transmission factors are lower for the period April to September when the path length through the atmosphere, optical air mass, has higher level of precipitable water and more dust particles.

3.8.2 THE EXTINCTION COEFFICIENTS: As mentioned in section 2.4 Bouguer's law (equation 2.1) may be used to represent the attenuation of the normal incidence radiation within the whole solar spectrum. Also, it may be used to represent the normal incidence radiation within different spectral bands [27]. The portion of the solar constant within the band of concern should be used in applying Bouguer's law to that band.

Bouguer's law was applied to the measured energy quantities IDN, Ii, Iv, Ir, Ik and Ie reduced to mean earth-sun distance and the extinction coefficients for the total spectrum (ADN), the infrared band (Ai), visible band (Av), red and infrared band (Ar), shortwave band (Ak) and the red band (Ae) were calculated at different hour angles throughout the year. The average value for each of these coefficients were calculated for the two periods of the year, April to September and October to March, at solar altitudes 60, 50, 40, 30, 20, 15 and 10 degrees. Table 3.11 lists these values and the corresponding average optical air mass m.

TABLE 3.11 Extinction coefficients for the whole solar spectrum and the five bands calculated at different solar altitudes α (degrees) throughout the year.

α	Period(*)	m	Extinction Coefficients					
			ADN	Ai	Av	Ar	Ak	Ae
60	1	1.09	0.340	0.306	0.338	0.325	0.312	0.482
50	1	1.21	0.234	0.277	0.340	0.296	0.319	0.451
40	1	1.48	0.267	0.217	0.295	0.233	0.281	0.371
	2	1.45	0.272	0.216	0.308	0.233	0.296	0.379
30	1	1.88	0.258	0.209	0.293	0.218	0.292	0.290
	2	1.85	0.225	0.151	0.294	0.181	0.265	0.476
20	1	2.77	0.277	0.175	0.276	0.182	0.282	0.242
	2	2.72	0.181	0.116	0.252	0.129	0.252	0.244
15	1	3.63	0.197	0.144	0.256	0.151	0.265	0.209
	2	3.62	0.157	0.094	0.234	0.109	0.231	0.250
10	1	5.32	0.189	0.142	0.250	0.145	0.269	0.166
	2	5.70	0.131	0.081	0.202	0.089	0.208	0.217

(*) Period 1 includes the months April to September.
Period 2 includes the months October to March.

In general, at the same solar altitude, the extinction coefficients are higher for the period April to September than for the period October to March. The ratio is 1.29 for the whole spectrum, 1.47 for the infrared band and 1.16 for the shortwave band. Also, it was found that:

$$(Ak/ADN)_1 = 1.15 \qquad (Ak/ADN)_2 = 1.4$$

$$(Ai/ADN)_1 = 0.79 \qquad (Ai/ADN)_2 = 0.66$$

$$(Ak/Ai)_1 = 1.45 \qquad (Ak/Ai)_2 = 2.1$$

where subscript 1 refers to the period April to September and subscript 2 refers to the period October to March.

CHAPTER 4

TURBIDITY OF THE ATMOSPHERE AND ABSORPTION OF SOLAR RADIATION BY ATMOSPHERIC WATER VAPOR

4.1 ATMOSPHERIC TURBIDITY

The basic relation for the depletion of solar radiation by the earth's atmosphere was given in chapter 2 by:

$$I = (R_0/R_i)^2 \int_0^\infty I_0(\lambda) \cdot e^{-A(\lambda)\cdot m} \cdot d\lambda \qquad (4.1)$$

Rewriting equation 4.1 in terms of transmission of the different components of the earth's atmosphere gives:

$$R \cdot I = \int_0^\infty I_o(\lambda) \cdot \tau_R^m(\lambda) \cdot \tau_D^m(\lambda) \cdot \tau_W^m(\lambda) \cdot \tau_O^m(\lambda) \cdot \tau_{CO_2}^m(\lambda) \cdot d\lambda \qquad (4.2)$$

where $I_O(\lambda)$ is the solar constant as a function of the wavelength λ,

I is the measured solar intensity at the ground,

R = $(R_i/R_o)^2$, the reduction factor for mean earth-sun distance,

R_i is earth-sun distance at time of observation,

R_O mean earth-sun distance,

$\tau_R(\lambda)$ transmission of a Rayleigh atmosphere, clean and dry atmosphere, of unit air mass,

$\tau_D(\lambda)$ transmission due to dust in a unit air mass,

$\tau_W(\lambda)$ transmission due to water vapor in a unit air mass,

$\tau_O(\lambda)$ transmission due to ozone in a unit air mass,

$\tau_{CO_2}(\lambda)$ transmission due to carbon dioxide in a unit air mass, and

m is the optical air mass.

The turbidity of the atmosphere is defined as the reduced transmission of the atmosphere, caused by absorption and scattering by solid or liquid particles, other than clouds, held in suspension. On the basis of the physical considerations several methods for measuring atmospheric turbidity have been proposed. Angström (1929, 1930) defined a turbidity coefficient β, the extinction coefficient at $\lambda = 1\mu$ and γ, a wavelength exponent. Another turbidity coefficient B, was defined by Schüepp (1949) to represent the extinction at $\lambda = 0.5\mu$. A third measure of turbidity, called Linke's turbidity factor T, was proposed by Linke as early as 1922.

4.1.1 THE TURBIDITY FACTOR, T: It is defined as the ratio of the extinction of direct solar radiation in the real atmosphere to that of a Rayleigh atmosphere, i.e., an atmosphere free of dust, water vapor and ozone.

In 1922 Linke derived a mathematical formula for a separation of the extinction by dust and the selective absorption by the gases of the atmosphere from the scattering by the molecules. He proposed that:

$$I_\lambda = I_{0\lambda} \cdot \exp(-a_R(\lambda) \cdot T \cdot m) \qquad (4.3)$$

where $a_R(\lambda)$ is the extinction coefficient of molecular scattering for clear dry atmosphere,

$I_{O\lambda}$ is the intensity of parallel monochromatic beam at air mass zero,

I_λ is the intensity of parallel monochromatic beam at the surface.

Linke's turbidity factor T expresses the total extinction with the molecular scattering as unity. For an ideal pure (clean and dry) atmosphere, T becomes one. When T equals 2.0, the extinction of the real atmosphere containing water vapor and dust is twice that of a perfectly clean atmosphere with no selective absorption. Therefore the value of T can never be smaller than one.

By integrating equation 4.3 and applying the reduction for mean solar distance, the total radiation of all wavelengths is given by:

$$I = 1/R \cdot \int_0^\infty I_0 \cdot \exp(-a_R(\lambda) \cdot T \cdot m) \cdot d\lambda$$

$$R \cdot I = I_0 \cdot \exp(-T \cdot \bar{a}_R(m) \cdot m) \qquad (4.5)$$

where $I_0 = \int_0^\infty I_0(\lambda)\, d\lambda$ represents the solar constant,

$\bar{a}_R(m)$ is the mean value over all wavelengths of the extinction coefficient in clean dry atmosphere, and is now a function of air mass m, and

T is the turbidity factor for total radiation of all wavelengths.

From equation 4.5 a formula for the computation of the turbidity factor is deduced as:

$$T = P(m) \cdot [\log(I_0) - \log(I) - \log(R)] \qquad (4.6)$$

where $P(m) = (m \cdot \bar{a}_R(m) \cdot \log(e))^{-1}$, and is given in table 6 of the IGY Instruction Manual 1958 [10].

The optical air mass is used in evaluation of the turbidity factor T. For high level stations, when tables are used for the computation of turbidity, the air mass m = 1 is not the vertical air mass, with the sun at the zenith, but an air mass which is p_o/p times the vertical one, where p_o is the pressure at sea level and p is the pressure at place of observation. Therefore the values which are obtained from the tables do not refer to the vertical air mass of unity. In order to compare data at stations with different elevations, the value of T must be related to the air mass vertically above a station at mean sea level. For stations which have a mean pressure that is more than 50 millibars lower than the mean pressure at sea level, the value of T should be reduced at sea level with the aid of the following relationship given in [10]:

$$T_p = 1 + (T - 1) \cdot (P(m_h)/P(m)) \qquad (4.7)$$

where T_p is the turbidity factor extrapolated to sea level,

$P(m_h)$ is the tabular value of the function P(m) at the relative air mass m_h, and

P(m) is the tabular value of the function P(m) at the optical air mass m.

4.1.2 ÅNGSTRÖM'S TURBIDITY COEFFICIENT, β: A more appropriate way of expressing the scattering of dust in the atmosphere independent of the molecular scattering for the non selective part of the solar spectrum has been introduced by Ångström, 1929 [2]. In the ultraviolet and visible portion of the solar spectrum, where there is almost no selective absorption apart from the ozone absorption at high layers, attenuation of solar radiation is caused only by dry air and dust in the atmosphere. For this part of the spectrum the combined effect of the scattering by dry air molecules and dust may be expressed by the following equation:

$$I_\lambda = I_{0\lambda} \cdot \exp-(a_R(\lambda) + a_D(\lambda)) \cdot m \qquad (4.8)$$

where I_λ, $I_{0\lambda}$, $a_R(\lambda)$ and m are as defined before, and

$a_D(\lambda)$ is the extinction coefficient of the atmospheric dust.

The separate effects of absorption and scattering are difficult to separate for dust, but as a compromise, Ångström [3] found that the extinction coefficient of the dust in the

atmosphere may be approximated in a form similar to that of the Rayleigh scattering coefficient. In 1929, 1930 he proposed the well known empirical relation for the wavelength dependence of extinction of solar radiation by dust given by:

$$a_D(\lambda) = \beta \cdot \lambda^{-\gamma} \tag{4.9}$$

where β is the turbidity coefficient,

γ is a wavelength exponent, and

λ is the wavelength.

The magnitude of the wavelength exponent γ depends on the average size of the dust particles in the atmosphere. For small particles like those demanded by the theory of Rayleigh, γ may be as large as 4.0. For larger particles it may decrease to a value between zero and 1.0. In practice γ remains between the limits 0.5 and 3. Ångström [4] found that $\gamma = 1.3 \pm 0.2$ to be a reasonable average value.

The turbidity coefficient β depends upon the amount of dust present in the atmosphere and for a constant value of γ, it is proportional to the amount of dust in the air. It is clear from equation 4.9 that the quantity β coincides with the dust extinction coefficient a_D for wavelength $\lambda = 1\mu$.

The method most widely used for determination of the turbidity coefficient is Ångström's original method recommended in the IGY Instruction Manual (1958). It is based on the fact that the extinction by dust in the atmosphere is assumed

to take place according to the criteria for equations 4.8 and 4.9, and the measurement of the radiation behind the Schott filter of RG2 glass and the total radiation without filter.

The RG2 filter transmits more than 90 per cent of all radiation of wavelengths above 0.63 micron. Practically the total water vapor absorption in the solar spectrum falls on the wavelengths which are transmitted. If the total radiation and the radiation behind the RG2 filter ($\lambda > .63\mu$) are measured, then the short wave radiation ($.29 < \lambda < .63\mu$) can be obtained, as discussed in chapter 3, as the difference between the total radiation and the filtered radiation. The effect of water vapor is eliminated.

Integrating equation 4.8 for wavelengths between zero and 0.63μ and applying the reduction factor R for mean sun-earth distance, the short wave radiation, Ik, is expressed by:

$$R \cdot Ik = \int_{0}^{0.630} I_0(\lambda) \cdot \exp(-m\, a_R(\lambda) - m\, a_D(\lambda)) \cdot d\lambda \qquad (4.10)$$

The integral value of 4.10 is represented in tables such as: Tables for Radiation intensity of the sun ($m\,cal \,.\, cm^{-2} \,.\, m^{-1}$) in relation to air mass m and the turbidity coefficient β for wavelength less than 0.630μ computed by Feussner (1932) or Hoelper (1939). The data in Table 7, given in the appendix to the IGY Manual [10], were calculated from these sources with due regard to the international Pyrheliometric Scale 1956, and the extraterrestrial solar spectrum by Nicolet

(1951). Also there are diagrams which represent the value of the integral 4.10 for different air masses and different values of β like those given by Ångström (1929) [2]. If the intensity of the short-wave radiation at different values of air mass m corresponding to different times at any place are calculated, then Ångström turbidity coefficient can be interpolated from the standard table or diagrams. Usually tables and diagrams for the turbidity coefficient β are built up to refer to a place of observation with the standard pressure, at mean sea level, of 1000 millibars. For elevated stations with atmospheric pressure lower than 950 millibars the value of the turbidity coefficient β should be reduced to standard pressure using the relation:

$$\beta_p = \beta \cdot p/p_o \qquad (4.11)$$

In integral 4.10, a somewhat larger value for a_R should be used to account for ozone absorption in the ultraviolet and visible regions of the solar spectrum.

4.1.3 SCHÜEPP'S TURBIDITY COEFFICIENT, B: Ångström's turbidity coefficient β refers to a wavelength of 1.0μm, which is outside the visible spectrum. Schüepp (1949) has substituted a turbidity coefficient B which refers to a wavelength of 0.5μm. Ångström [7] found by observation that in the center part of the visible spectrum

$$B = 0.434\ \beta \cdot 2^{\gamma}$$

The coefficients B and β are not related by a constant factor, but depend specifically on the value of γ. However, calculations for B are often made by letting $\gamma = 1.3$ as suggested by Ångström. Then

$$B = 1.069\,\beta$$

A direct measurement of B can be obtained by using the Volz type G Sunphotometer.

4.2 DETERMINATION OF LINKE'S TURBIDITY FACTOR FOR EDMONTON

Table 6 of the IGY Instruction Manual 1958 [10] was divided into several intervals with each interval covering one unit of air mass. A polynomial was fitted for each interval between the values of the air mass m and the factor P(m) using a least square technique. Table 4.1 shows the ten polynomials used for calculating the factor P(m) for any given value of air mass m in this study.

The turbidity factor T for Edmonton was determined from equation 4.6 using the solar constant $I_0 = 1.98$ cal . cm^{-2}. min^{-1}, the values for the reduction factor R from reference [25], the measured total direct normal solar radiation at Edmonton in cal . cm^{-2} . min^{-1} and the calculated value of P(m). Then the extrapolated turbidity factor T_p was determined according to equation 4.7. For each day, T_p was calculated at hourly intervals starting from hour angle zero, at solar noon, for

TABLE 4.1 Polynomials for calculating the factor P(m) as a function of the air mass m

P(m)	$= 112.39 - 213.96 \cdot m + 180.99 \cdot m^2 - 56.08 \cdot m^3$	$0 < m \leq 1$
P(m)	$= 55.81 - 49.78 \cdot m + 20.06 \cdot m^2 - 2.95 \cdot m^3$	$1 < m \leq 2$
P(m)	$= 25.97 - 5.65 \cdot m - 1.45 \cdot m^2 + 0.024 \cdot m^3 + 0.46 \cdot m^4 - 0.131 \cdot m^5 + 0.01 \cdot m^6$	$2 < m \leq 3$
P(m)	$= 8.81 + 5.06 \cdot m - 2.48 \cdot m^2 + 0.29 \cdot m^3$	$3 < m \leq 4$
P(m)	$= 8.06 + 2.52 \cdot m - 1.04 \cdot m^2 + 0.09 \cdot m^3$	$4 < m \leq 5$
P(m)	$= 13.64 - 2.02 \cdot m + 0.12 \cdot m^2$	$5 < m \leq 6$
P(m)	$= 9.11 - 0.59 \cdot m + 0.004 \cdot m^2$	$6 < m \leq 7$
P(m)	$= 8.031 - 0.408 \cdot m$	$7 < m \leq 8$
P(m)	$= 7.309 - 0.318 \cdot m$	$8 < m \leq 9$
P(m)	$= 6.752 + 0.256 \cdot m$	$9 < m \leq 10$

both forenoon and afternoon periods. Figure 4.1 shows the daily average value of T_p for Edmonton and the mean monthly values. The latter are listed in table 4.2.

TABLE 4.2 Mean monthly value of Linke's turbidity factor T_p for Edmonton

Month	T_p	Month	Tp
January	2.01	July	3.26
February	2.08	August	3.22
March	2.49	September	2.75
April	2.92	October	2.29
May	3.26	November	2.09
June	3.37	December	1.98

T_p is lowest in December and January and increases to a flat peak in the months May through September. The increase between winter and summer values of T_p is partially due to the increase of absorption in the near-infrared bands. The mean yearly value of T_p, averaging all data is 2.64. The merit of T_p is that it can be found from measurement of the intensity of total solar radiation. However, T_p is affected by absorption of solar radiation in the near-infrared water

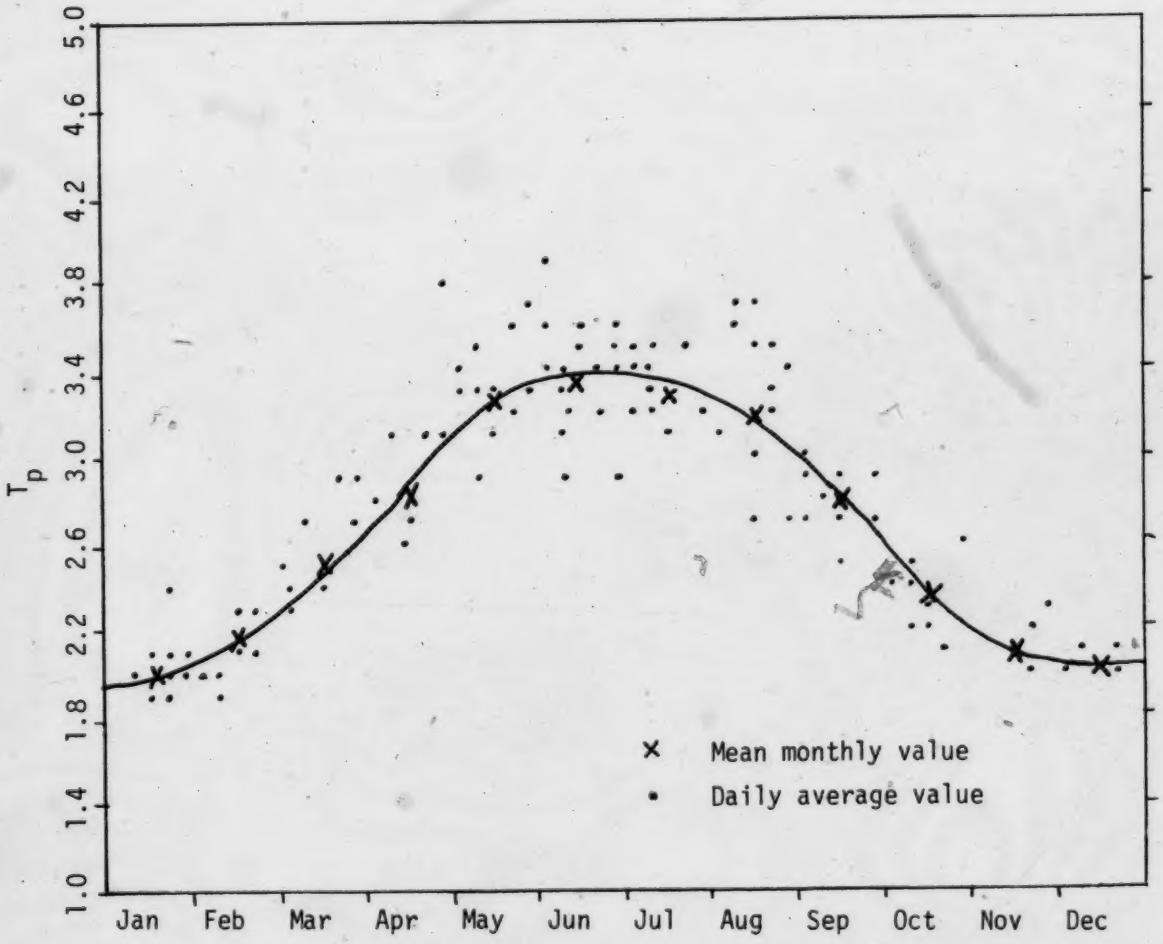

Figure 4.1 Annual variation of Linke's turbidity factor for Edmonton.

vapor bands. Therefore, T can not essentially be considered as a strict measure of the atmospheric turbidity alone [24].

4.3 DETERMINATION OF ÅNGSTRÖM'S TURBIDITY COEFFICIENT FOR EDMONTON

Ångström turbidity coefficient β has been computed for Edmonton according to Ångström's original method. First, the hourly values of the radiation measured by the RG2 filter were prepared (as discussed in Chapter 3). Then these values were subtracted from the corresponding hourly values of the total normal incidence radiation (in cal. cm^{-2}. $min.^{-1}$) and the differences were reduced to mean solar distance so the shortwave radiation defined by $\lambda < 630m\mu$ was obtained. This radiation can be regarded as free from selective absorption and was used for determination of β by interpolation from table 7 given in the appendix of the IGY Instruction Manual. This table is based on the use of $\gamma = 1.3$. Then the β values thus derived were reduced to β_p according to equation 4.11.

Table 4.3 lists the monthly average value of Ångström's turbidity coefficient β_p for Edmonton and figure 4.2 shows the annual variation of β_p. The annual trend of β_p is similar to that for Tp. The peak in β_p occurs in May and June reaching an average value of 0.048 and the lowest value of 0.01 occurs in the winter months. The mean value of β_p over the year was found to be 0.026.

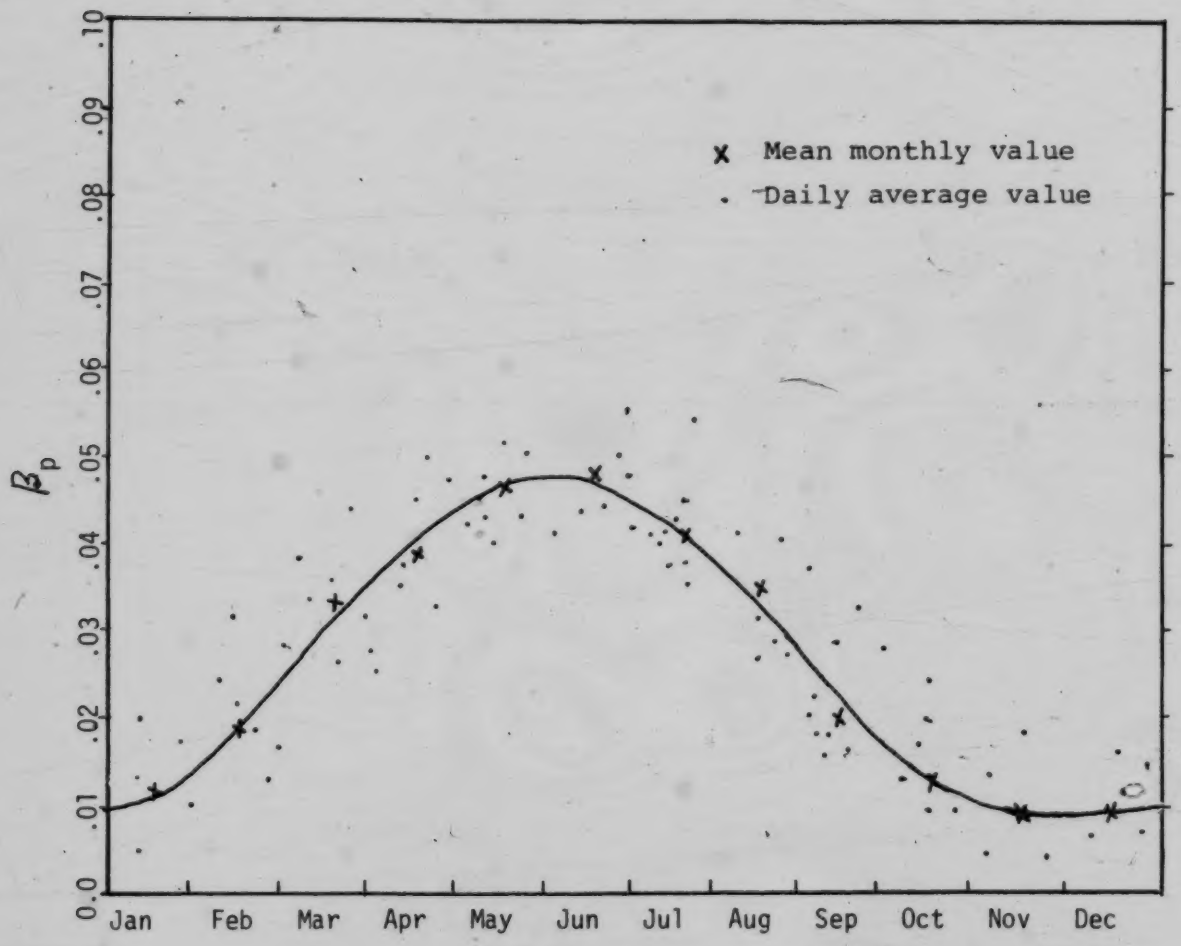

Figure 4.2 Annual variation of Ångström turbidity factor, β_p, for Edmonton.

TABLE 4.3 Mean monthly value of Ångström's turbidity factor β_p for Edmonton

Month	β_p	Month	β_p
January	0.012	July	0.041
February	0.019	August	0.037
March	0.034	September	0.018
April	0.038	October	0.012
May	0.047	November	0.008
June	0.048	December	0.010

The seasonal variation of β_p with a pronounced maximum in the early summer months is a well known phenomena [24]. The obvious cause of this must be that on account of the rapid heating of the ground in spring and early summer and that consequently dust particles are then carried most effectively from the ground to the higher layers of the atmosphere, while during winter the surface is covered by snow much of the time, suppressing the dispersion of surface dust.

4.4 ABSORPTION OF SOLAR RADIATION BY ATMOSPHERIC WATER VAPOR

In the near infrared regions of the solar spectrum ($\lambda >$ 630 mμ), absorption by water vapor and absorption by carbon

dioxide dominate the attenuation of radiation. This attenuation occurs by a series of absorption bands each comprised of hundreds of narrow individual absorption lines, which merge to form the bands. The wings of these numerous lines contribute a definite amount to the continuum extinction. So the infrared extinction is comprised of two parts: a continuum extinction at all frequencies, caused by scattering and the wings of absorption lines, and a selective absorption within each individual line contributing to the total absorption band. The absorption is mainly caused by the water vapor and is simply denoted as water vapor absorption.

Different formulas for the calculation of the water vapor absorption in the infrared regions of the solar spectrum have been derived by scientists. As a compromise the water vapor absorption is expressed as a function of the total amount of water vapor, in the zenith direction, between the surface of the earth and space, known as the precipitable water. The amount of precipitable water, in centimeters, is the thickness of liquid water which would be formed if all the water in the zenith direction, vertical column, were condensed at the surface.

In 1961 Ångström [5] has derived the following formula for the infrared absorption (the region where the main water vapor bands are found is 0.75 to 2.1 μ) by the water vapor in the case of a perfectly clear atmosphere (turbidity coefficient $\beta = 0$) at standard sea level pressure

$$WA = 0.31 - 0.21 \exp(-0.23\ w \cdot m_h) \qquad (4.12)$$

where WA is the infrared absorption by the water vapor (in $cal.cm.^{-2}min.^{-1}$),

w is the precipitable water content of the vertical column (in cm) and

m_h is the relative air mass.

In 1964 Ångström[6] expanded his formula to take regard also for the influence of scattering within the wavelength region where the main water vapor bands are found, viz. at 0.75 to 2.1 μ. He also added two corrections for the pressure dependence of the absorption and for absorption above 2.1μ. He proposed that for $m_h.w$ between 0.5 and 10 and $\beta < 1.0$, the infrared absorption by water vapor may be calculated by the equation:

$$WA = 0.163\ (w \cdot m_h)^{0.30} \cdot (0.81)^{m_h \cdot \beta} \qquad (4.13)$$

where β is Ångström's turbidity coefficient. This equation is applicable to the average conditions at stations near to sea level with uncertainty in deriving values for WA of at least ±5 percent [6].

4.5 DETERMINATION OF WATER VAPOR ABSORPTION AT EDMONTON

The water vapor absorption, WA, at Edmonton was calculated according to equation 4.13, using the calculated relative

air mass values for Edmonton, the average daily precipitable water values for forenoon and afternoon obtained from reference [11] and the β values determined for Edmonton in section 4.4. For each day WA was calculated at hourly intervals for both forenoon and afternoon periods then the daily average value was calculated. Table 4.4 lists the monthly mean value of the water vapor absorption, WA, at Edmonton and figure 4.3 shows the annual variation of WA. The atmospheric water vapor absorption shows higher values in the summer months with the maximum of 0.245 cal.cm.$^{-2}$min^{-1} (54.19 Btu.ft.$^{-2}$hr^{-1}) in August. The lowest values occur in the months October to March with an approximate average value of 0.18 cal.cm.$^{-2}$min^{-1} (39.82 Btu.ft^{-2}.hr^{-1}). These correspond to an amount of precipitable water of 1.84 cm (0.724 inches) and 0.48 cm (0.19 inches), respectively.

TABLE 4.4 Mean monthly value of water vapor absorption at Edmonton

Month	WA	
	$cal.cm.^{-2} min^{-1}$	$Btu.ft.^{-2}hr^{-1}$
January	0.178	39.37
February	0.180	39.82
March	0.181	40.03
April	0.182	40.26
May	0.185	40.92
June	0.210	46.45
July	0.215	47.56
August	0.243	53.75
September	0.218	48.22
October	0.184	40.70
November	0.180	49.82
December	0.176	38.93

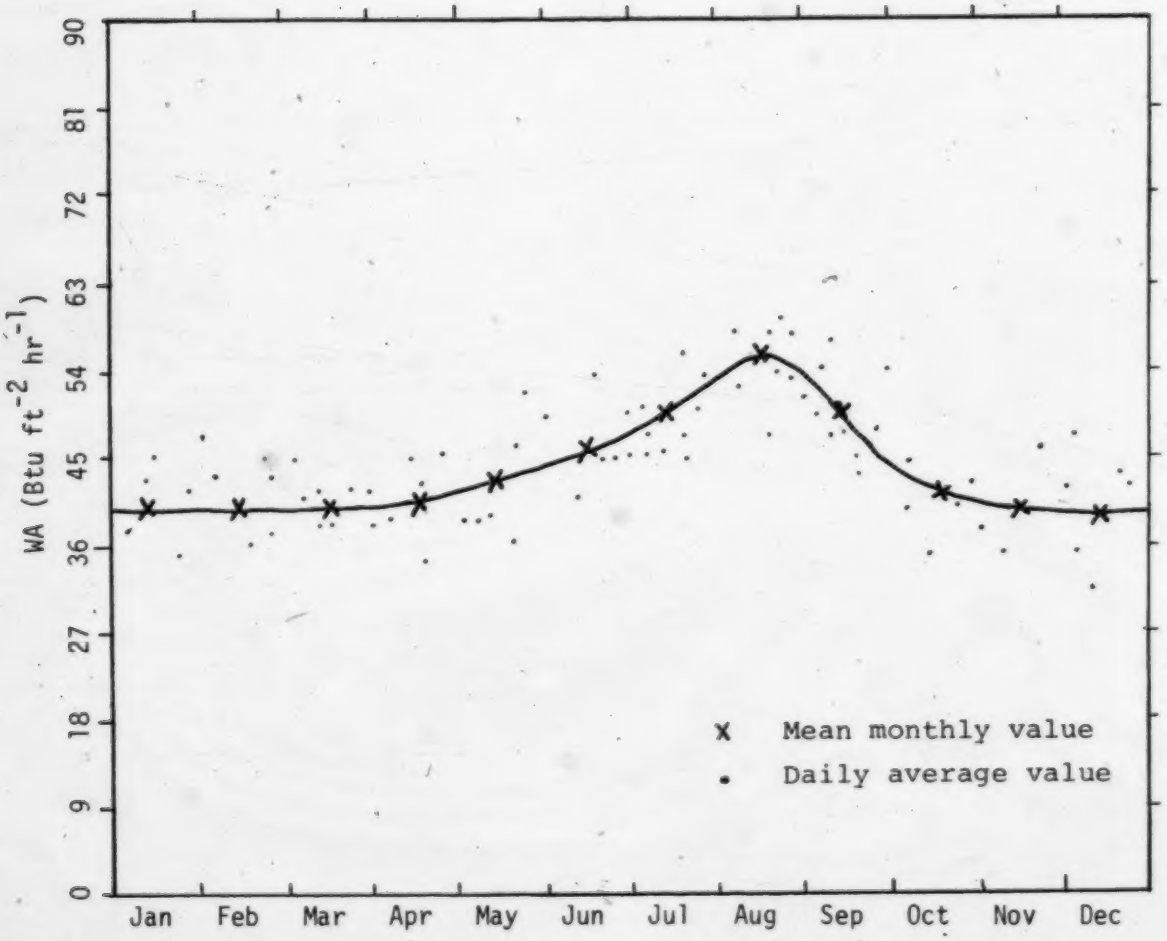

Figure 4.3 Annual variation of water vapor absorption, WA (Btu ft^{-2}hr^{-1}), at Edmonton.

CHAPTER 5

DISCUSSION AND CONCLUSIONS

In this study, solar radiation measurements at Edmonton, Alberta, Canada were analyzed for the period from May 1972 to September 1975. The data consisted of records of clear sky direct normal incidence radiation within the whole spectrum and its spectral components passing through the RG2 and RG8 filters. The spectrum was divided into five bands defined by the wavelength intervals: $\lambda < 626m\mu$ (shortwave), $\lambda > 626m\mu$ (red and infrared), $\lambda < 690m\mu$ (visible), $\lambda > 690m\mu$ (infrared) and $626 < \lambda < 690m\mu$ (red). In order to study the effect of the atmospheric scattering and water vapor absorption on the solar energy more attention was given here to the shortwave and infrared bands. The intensity of the shortwave radiation received at the earth's surface is mainly dependent on atmospheric scattering while the intensity of the infrared radiation is mainly dependent on the absorption by the atmospheric water vapor.

5.1 APPARENT SOLAR CONSTANT AND APPARENT EXTINCTION COEFFICIENT

The apparent solar constant I^* and the apparent extinction coefficient A have been calculated from the total direct normal incidence radiation IDN and the optical air mass m using the equation:

$$IDN = I^* \exp(-Am)$$

The annual variation and the monthly average values for I^* and

A are reported in section 2.4. The mean annual values obtained are 346 Btu.ft^{-2}.hr^{-1}. for I^* and 0.122 for A. The results are compared with the values obtained by Sadler [28] for the same location for the period from 1965 to 1968. The present results show about 5 percent lower values for I^* for April to August, inclusive. A better agreement appears for the rest of the year. The present values for A are slightly lower for January to September and slightly higher for October to December. The simplicity of this method used to represent the solar insolation is desirable in practice, but additional investigation is required to determine the effect of the climatic conditions on the values of I^* and A. Since the recording station is located near the center of the city, consideration should be given to the dust content in the atmosphere in order to arrive at more representative values of I^* and A.

5.2 DIURNAL AND ANNUAL VARIATIONS OF THE DIRECT RADIATION AND ITS SPECTRAL COMPOSITION

The annual variation of the total direct normal incidence radiation and its composition within the five spectral bands at hour angles 0 to 6 is shown graphically in sections 2.6 and 3.5. The monthly average values are also reported. These values occur at about the third week of the month but measurements on adjacent days may show up to 10 percent variation

from the mean. The maximum intensity of the total direct radiation of about 305 Btu.ft^{-2}.hr^{-1} occurs in March and April at solar noon. The maximum intensity of the infrared radiation of about 182 Btu.ft^{-2}.hr^{-1} occurs also in March and April when the precipitable water in the atmosphere is low. Lower energy values are found in the summer months as the precipitable water level increases in the atmosphere. The maximum intensity of the shortwave radiation of about 125 Btu.ft^{-2}.hr^{-1} occurs in the summer months at solar noon when the path length through the atmosphere is relatively short. The available energy decreases as the hour angle deviates from solar noon. The decrease is more rapid after hour angle 2 due to rapid increase in the path length of the radiation through the atmosphere.

The infrared fraction of the direct radiation has minimum value during the summer months (for all hour angles), although the path length through atmosphere is relatively short. This is due to the larger quantities of precipitable water during this season. The red fraction of the direct radiation has a mean value of 6.5 percent with slight annual variation at all hour angles. The shortwave fraction of the direct radiation has a maximum during the summer months and decreases gradually during the rest of the year, a characteristic which occurs at all hour angles. This fraction decreases as the hour angle increases from solar noon because of the increase in the path length through the atmosphere. As a result, the infrared

fraction increases approximately in proportion to the decrease in the shortwave fraction with increasing hour angle.

5.3 VARIATION OF THE INFRARED AND SHORTWAVE FRACTIONS WITH SOLAR ALTITUDE AND OPTICAL AIR MASS

The fraction of the direct radiation within the infrared band increases from about 54 to 62 percent while the fraction in the shortwave band decreases from about 40 to 35 percent as the solar altitude decreases from 60 to 20 degrees. For further decrease in altitude, these values change faster reaching 74 percent within the infrared band and 20 percent within the shortwave band at 5 degrees.

By representing the infrared and the shortwave fractions as functions of the optical air mass, linear relationships seemed reasonable and have been computed by the least squares method. For the same optical air mass, the infrared fraction is less in the summer than in the winter by about 2.5 percent. On the other hand, the shortwave fraction is about 1.5 percent higher in the summer.

5.4 ATMOSPHERIC TRANSMISSION FACTORS AND EXTINCTION COEFFICIENTS

For the same solar altitude and approximately the same optical air mass, the intensities of direct radiation within

the whole spectrum and the five bands reduced to mean earth-sun distance are higher in winter than in summer. This is consistent with higher atmospheric transmission factors in winter when the precipitable water and the dust content in the atmosphere are lower than in summer. The ratio of the extinction coefficient in summer to that in winter is 1.29 for the whole spectrum, 1.47 for the infrared band and 1.16 for the short band. In summer, the ratio of the extinction coefficients of the infrared band and the shortwave band to the extinction coefficient for the whole spectrum are 0.79 and 1.15, respectively. The corresponding values in winter are 0.66 and 1.44, respectively.

5.5 ATMOSPHERIC SCATTERING AND ABSORPTION

To render the results from Edmonton directly comparable with those from other places, it was regarded appropriate to determine some parameters that facilitate the treatment and give the results a general character. Three such parameters are: Linke's turbidity factor, Ångström's turbidity coefficient and the water vapor absorption.

Linke's turbidity factor T_p has shown a marked annual variation with high values in summer and low values in winter. The mean value over the year is 2.64. The increase between winter and summer values of T_p is due to the increase of dust and other aerosol particles in the atmosphere. It is also

partially due to the increase of atmospheric water vapor in the atmosphere in the summer.

The annual trend of Ångström's turbidity coefficient β_p is very similar to that for T_p, and for the same reasons. The yearly mean value for β_p is 0.026.

The atmospheric water vapor absorption is found to be 47.0 Btu.ft^{-2}.hr^{-1} (0.213 cal cm^{-2} min^{-1}) with an annual variation indicating a maximum in July and August and a minimum in the winter months. This corresponds to an amount of precipitable water of 0.465 inches (1.16 cm) in the vertical column of the atmosphere.

REFERENCES

1. American Society of Heating, Refrigerating and Air Conditioning Engineers (ASHRAE), 1967: Handbook of Fundamentals, Chap. 22, pp 386-394.

2. Ångström, A., 1929: On the Atmospheric Transmission of Sun Radiation and on Dust in the Air, Geografiska Annaler, H.2, pp 156-166.

3. _____, 1930: On the Atmospheric Transmission of Sun Radiation II, Geografiska Annaler, H.2 and 3, pp 130-159.

4. _____, 1961: Techniques of Determining the Turbidity of the Atmosphere, Tellus, 13, 2, pp 214-223.

5. _____, 1961: Absorption of Solar Radiation by Atmospheric Water Vapor, Arkiv för Geofysik, Band 3, nr 23, pp 557-565.

6. _____, 1964: On the Absorption of Solar Radiation by Atmospheric Water Vapor. II, Arkiv för Geofysik, Band 4, nr 24, pp 503-511.

7. _____, 1964: The Parameters of Atmospheric Turbidity, Tellus, 16, 1, pp 64-75.

8. _____, 1970: On Determinations of the Atmospheric Turbidity and Their Relation to Pyrheliometric Measurements, Advances in Geophysics, 14, pp 269-284.

9. _____ and A.J. Drummond, 1961: Basic Concepts Concerning Cutoff Glass Filters Used in Radiation Measurements, Jour. of Meteor., 18, pp 360-367.

10. Annals of the International Geophysical Year, 1958: part VI, Pergamon Press, New York.

11. Atmospheric Environment Service, 1972-1975: Monthly Bulletins of Upper Air Data, Downsview, Ontario.

12. Brooks, F.A., 1960: Introduction to Physical Microclimatology (chap. 2), University of California, Davis, California.

13. Brooks, F.A. and W. Miller, 1963: Availability of Solar Energy, in "Introduction to the Utilization of Solar Energy", edited by Zarem and Erway, McGraw-Hill, Inc., New York.

14. Cooper, P.J., 1969: The Absorption of Solar Radiation in Solar Stills, Solar Energy, 12, 3, pp 333-346.

15. Drummond, A.J. and A. Ångstrom, 1967: Solar Radiation Measurements on Mauna Loa (Hawaii) and Their Bearing on Atmospheric Transmission, Solar Energy, 11, 3-4, pp 133-141.

16. Dunkelman, L. and R. Scolnik, 1959: Solar Spectral Irradiance and Vertical Atmospheric Attenuation in the Visible and Ultraviolet, J. Opt. Soc. Am., 49, 4, pp 356-367.

17. Eppley Laboratory, Inc., 1960: Generalized Transmission Data for Schott OG1, RG2 and RG8 Filters as Supplied in Eppley Normal Incidence Pyrheliometers, Newport, Rhode Island.

18. Fritz, S., 1957: Solar Energy on Clear and Cloudy Days, The Scientific Monthly, pp 55-65.

19. Gates, D.M., 1966: Spectral Distribution of Solar Radiation at the Earth's Surface, Science, 151, 3710, pp 523-529.

20. Hay, J.E., 1977: An Analysis of Solar Radiation Data for Selected Locations in Canada, Climatological Studies Number 32, Atmospheric Environment Service, Downsview, Ontario.

21. Johnson, F.S., 1954: The Solar Constant, J. Meteor. 11, 6, pp 431-439.

22. K and E Solar Ephemeris, for the years 1972-1975, and Surveying Instrument Manual, Keuffel & Esser Co., New York.

23. Latimer, J.R., 1972: Radiation Measurement, IFYGL, Technical Manual Series No. 2, Information Canada, Ottawa.

24. _____, 1974: Observation of Direct Solar Radiation and Atmospheric Turbidity at Toronto-Scarborough from 1960-1970, CMRR 1/74, Atmos. Environ. Service, Downsview, Ontario.

25. Nautical Almanac for the Years 1972-1975, U.S. Government Printing Office, Washington.

26. Petterssen, S., 1969: Introduction to Meteorology, third edition, McGraw-Hill Inc., New York.

27. Robinson, N., 1966: Solar Radiation, Elsevier Publishing Company, New York.

28. Sadler, G.W., 1970: Measurement of Apparent Solar Constant and Apparent Extinction Coefficient at Edmonton (Alberta) Canada, Solar Energy, 13, pp 35-41.

29. _____, 1974: Solar Radiation at Edmonton, Alberta, Dept. of Mechanical Engineering, Univ. of Alberta, Edmonton, Alberta.

30. _____, 1978: Characteristics of Clear Sky Normal Incidence Solar Insolation Measured with the RG2 Filter, Dept. of Mechanical Engineering, Univ. of Alberta, Edmonton, Alberta, Solar Energy, 20.

31. Siriwong, S., 1972: Solar Insolation at Edmonton, Alberta, unpublished M.Eng. project, Dept. of Mech. Eng., Univ. of Alberta, Edmonton, Alberta.

32. Thekaekara, M.P., R. Kruger and C.H. Duncan, 1969: Solar Irradiance Measurements from a Research Aircraft, Applied Optics, 8, 1717.

33. Thekaekara, M.P., 1970: Proposed Standard Values of the Solar Constant and the Solar Spectrum, J. Environ. Sc., 13, 4, pp 6-9.

34. Threlkeld, J.L. and R.C. Jordan, 1958: Direct Solar Radiation Available on Clear Days, Transactions Am. Soc. of Heating and Air-Conditioning Engineers (ASHAE), 64, pp 45-68.

35. Threlkeld, J.L., 1970: Thermal Environmental Engineering (chap. 14), second edition, Prentice-Hall, Inc., Englewood Cliffs, N.J.